UNIVERSITY OF TWENTE.

de Vries & van de Wiel
Dredging & Environmental Solutions

SAND DUNE BEHAVIOR PREDICTIONS FOR DREDGING APPLICATIONS

MSc thesis in Civil Engineering and Management

Alex Rojals Mainar
s2010674

Enschede, July 2018

Water Engineering and Management Department

SAND DUNE BEHAVIOR PREDICTIONS FOR DREDGING APPLICATIONS

Alex Rojals Mainar
s2010674

MSc Thesis in Civil Engineering and Management
Enschede, July 5, 2018
To be presented in public on July 12, 2018
11:00h, OH-110, de Horst

University of Twente
Faculty of Engineering Technology
Department of Water Engineering and Management
PO Box 217
7500 AE
Enschede, the Netherlands

Members of the committee:

Prof. dr. S.J.M.H. Hulscher	Head of the committee, University of Twente
Dr. J.J. Warmink	Supervisor, University of Twente
A. Mol	Supervisor, De Vries & Van de Wiel
Ir. M.R.A. Gensen	Committee member, University of Twente

ACKNOWLEDGEMENTS

This report is the result of my Master Thesis for the Master in Civil Engineering at the *Universitat* Politècnica de Catalunya (UPC). The project was performed at the University of Twente, in collaboration with De Vries & Van de Wiel (DEME-Group), during an academic Erasmus Exchange. Therefore, it represents the culmination of my academic life, which I can gladly say that not only took place in Barcelona but also in Milan, Italy and Enschede, The Netherlands.

Writing this master's thesis gave me the opportunity to get an insight on the hydrodynamic and morphodynamic processes and river configuration of the Netherlands and allowed me to discover a whole new engineering world under the rivers' water surface. The realization of this work could not have been possible without the help of many people whom I would like to thank. First, I need to thank the University of Twente for accepting me and treating me as one of their own and De Vries & Van de Wiel for giving me the possibility to work with them on this project. Therefore, I am grateful to my daily supervisors, Jord Warmink and Arjan Mol, for their guidance throughout the past 9 months, Suzanne Hulscher for her knowledge on the topic and feedback, and to all the actors in both institutions involved in the project, who agreed on having meetings and giving me all the information I needed.

Undoubtedly, nothing of this would have been possible without the help and support of my family to which I am really thankful. They always believed in my abilities and offered me all the means to study whatever and wherever I wanted. During my stay in the Netherlands I had the opportunity to meet a bunch of new people from all over the world who encouraged me to keep on working. A special mention to the guys from room HT 307 and HT 305 who always gave me new ideas and recommendations for my work. To my closest friends in Barcelona (PDA crew), thanks for always listening to my civil engineering projects and stories even though you had severe struggles to understand it.

Last but not least, no words can thank the help I received from a man that was a total stranger 3 years ago. A man you can always call for help and he will be there no-questions-asked. Enric Consegal, ja saps que aquest treball no seria ni la meitat del que ha acabat sent sense la teva ajuda. Sincerament, totes les gràcies que et pugui donar es quedaran curtes. Gràcies per tot el feedback que m'has donat, gràcies pel suport moral durant tota la tesis i gràcies per, tot i ser a 700km de distància, poder ser un amic amb qui poder comptar sempre. Molta sort en la teva nova experiència al nou continent. T'ho mereixes.

And a big thanks to you, the reader. I hope you enjoy reading this report.

Alex Rojals Mainar
Enschede, July 2018

ABSTRACT

Located at the confluence of several major Western-European rivers flowing into the North Sea (Rijn-Maas-Scheldt delta), the flat and low-lying conditions of the Netherlands are suitable for the development of sand dunes. These bedform patterns vary both in spatial and temporal scales according to the hydraulic conditions and their continuous development and migration could interact with human activities. Being able to predict these riverbed patterns is of great importance for the maintenance of the minimum draught levels of rivers to ensure navigation.

The present thesis is a case study in the river system placed within the Rijn and Maas tidal areas (*West-Nederland Zuid)*. The project, in collaboration with the external company De Vries & van de Wiel (DEME-Group), aims to explore the characteristics and progression of the river sand dunes and develop a tool to forecast their morphological behavior. The approach is made by calibrating a dune evolution model to the area conditions. Forecasting solutions are presented for dune height and dune length development, as well as for migration rates.

The report follows a quantitative and qualitative research on the area. According to the model limitations, the study focuses on two different properties areas located at the Beneden Merwede (BEM) and the Boven Merwede (BOM), where sand dunes develop. The former comprises a straight river segment within a groyne field while the later lays at the inner bank of a river bend. Both areas present a predominant seaward uni-directional flow with diurnal discharge variations due to the perceived downstream sea-boundary tidal effects. A manually collection of the sand dunes' characteristics through consecutive survey periods allows to study the dunes' migration and growth rates, getting an insight on which and to what extent are the most important processes involved in their behavior patterns.

The dune evolution model of Van Duin (2017) is applied and calibrated in both areas, capable of reproducing the observed dune heights development. Nonetheless it fails to properly predict the hydrodynamics and underestimates the water depths. The varying conditions in both areas resulted in two different models and scaling relations with slightly different parameters. The developed tool is capable to provide a range of possible dune heights and migration rates. A performance analysis determined that considering monthly averaged discharges the models still predict a proper dune development. The particular characteristics of BOM suggest that its final calibrated model is very specific to the area, limiting its use to other non-equally locations, whereas the more common and englobing characteristics of the BEM area make its supposition and incorporation into the rest of the project area more feasible.

CONTENTS

LIST OF FIGURES

LIST OF TABLES

1. Introduction

River sand dunes are of great importance for the determination of the commercial draught levels of rivers. The flat and low-lying conditions of the Netherlands are suitable for their development. While it is the place of confluence of several major Western-European rivers, flowing into the North Sea (Rijn–Maas–Scheldt delta), the country has a long history of adapting the natural water and river systems to user functions, resulting in a highly developed water infrastructure and an extensive network of inland waterways which serve the commercial shipping needs. Therefore, the system requires periodical maintenance to ensure a proper commercial service.

Those rivers and watercourses respond to dynamic processes and due to the sandy composition of the largest Dutch rivers, a series of bed patterns are formed resulting from an instability on the interface of the mobile sandy bed and water flow. This instability is responsible for sediment transport gradient and the development of different bedforms such as ripples, dunes and bars (Kennedy & Odgaard, 1991). In many rivers, dunes are the dominant bedforms; river sand dunes are asymmetrical flow-transverse bedforms, whose steep face points downstream and migrate slowly downstream. They form during lower regime conditions, Froude number, *F*, below one, and they are associated with river surface fluctuation out of phase with the bed fluctuations. They are found in beds with sediment sizes ranging from medium sand to gravel, from 0.2mm to 30mm (e.g. Van den Berg & Van Gelder, 1993; Kostaschuk, 2000; Best, 2005). Their height is in the order of 10 to 30% of the water depth and their length (distance between two consecutive crests) is approximately 10 times their height (e.g. Van Rijn, 1984).

Sand dunes and superimposed ripples, vary in both spatial and temporal scales, splitting and merging (e.g. Paarlberg et al., 2010; Warmink et al., 2014; Naqshband et al. 2014), and their continuous development and migration could interact with human activities e.g. uncovering pipelines or other constructions beneath the river bed or affecting on the navigation draft of rivers. For it, maintaining a minimum water depth is crucial to satisfy navigational purposes, being able to identify and predict the critical locations of these bed patterns and their associated morphological time scale for dredging operations.

Hence, a lot of research has been done to model the sediment transport and predict the development of sand dunes, from equilibrium state formulations (e.g. Yalin, 1964; Van Rijn, 1984) to more complex dynamic processes models (e.g. Paarlberg, 2009; Nabi et al., 2013). New principles are continuously found or understood through flume and field observations, such as flow separation (Paarlberg et al., 2007) and dune interactions mechanisms (Gabel, 1993; Martin & Jerolmack, 2013). However, the origin, development and dynamics of sand dunes are far from being fully understood.

1.1. Case description

The present thesis is part of a project in collaboration with the external company De Vries & Van de Wiel (DEME-Group). De Vries & Van de Wiel is responsible for the maintenance of several river branches (contract areas) in the Rijn-Maas Delta by ensuring minimal draught levels for navigation. Figure 1 gives an overview of these different contract areas. By combining measurements and model forecasts, De Vries & Van de Wiel tries to get more insight in the morphological behavior of the river system so dredging activities can be optimized. Since the characteristics of river dunes significantly influence the draught level in a river, the understanding of their behavior plays an important role. Therefore, the study focuses on a river system comprising the following rivers:

- Amer
- Nieuwe Maas
- Hollandsche IJssel
- Lek
- Noord
- Boven Merwede
- Beneden Merwede
- Nieuwe Merwede
- Hollandsch diep
- Bergsche Maas
- Oude Maas

The area is mainly dominated by the discharges at the river Waal, the river Maas, the river Lek and the tidal influences at the downstream sea boundary. Daily tide effects are visible up to the conforming upper boundaries at the measuring stations at Tiel at the river Waal, Hagestein Boven at the river Lek and Megen at the river Maas. Therefore, the tidal impacts are perceived in a higher or lower intensity all over the area. The more downstream, and so the closer to the sea boundary, the more discharge variations due to tidal inflow (flood) and outflow (ebb) currents in the delta, which along with low upstream river discharge quantities may result in reverse flow at the most downstream locations.

De Vries & Van de Wiel performs forecast predictions of the hydrological and morphological processes of the complete extension using a Delft3D model. The model uses a coarse grid and the characteristic discharge climate for the actual considered months, being only able to predict large-scale morphological development. Hence, small-scale patterns such as sand dunes are not taken into account. Nonetheless, there is a lack of short term river dune evolution predictions under realistic varying discharge waves, for which a thorough study of the sand dunes dynamics in the area is needed.

The availability of bathymetric data corresponds to past surveys carried out by De Vries & Van de Wiel, starting in the first quartile of 2016. The time period between survey campaigns may vary depending on the relevance and hinders of the area, being 3 months apart on average. When dredging operations take place in an area, surveys are held before and after the works. The specific hydrological data for each location, needed as inputs for the model, e.g. discharge, water depth, water level and flow velocities, are obtained after 37 model runs with pairs of varying upstream discharge conditions at the river Waal (Tiel) and the Maas (Megen).

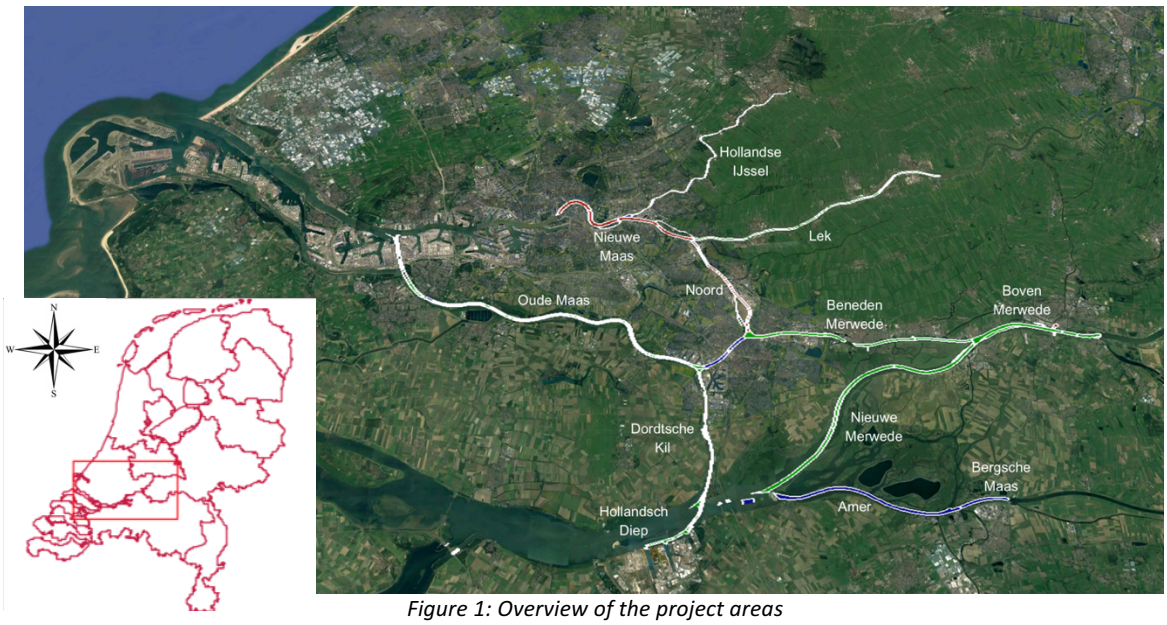

Figure 1: Overview of the project areas

1.2. Theoretical background

Under unidirectional predominant flows, river dunes exhibit an asymmetric shape in the downstream direction, with a gentle stoss side and a steep lee side after the crest. The resulting river surface is out of phase with the bed fluctuations. The water level is high at the troughs and low at the crests. Therefore, the flow is accelerated as it goes up the stoss side of the sand dune, reaching maximum depth-averaged velocities at the crest. Recirculating eddies can develop at steep lee sides of dunes, resulting in a flow separation zone where flow rotation and reverse circulation can be found (Paarlberg, 2009; Warmink et al., 2014).

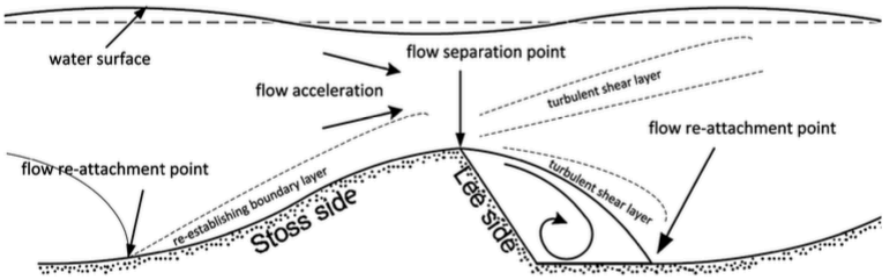

Figure 2: Flow dynamics over a dune with emphasis on flow separation. Source: (Warmink et al., 2014).

Dunes develop or degrade due to the combined erosion and sedimentation processes. Resulting from the time-dependency of dune evolution to adapt to the changing flow conditions by means of sediment transport, their development is delayed relative to changing discharges, leading to a hysteresis in dune properties against water discharge. (e.g., Ten Brinke et al., 1999). Differences in dune height can be identified for the equal discharges in the rise or fall stages of the flood wave, see Figure 3, bottom plot. Dunes continue to develop about 20% in height after the peak discharge.

Hysteresis effects can also be found when plotting the water levels against the discharge (Figure 3, upper plot). These effects are attributed to the accelerations and decelerations during the passage of a flood wave and to the time-dependent dune evolution and the coupled changing bed roughness during the flood event.

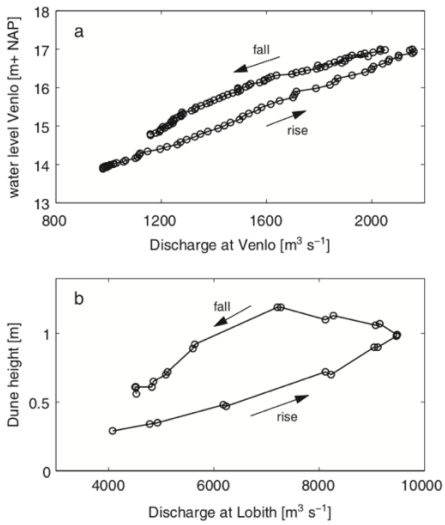

Figure 3: Hysteresis in water level and dune height for floods in the River Meuse at Venlo and River Rhine near the Pannerdensche Kop, respectively. Source: a.(Termes, 2004), b.(data from Directorate Eastern Netherlands (DON) and the Head Office of Rijkswaterstaat))

Within a river bed, sand dunes with different dimensions, lengths and amplitude, coexist and interact. Dune comportment mechanisms are governed by dune amalgamation, superposition and splitting (Gabel, 1993; Martin & Jerolmack, 2013). The presence of superimposed small river dunes on larger dunes, which migrate at higher velocities than the host dunes, are responsible for trough filling and merging of dunes, as well as dune splitting due to the flow separation zone.

1.3. Research Gap

River sand dunes are highly dynamic and show a complex behavior evolution. A single dune grows or decays according to the flow characteristics. Additionally, the flow and the dune behavior is affected by the interaction between surrounding dunes and the superimposed ripples or small perturbations upon them. The approach used by De Vries & Van de Wiel do not take into account these small-scale morphological developments. Instead, by using the Delft3D model, the large-scale bathymetry changes are predicted and added to the the actual measured river bed. By doing so, sand dunes and other detailed features come back in the forecast as they were present in the initial measured bathymetry, although their morphological development is not predicted by the model.

To fill the gap in De Vries & Van de Wiel's methodology, the morphological single dune model of Van Duin (2017) is presented. The model will be calibrated to the observed dunes' behavior in order to provide the expected dune characteristics in a future scenario. The two models are meant to be used separately. Therefore, the results out of the new tool are to be included to the main model as additional information of the estimated changes on the sand dunes characteristics.

1.4. Research Objective & Questions

The objective of this research is:

To develop a tool for the prediction of the dynamic behavior of the sand dunes within the Dutch river system in the Rijn-Maas Delta (De Vries & Van de Wiel contract areas, West-Nederland Zuid).

In order to be able to achieve the objective, three different steps in form of research questions are formulated:

1. *Which are the most important areas for the development of sand dunes?*

Not all river branches comprised in the river system present the same conditions (discharge, tidal influences and reverse flux, bed slope or grain size). Therefore, not all rivers are likely to develop significant sand dunes of considerable characteristics for the purposes of this thesis. In order to determine which are the most vulnerable areas of the project extension, the riverbed bathymetry obtained from past survey measurements will be analyzed detecting the presence of these features.

2. *What are the most important processes involved in dune characteristics and behavior?*

Within the selected study areas, the resulting dune characteristics for each of the survey periods will be collected and analyzed. Moreover, comparing consecutive survey periods data put against the particular discharge for that period, the most influent parameters in dune growth (in height and length) and migration will be determined.

3. *To what extent can a dune evolution model simulate the observed dunes' behavior?*

The previously examined dune dynamics of each study area and for each of the survey dates, will serve as reference dune attribute levels to which calibrate and validate the dune evolution model. The forecasted results will require to fit in the defined intervals of the dune height, length and migration observed with the surveyed data.

1.5. Methodology

In this section, the methodology that will be applied and the necessary steps in order to solve each research question are presented.

The first part of the research (Research Question 1) consists on the determination of the main areas where significant accumulations of sediment occur, in the form of sand dunes, followed by a selective analysis of these bed patterns evolution. This will lead to the understanding of the hydrodynamic characteristics and river bed morphodynamics seen around the project extension. Therefore, this first enquiry will serve to identify the locations in which sand dunes develop.

The analysis on the complete area will focus on past survey data of river bathymetry and flow characteristics, concerning discharge quantity, water depths and flow velocities as well as the flow predominant direction. Riverbed levels will be plotted by making use of contour line plots with MATLAB, from which two main sand dunes field areas will be distinguished and selected. The area selection strategy follows criteria in which areas will be quantified in terms of availability of different surveyed time-periods, dune presence and changes in time.

Previous or expected dredging operations enhance an additional interest on the area. Due to the model's limitations, areas presenting reverse flow due to the tidal influences will not be considered. Selected areas will have different characteristics in order to extend the analysis from different approaches. After the area selection, various longitudinal profiles will be traced covering the region extension, from which significant dunes with potential to develop and surpass the minimum contractual river draft will be chosen and tracked. In the absence of an accurate tool to gather the dunes' data, their characteristics will be manually collected.

Different consecutive surveys will be compared to be able to analyze the behavior throughout time of the bed patterns and the determination of dune characteristics such as dune dimensions, dune growth and migration rates for each of the study areas. An exhaustive analysis of the obtained data will follow (Research Question 2) in search for relations and trends between different dune parameters. The dune parameters (dune height, length, steepness, migration and growth) will also be related to the previous discharge conditions to get more insight in the dune forming processes.

Furthermore, using the Van Duin (2017) model the observed behaviors are intended to be reproduced (Research Question 3). The dune evolution model will be calibrated upon dune height. The morphological conditions, bed slope, *i*, and grain size, d_{50}, are spatially dependent and exact data for each area is often a constraint, resulting in an interval of possible values. After, a sensibility analysis of the model's performance will be done based on changing the parameters. From this analysis the most extreme morphological conditions will be modelled as upper and lower range bounds of simulated values, which would be validated with respect to the bandwidth covered by the standard deviation of the mean of observed dunes heights for each period $[\mu_i - \sigma_i, \mu_i + \sigma_i]$, including 68.2% of the data. Given the lack of the model to provide accurate migration rates, another approach will be suggested to obtain a reasonable range of results fitting the analyzed survey data.

The model is meant to be used to predict future scenarios (with stochastic forcing discharges) to which the exact discharges are unknown. Therefore, a final model performance analysis will be held in which the considered discharge quality will be lowered by (1) applying larger block-averaged periods or (2) supposing more general data following the most frequent discharges per month after a long-term timeseries data set. For each of the discharge scenarios, the coverage and accuracy to the surveyed data for the resulting intervals of possible values for dune height will be compared.

2. Selection of the most important areas for the development of sand dunes

The extensive river system area, located within the Rijn and Maas estuaries and the Rotterdam Harbor, is mainly dominated by the upstream discharges at the river Waal, the river Maas and the river Lek and the tidal influences at the downstream sea boundary. Tidal effects are shown to spread up to Tiel, at the river Waal, up to Hagestein at the river Lek and up to Megen at the river Maas. Therefore, the effects are seen all over the area. The more downstream, and so the closer to the sea boundary, the more discharge variations are found within a day due to the tidal flood and ebb (inflow and outflow) currents. Under low river discharge conditions, the most downstream areas can even show reverse flow.

If reverse flow conditions are met, it can affect the sand dunes' shape, which present an asymmetric configuration with a gentle stoss side and a steep lee side, pointing and moving streamwards. Consequently, a bidirectional flow may disturb their growth development and migration.

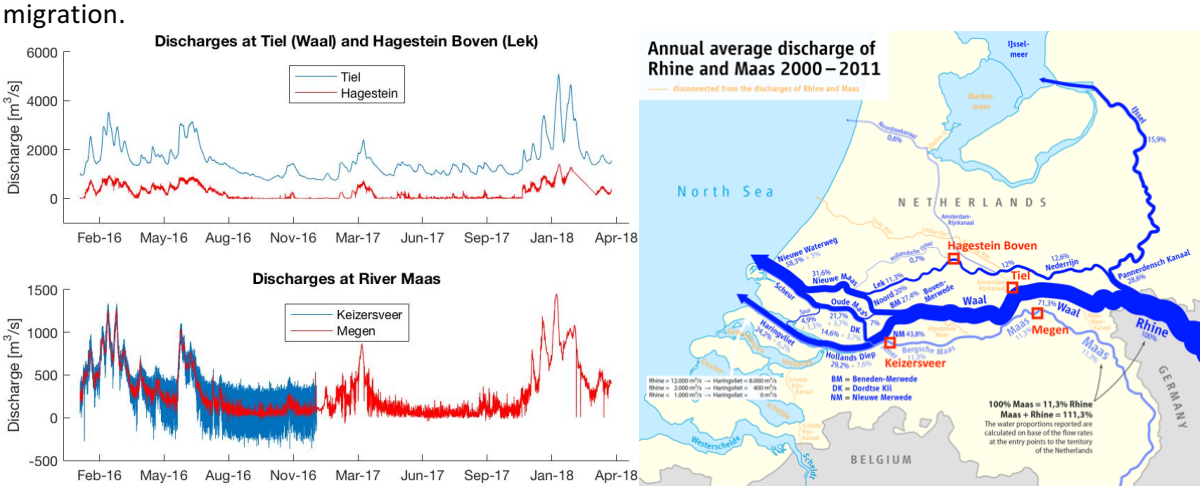

Figure 4: Measured discharges for the studied period at river Waal (Tiel), Lek (Hagestein Boven) and Maas (Megen and Keizersveer), and averaged discharge distribution for the Rijn and Maas rivers, source: (Dörrbecker, 2018)

The observed discharges at different measuring stations (Figure 4, left), provided by *Rijkswaterstaat*, clearly show the consequences of the different upper and bottom boundary conditions on the area. The river Waal and the river Lek present similar discharges, not in quantity but in shape, with clearly large discharges at Tiel (Waal) and lower flows in Hagestein Boven (Lek river), as both being distributaries of the Rijn river (see Figure 4 right). Small amplitude sinusoidal variations due to the tides at the North Sea can be seen in Hagestein Boven, which are not as visible at Tiel, as a result of the lower upstream discharges. When considering the two discharge points at the river Maas, the same principle of counteraction of flood tidal currents and upstream river discharge is found, observing sinusoidal tidal effects during low discharges at Megen, even concerning negative discharges and therefore reverse flow. Moreover, the closer to the sea, that is, the more downstream, the major is the effect of tides. The effect of tides causes larger amplitude discharge variations in Keizersveer (Amer) involving the same upstream river discharge conditions as in Megen.

These tidal current consequences on the predominant discharge flow are also perceptible when observing the river bed in different time periods. A comparison of two different contour line maps of the surveyed bathymetry depth in a downstream location at the river Lek near Schoonhoven, shows the shape-changing behavior of sand dunes when the predominant flow is reversed. The first surveyed data is from the 11th January 2016, right at the beginning of the wet period, while the second bathymetry data was collected after the wet period on the 2nd July 2016. Particularly, the first survey corresponds to a period with low river discharges during the previous days (late 2015), which added to the large tidal influence due to the downstream location of the area, it shows intermittent reverse flow conditions.

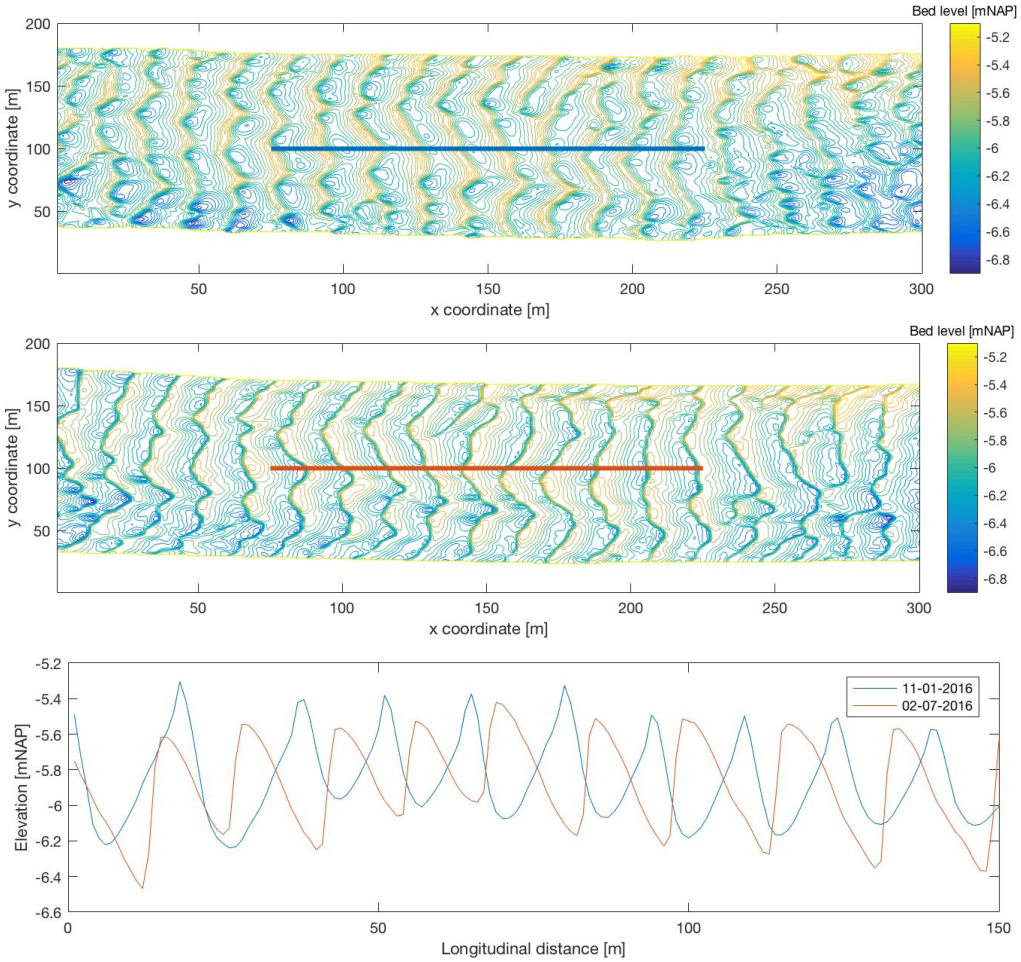

Figure 5: Contour lines of the river bed at Lek near Schoonhoven for the 11-01-2016 (above) and 02-07-2016 (below) and longitudinal profiles. Predominant flow from right to left

Figure 5 shows for both time periods different visible stripes defined by close contour lines, which clearly outline the crests of the sand dunes. At one side of the crests, the contour lines appear more spread out, delimiting the low steep dune stoss side. On the other edge, the lines are closely distributed which remark a steep slope area, the dune lee side. During the first survey, sand dunes look more asymmetric and pointing to the right (upstream) due to the tidal reversing effects on the predominant flow during the previous days, while on the lower plot these features are shown to be downstream pointing and complete asymmetrical.

2.1. Areas selection

As observed in Schoonhoven, the contour conditions are totally variable in time, but also in space within the complete extension of the contract areas. Not all rivers present the same flow conditions, nor all rivers have the same bed sediment characteristics, resulting in different morphodynamics. Therefore, not all rivers are likely to develop sand dunes. A closer look in the area would lead to the understanding of the hydrodynamic and morphodynamic processes, giving the possibility of disregarding much, or complete, of the rivers' data and select the most important areas for the appearance of sand dunes for a further analysis.

Due to the incompatibility of the chosen river dune evolution model to considerate reverse flow, the model will be used as a tool to provide a future prediction of these bed patterns behavior only in uni-directional predominant flow areas which present asymmetrically downstream pointing sand dunes. Accordingly, by analyzing past surveyed data from all rivers' bathymetry, provided by *De Vries & van de Wiel*, and by evaluating the upstream river discharges at Tiel (Waal), Megen (Maas) and Hagestein Boven (Lek) measuring stations, as well as the predicted Delft3D model outputs for every

specific area, both provided by the *Watermanagementcentrum Nederland (WMCN)* of the *Rijkswaterstaat*, smaller study areas will be selected according to the following criteria:

Criteria to identify study areas:

- Availability of river bed surveyed data (number of different time-periods)
- Recognition of large (in height and length) sand dunes potentially relevant to be dredged
- Dynamic behavior in time and space of sand dunes (dune height and length, growth and migration rate)
- Asymmetric and downstream pointing sand dunes. Avoiding areas with reverse flow
- Previous or expected future dredging operations (identifying problematic areas)

Studied areas

The seven initial contractual areas in which sand dunes where found are shown in Figure 6.

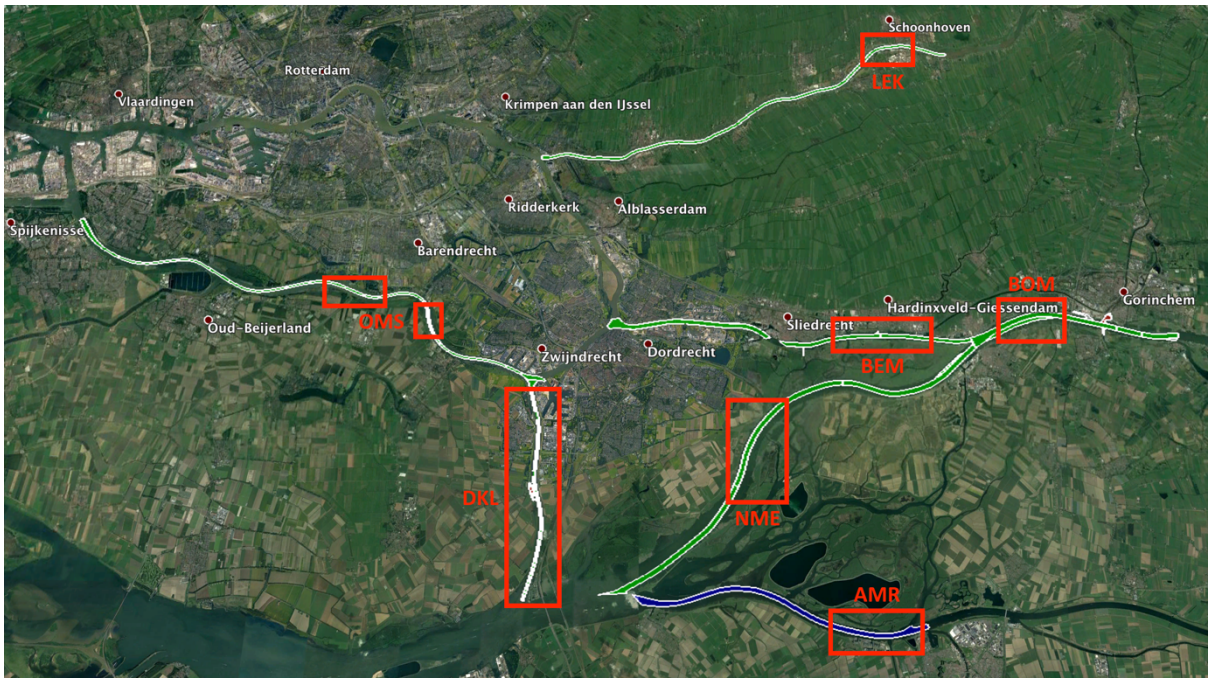

Figure 6: Overview of the studied contractual areas and their main location presenting sand dunes

Multiple contractual areas presented the formation of sand dunes. Nevertheless, dunes do not develop in all the extension of the area so their most predominant sand dunes areas are highlighted. Table 1 reflects the characteristics of each area following the selection criteria.

Table 1: Studied areas presenting sand dunes and their fit in the selecting criteria

Study Area	*Reverse flow*	*Significant (in height) dunes*	*Dredging nearby*	*Availability of data*
BEM (Boven Merwede)	Yes, but predominant downstream flow	Yes	No	High
AMR (Amer)	Yes, but predominant downstream flow	No	No	High
BOM (Boven Merwede)	No	Yes	Yes	High
DKL (Dordtsche Kil)	Yes	Yes	Yes	High
LEK	Yes	No	No	Low
OMS (Oude Maas)	Yes	Yes	No	Medium
NME (Nieuwe Merwede)	No	No	No	Medium

BEM and BOM areas are selected as they fit in the selecting criteria. Both areas present different characteristics, as seen in Table 2, which involve dissimilarities in the hydrodynamics. These

differences allow to extend the analysis and the model application from two diverse approaches.

Table 2: Generic characteristic of each selected area

Overview	*Area 1: BEM*	*Area 2: BOM*
Location characteristics	Straight river segment (center)	Curved river segment (inner bank)
Number of time periods	8	9
Number of profiles	3 (15m apart)	5 (30m apart)
Longitude of profiles	2680 meters	1404 meters
Unidirectional flow	No but predominant unidirectional flow	Yes
Dredging nearby	No	Yes

Area 1: Beneden Merwede (BEM)

The first selected study area is located in the upstream part of the Beneden Merwede (km 964-966). It comprises of a practically straight river segment 2680-meter-long, delimited both sides within a groyne field, with groynes spaced every 250 meters. Sand dunes of not more than 1.5 meters high and 80 meters long are spread out all over the center of the rivers width. There is a vast amount of surveyed measurements for this area, with 8 different time-periods comprising from the 25th of February of 2016 to the 9th of March of 2018.

The groyne field characteristic of this segment, clearly visible with the lateral scour holes at the heads of each groyne (Figure 8), added a last relevant point for the selecting criteria. The groyne field provides a more stable flow in the center of the channel, ensuring that the transversal sand dunes crests would migrate almost perpendicular to the river course. Nevertheless, to guarantee that possible secondary flows do not affect the measured data, 3 parallel and 15-meter apart profiles were drawn from the center of the water way, in order to get bathymetric profiles while enabling the possibility to analyze each dune behavior from different lineal observations (Figure 9). With this 3-way approach, the above mentioned possible local imperfections, which could alter the profile observed dune shape, will be surpassed. As the area presents standard flow characteristics controlled by groynes and a regular bathymetry along the width, considering width-averaged discharges and water depths will suppose a good approximation.

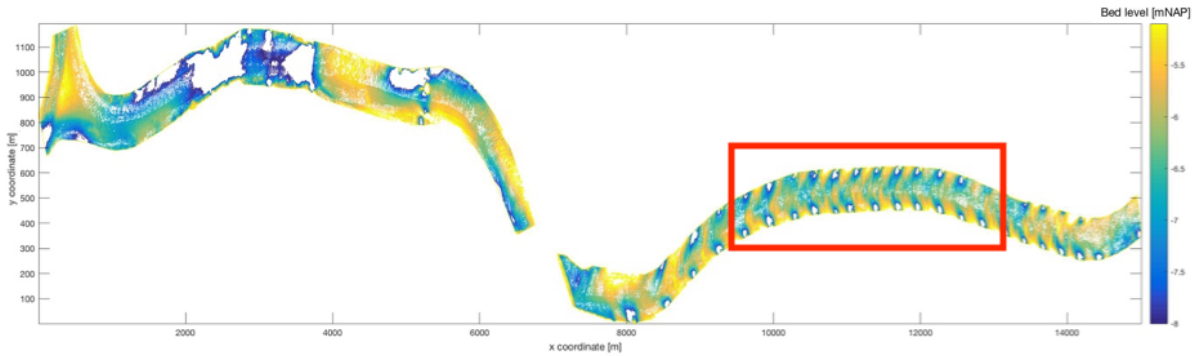

Figure 7: Overview of the bed level in 27-02-2017 and the selected area. Contour lines in mNAP. Flow from right to left

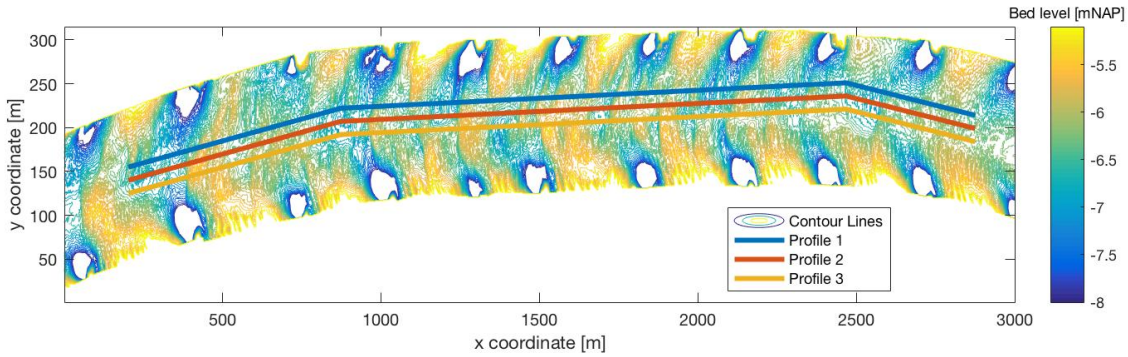

Figure 8: Selected area and defined profiles. Contour lines in mNAP

Note that all vertical axes have been exaggerated with respect to the horizontal axes.

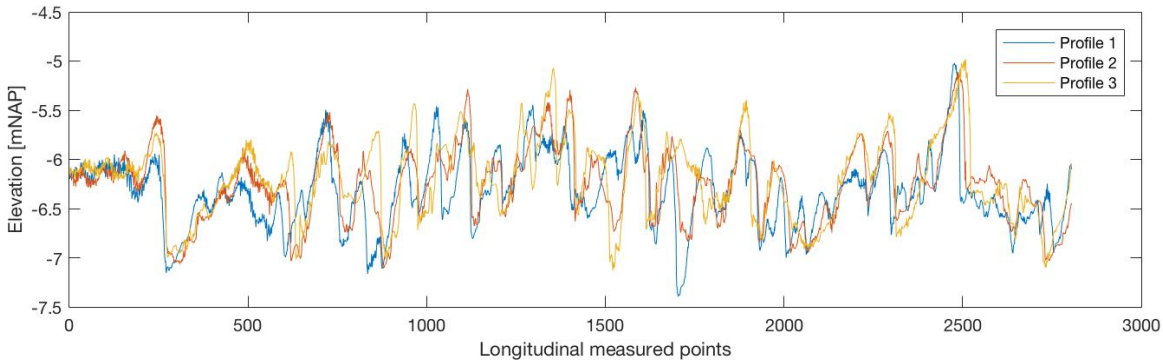

Figure 9: Superposition of the 3 profiles. Flow from left to right

Moreover, the discharge outcomes of the model provided by *Rijkswaterstaat* display that the tidal effects in the area propitiate negative discharge values for a short period a day (Figure 10). These negative discharges are shown to reach up to 700m^3/s during the lowest upstream discharges at Tiel in dry periods. A quick application of the Shields formulation for the determination of the beginning of motion of the bed material, reveals that for the area characteristics the occurrence of sediment transport ($\tau_b > \tau_{crit}$) starts around discharge values higher than 400m^3/s. However, the majority and predominant flow is unidirectional and positive. Negative discharges are found on a year-average for 2.5 hours each tidal period and reverse flow values larger than the threshold of 400m3/s take place during 2 hours in the worst scenario. Therefore, the area was not disregarded. Additionally, by observing the different time-periods profiles, sand dunes show a natural asymmetric shape with a stoss and lee side pointing downstream in all of them, as it would be expected for a constantly unidirectional flow.

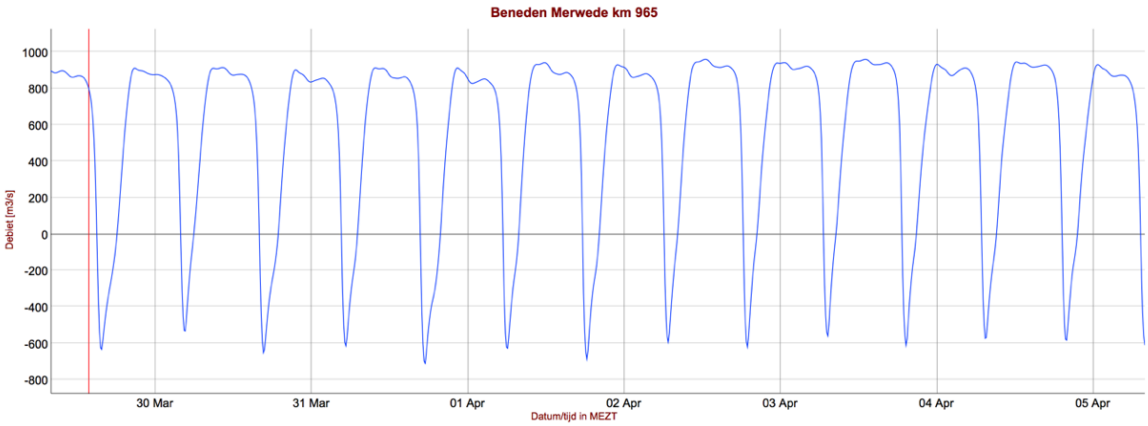

Figure 10: Model predicted discharges at the BEM area

The model simulated discharges shown in Figure 10, presenting an averaged maximum negative discharge of 600m^3/s, which correspond to a period in which the measured flow in Tiel was 1500m^3/s. The same discharges were evaluated at the BEM area from June 30th to July 2nd of 2018 which showed negative discharges slightly exceeding 700m^3/s. During that period, the discharges at Tiel were around 1100m^3/s. An overlook on a long timeseries measurements at Tiel reveals that the averaged minimum discharges have an approximate value of 1000m^3/s. Therefore, estimating the most negative discharges as 700 m^3/s is presumed as a good approach. Nevertheless, for a better accuracy more data during low upstream discharges should be compared, which was not available at the moment.

Area 2: Boven Merwede (BOM)

Alternatively, a second area was chosen upstream of the preceding with comparatively different characteristics, located in the lowest part of the Boven Merwede (km 958-960). In the zone, sand

dunes appear to be slightly lower than 1 meter in height and on average 70 meters long, and their crests are completely oblique to the river course. 9 different time periods surveyed data are available for this region, starting the 29th of February 2016 until the 22nd of January 2018.

The selected area is found on a river curve (Figure 11), meaning that the hydrodynamics are much more complex as secondary flow is generated, making it an interesting area to study the sand dunes' behavior and to simulate it with a 2DV dune model which cannot directly take into account this phenomenon. The characteristic clock-wise helical flow pattern drastically influences the dispersion of suspended or dissolved matter. In addition, the bed topography in a bend often differs strongly from the one in a straight reach such that it can even become limitative to the navigability of the river (De Vriend, 1981). This phenomenon produces a displacement of the talweg towards the outer bank of the curve, and a zone of deposition in the opposite bank, as seen in Figure 11. For that, dredging operations took place 3 times within the last 2 years (Table 3) in the shallowest area used as a mooring area, off-limits of the commercial navigational path but within the contractual limits, named Ankervak.

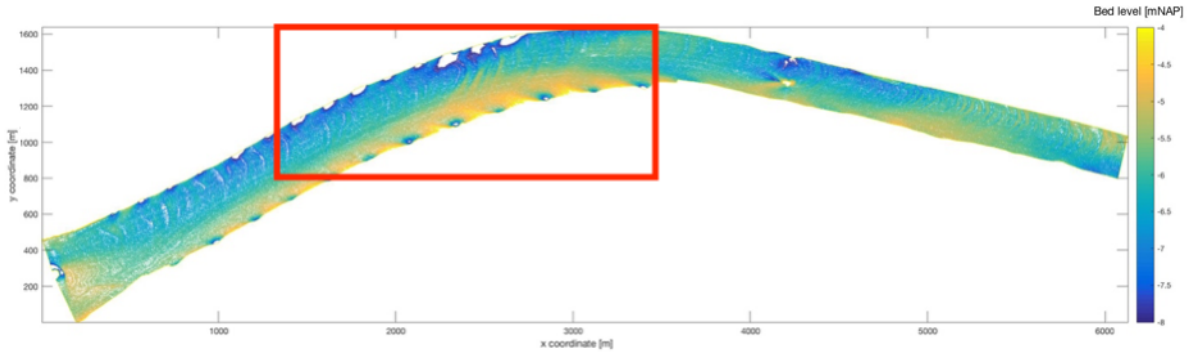

Figure 11: Overview of the bed level in 29-02-2016 and the selected area. Contour lines in mNAP. Flow from right to left

Table 3: Dredging in the Ankervak area

Day	Initial volume (above contractual depth) [m^3]	Final volume [m^3]
05-Apr-2016	4183	26
29-Sep-2016	3086	67
15-Feb-2018	3495	679

Given the particular characteristics of the area and the obliquity of the sand dunes, 5 different profiles of 1404 meters long were drawn from the shallowest inner bank to the center of the river width, spacing each other 30 meters (Figure 12 and Figure 13). The profiles cover the shallowest area, potentially critical to develop sand dunes above the contract threshold depth. Aware of the particular flow and bathymetry along the width of the river bend, the consideration of width-averaged discharges and water depths in the model will suppose an overestimation of the dunes characteristics for the inner bank and shallow considered area.

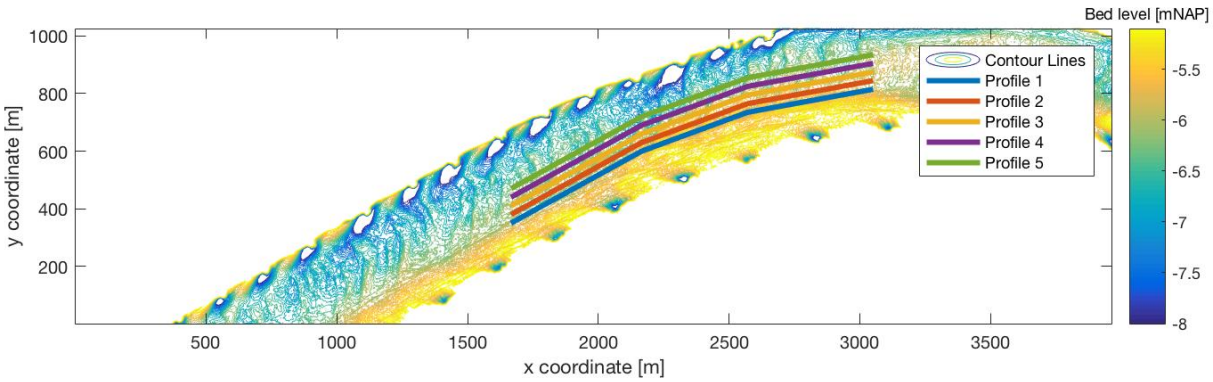

Figure 12: Selected area and defined profiles (09-05-2017). Contour lines in mNAP

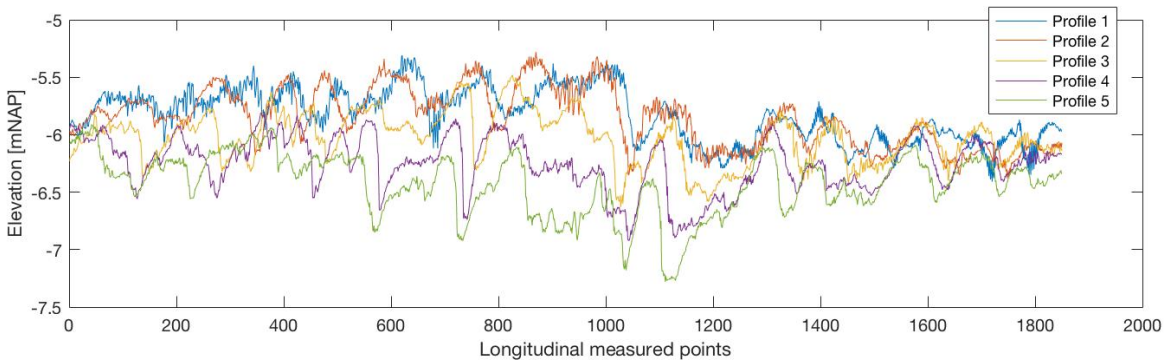

Figure 13: Superposition of the 5 profiles. Flow from left to right

Additionally, the model output discharges (Figure 14) show that there is a large daily variation on the area due to the tidal currents at the downstream boundary of the system. Nevertheless, the great amount of water coming from upstream prevents reverse flow.

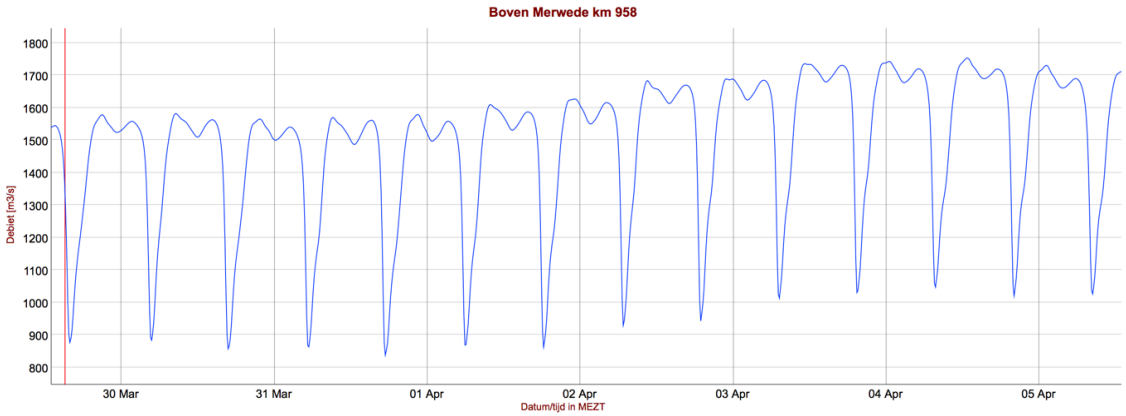

Figure 14: Model predicted discharges at the BOM area

The above shown simulated discharges at the BOM area correspond to a period with measured averaged discharges at Tiel of 1500m^3/s. Other low upstream discharge periods were evaluated and no negative discharges were observed at the BOM area.

2.2. Dunes selection

After extracting every profile for each of the time steps, all the dunes information needed to be extracted. The collected data consisted on dune crest position and height, as the highest point of the dune, and both front and rear through position and height as the minimum points, with which dune height and length and dune migration and growth between periods could be calculated. Dune height, *H,* was extracted as the value from the crest to the closest through, while dune length *L* was supposed as the horizontal distance between troughs (see Figure 15). On the other hand, dune migration was computed as the difference in crest position for the same tracked dune from one period to the consecutive surveyed data, and dune growth as the difference in dune height for each single dune for consecutive surveys.

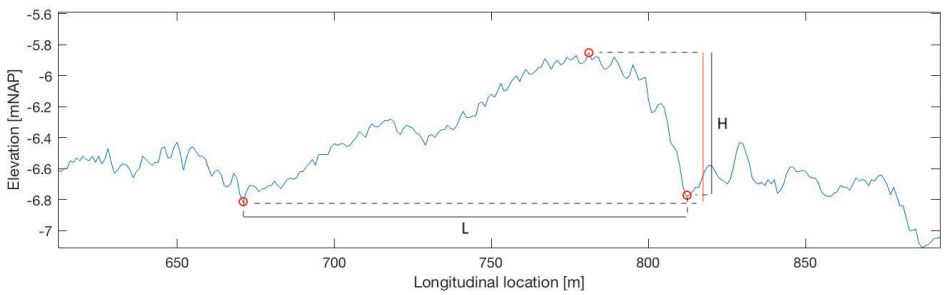

Figure 15: Sketch of dune characteristics (H and L) extraction. Dune D3.1 at the BEM area on Feb-17 shown as example

Given the irregularity of the riverbed, accounting with areas of deposition or erosion and therefore, higher or deeper parts than the depth given by the bed slope, no automatic tool to detect and collect the dunes (e.g. Van der Mark & Blom, 2007) was able to be used properly. The tool developed by Van der Mark & Blom (2007) is mainly based on the detection of the number of times the signal crosses the average height line to recognize the dunes. So eventually, the small amplitude ripples and the uncertainty of the survey method resulted in noisy bathymetric signals, what hinders the detection of proper dunes by implementing the said tool. Therefore, sand dunes were finally selected manually by following the succeeding criteria:

Criteria to select the dunes

- Only average to high dunes, according to de Vries & Van de Wiel's interests on the most problematic dunes
- Easily recognizable in all the profiles, avoiding lateral inclusions of other oblique dunes
- Easily recognizable in all the time periods
- Easy to follow from the first time-step to the last one or for as many periods as possible
- Avoiding, if possible, dunes that split or merge in order to be able to calculate migration and growth rates for the corresponding dune

This resulted in the selection of 10 different dunes for the BEM area and 10 dunes for the BOM area, which were identified, followed and tracked to obtain their behavior. Figure 16 presents a visual example of the chosen dunes for each area's middle profile. Note that not all dunes where possible to track for all periods and profiles.

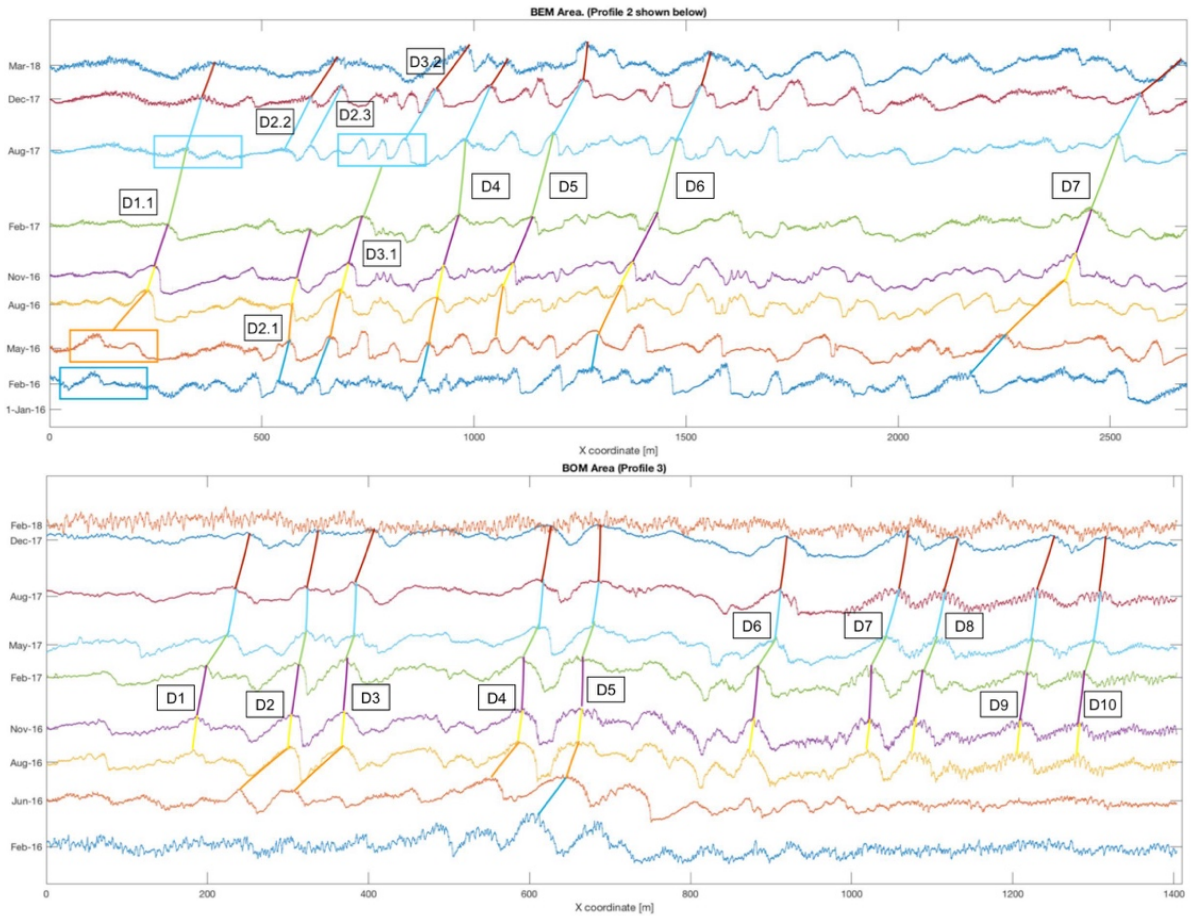

Figure 16: Dunes selection and tracking for BEM area (top) and BOM area (bottom). The D denotes the identified dunes

It is important to remark that for the 9th and last period of the BOM area, the bathymetry presents a very flattened and noisy signal, not linkable to ripples or other superimposed smaller-scale bed patterns. Therefore, due to the difficulty in determining the shape of the dunes, this time period was discarded. Moreover, the first profile for the BOM area, which was also the closest to the left bank and the *Ankervak* deposition area, presented flattened profiles in every time period so it was also rejected, ending with a total of 8 corresponding survey periods for each area and 3 and 4 profiles for BEM and BOM areas, respectively. Therefore, a maximum of 3x10 dunes and 4x10 dunes considering all the profiles were tracked for BEM and BOM, for each of the 8 time periods. However, not all dunes were possible to be followed in all the profiles or surveys and periods present a lower number of collected dunes (Table 4).

Table 4: Total number of collected dunes per time-period and area

Period	BEM	BOM
1	17	8
2	23	13
3	20	35
4	20	35
5	21	35
6	23	31
7	23	30
8	16	30

Unfortunately, the manual dune detection and data compilation procedure forced a larger criteria and a reduction of the selected data, for that cause some additional large dunes that did not meet all the requirements were left to track. Therefore, further studies should be supported by a more encompassing selective methodology, for which the only necessary criterion would be to focus on large and more stable dunes with potential to become a threat for the minimum contractual depth, and obviate smaller-scale dynamic dunes.

A range of observed heights and lengths of the sand dunes per each survey period and area are obtained. Below, Figure 17 for the BEM area and Figure 18 for the BOM area, display the boxplots of each survey data set distributed along the abscise axis according to the corresponding date in which the observation was made. On the same plots, the specific discharge found at each area is shown for a visual understanding of the dune height and dune length evolution. The exact values per each time-period data and their fit in a Normal Gaussian distribution can be found in APPENDIX A.

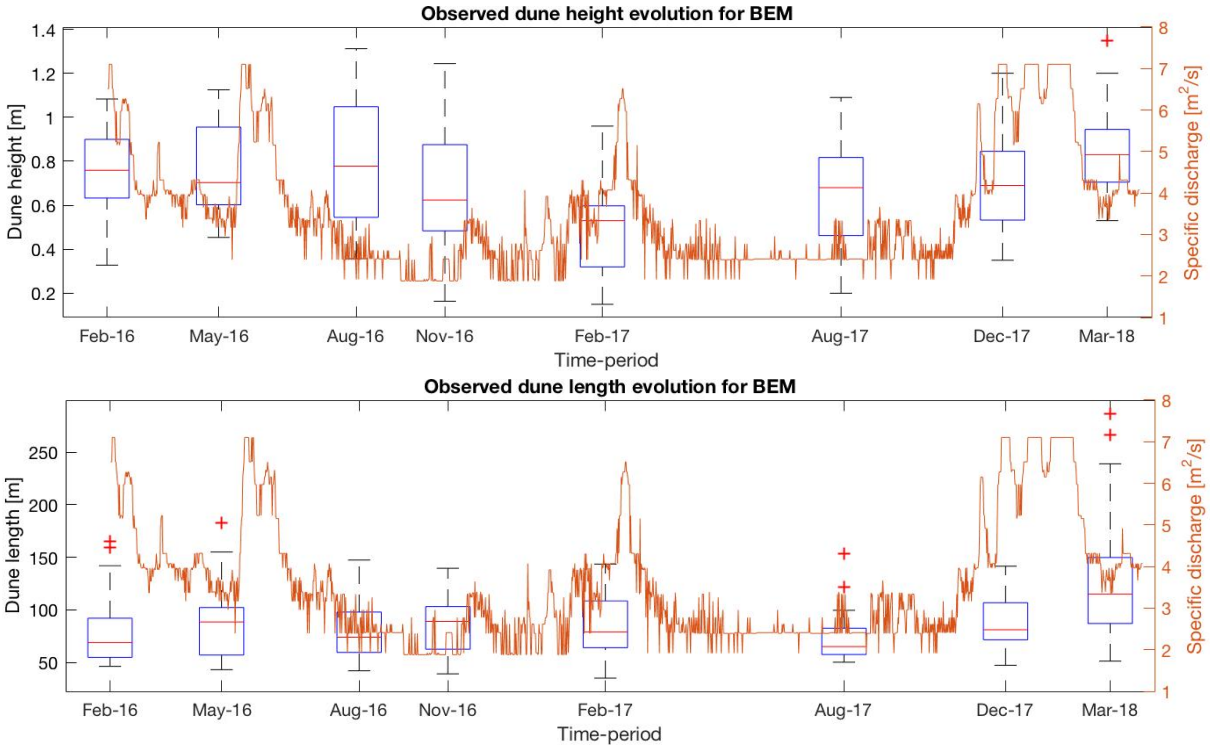

Figure 17: Surveyed dune height (top) and length (bottom) and specific discharge at the BEM area

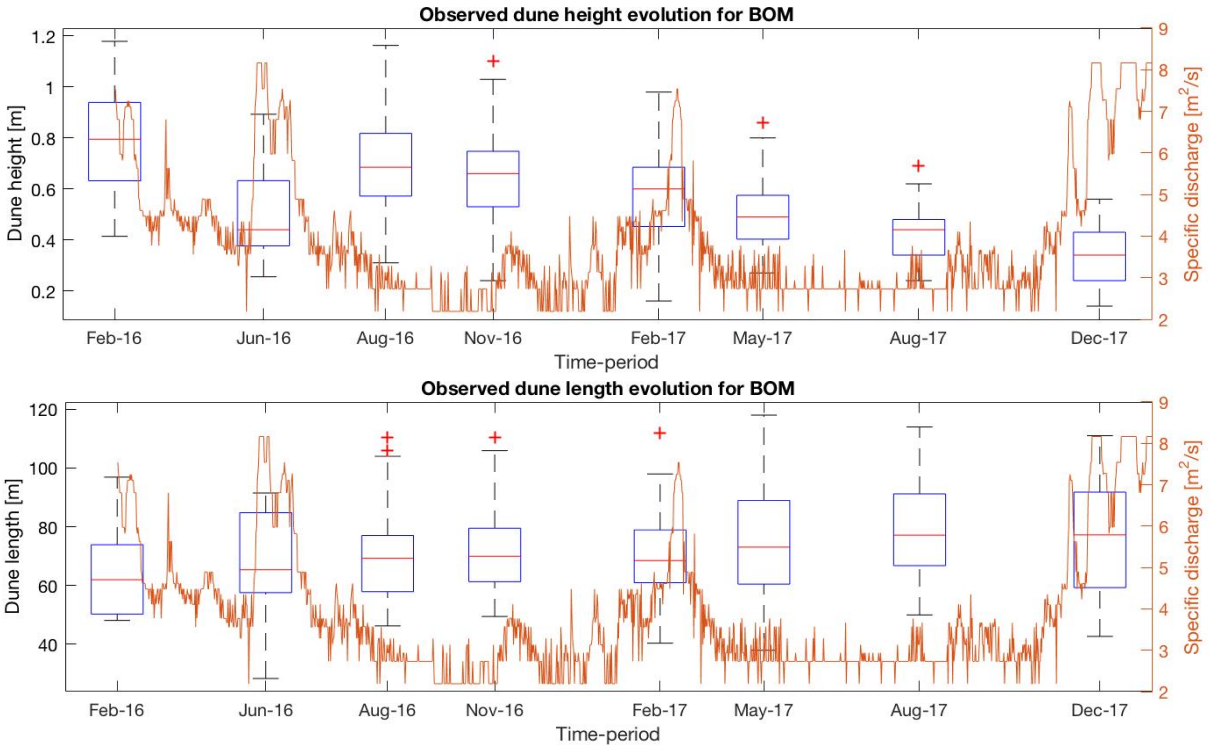

Figure 18: Surveyed dune height (top) and length (bottom) and specific discharge at the BOM area

3. Data Analysis

This chapter describes the behavior of the selected dunes analysis in terms of dune height, dune length, migration rate and growth rate, and tries to find a link between this behavior and the corresponding period discharges. The aim of the analysis is to check whether the selected dunes have characteristics as expected, leading to a better understanding of the physical processes in both study areas, thus, the understanding of the dunes development, which later will be tried to be replicated with a geomorphological model in order to be able to predict future developments.

Migration rates and growth or decay rates are computed from one survey period to the consecutive one, periods being from 66 to 177 days long in BEM and from 70 to 121 days in the BOM area (see Table 5).

Table 5: Number of days between consecutive survey campaigns

BEM Area		*BOM Area*	
Feb-16 to May-16	83	***Feb-16 to Jun-16***	99
May-16 to Aug-16	102	***Jun-16 to Aug-16***	83
Aug-16 to Nov-16	66	***Aug-16 to Nov-16***	72
Nov-16 to Feb-17	117	***Nov-16 to Feb-17***	111
Feb-17 to Aug-17	177	***Feb-17 to May-17***	70
Aug-17 to Dec-17	120	***May-17 to Aug-17***	105
Dec-17 to Mar-18	78	***Aug-17 to Dec-17***	121

3.1. Dune behavior and discharges results

For a better understanding of the obtained data at each study area, the following dune development charts are presented. The middle and right plots in Figure 19 show the mean values at each time-period for the dune height and length, and dune migration and growth rates, superposed upon the discharge at the Waal upstream boundary at Tiel (red line). Additionally, a generic profile development in time is plotted on the left, to be able to graphically link and contrast the data to the observed profiles. The resulting data and plots for each profile can be seen individually in the APPENDIX B.

On a general basis, it can be seen that migration (Figure 19, black line on right plots) is an accumulative process and responds to the area below the discharge line, which will lead to the identification of a tendency between the average previous discharge and the migration rate (Figure 22). On the other hand, as for the growth ratio (Figure 19, blue line on right plots), the outcomes of the analysis show that positive dune growth is mainly visible after periods with high discharge or presence of floodwaves (Notice the blue dotted line representing the 0 value). Nevertheless, its growth or decay magnitudes seem to depend on far more parameters, such as the initial dune dimensions, the relative time-distance to the peak discharge (rising or falling limb of the floodwave) and the discharge shape through the period (beginning and ending values).

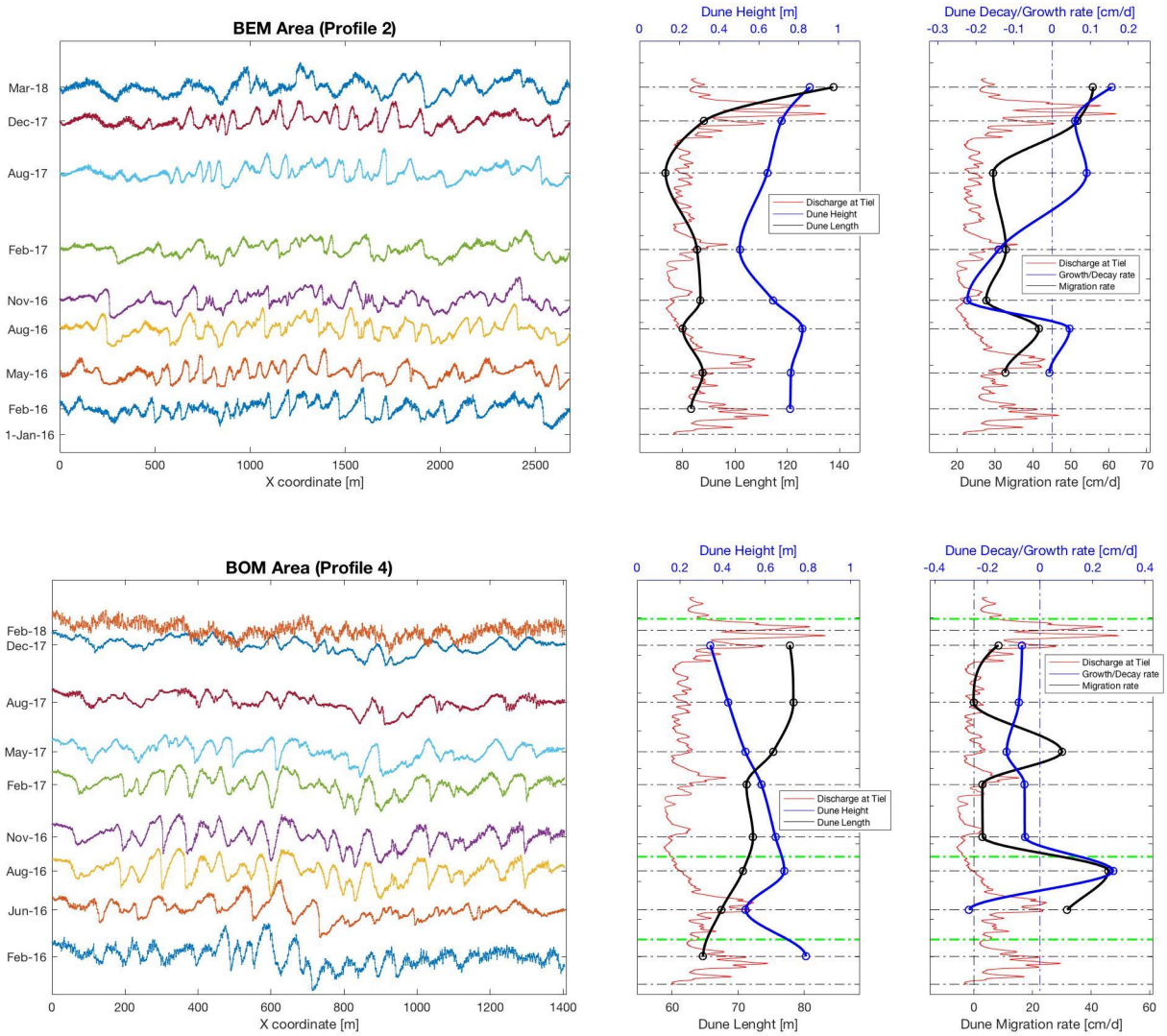

Figure 19: Bed level evolution and dune behavior (H, L, M and G) upon discharge at the river Waal (Tiel) at the BEM area (top) and the BOM area (bottom). Green lines represent the dredging campaigns in the Ankervak area

Observations have shown that changes in flow resistance are out of phase with flood intensity. Consequently, dune development is delayed relative to changing discharges and maximum dune dimensions occur later than the maximum discharge (e.g. Ten Brinke et al. 1999; Julien et al. 2002).

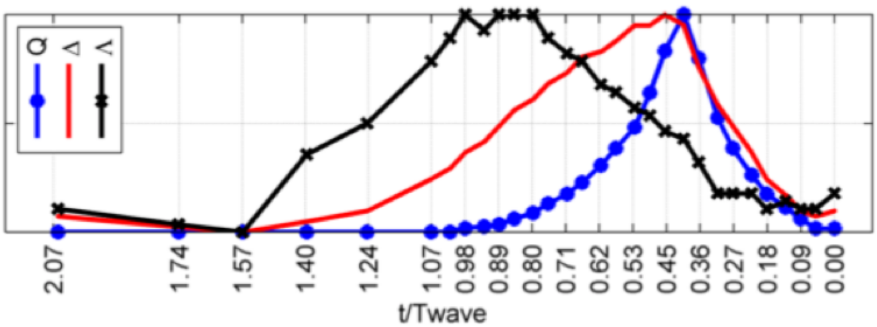

Figure 20: Dune height (Δ) and length (Λ) hysteresis to floodwave discharge (Q) in time, normalized between 0 and 1. Source: (Warmink, 2014).

Hence, taking in mind the hysteresis in dune development seen in Figure 20, the height behavior along all periods and its corresponding growth ratio are justified. Martin & Jerolmack (2013) showed substantial hysteresis on the Rijn river in the Netherlands, with fast adaptation times at the rising limb of the floodwave and large adjustment time scales during the falling stage. Therefore, disregarding

some deviations to the expected values, the averaged dune height values for each period respond accordingly to the upstream discharge and the out of phase maximum dune dimensions after a peak discharge and its subsequent slower recovery development to the new equilibrium state.

Dune length behavior remains still incomparable, presenting two different development shapes on each area. Gabel (1993) after measuring bed profiles in the Calamus River in Nebraska, concluded that dune length increases due to both the growth of individual dunes and the amalgamation of dunes, while it decreases because of both dying-out of dunes as well as dune splitting, induced by superimposed bedforms. Moreover, Paarlberg et al. (2006) indicated that a changing dune length is expected to be related to the influence of flow separation on equilibrium dune dimensions. Martin and Jerolmack (2013) also stated that trough-filling is responsible for the decay of the primary dunes that developed during the flood wave. Thus, merging and splitting could also explain some irregularities in the obtained data trends.

Merging and splitting

The last period of the BEM area presents a large range of length values indicating that merging took place. Moreover, merging in the same area is also observed from Feb-16 to May-16, both periods belonging to a high upstream discharge stage, whereas splitting is clearly seen from Feb-17 to Aug-17, during a large and low flow period. The BOM area shows merging during the first period Feb-16 to Jun-16 and both merging and splitting are seen from Jun-16 to Aug-16, during a period with a floodwave and posterior decreasing of the discharges to the lowest values. Finally, small indices of merging are seen from Feb-17 to Apr-17 along with the increasing discharges at the 2017 wet season, as bigger dunes merge into a unique entity with smaller superimposed disturbances.

The occurrence of merging and splitting suggests that merging occurs during peak discharges, either at the increasing phase or at the decreasing stage of the floodwave. However, due to the lack of survey periods before and after floodwaves, it was not possible to specify in which stage this event occured. Dune splitting seems to take place mainly during low discharges. According to Warmink (2014), matching with the previously analyzed data, after $t/T_{wave} = 1$ (T_{wave}, floodwave duration) the discharge remains constant and superimposed bed forms appear on top of the large primary dunes in both flume and field data (Figure 20). These superimposed bed forms migrate and thereby slowly create splitting or fill the troughs of the primary dunes.

3.2. Dune height and dune length

The averaged dune values for the BEM area oscillate between 0.504 and 0.857 meters in height and 73.57 to 137.64 meters in length for the 8 different periods. On the other hand, for the BOM area, mean dune height fluctuates from a lower value of 0.344 to 0.791m and mean dune length from 64.68 to a maximum of 78.37 meters. Keeping in mind the uncertainty in the collecting methodology and the ambiguity of the given values, it can be concluded that the BEM area presents higher and longer dunes than the BOM area. Both dune height values and length correspond to the possible expected range of values.

There is a wide array of scaling relations to determine dune dimensions (Bradley, 2017). Despite the lack of consensus on the mechanism that controls dune dimensions, the most commonly used scaling relations link dune dimensions to boundary layer thickness, usually assumed to be flow depth in rivers, so as the simple relation proposed by Yalin (1964). The expected values of the water level respect to NAP, provided by the model of Rijkswaterstaat, are similar for both areas. Therefore, given that the bathymetric level is on average higher in the BEM area than in the BOM area, the later referring to the inner part of the river bend with sediment deposition and shoaling waters, it would explain why the former has slightly higher values in both dune dimensions. In fact, in the BOM area the more to the center of the river course, the lower is the riverbed and the larger the water depth, which explains why sand dunes are on average higher for the most outer profiles (Table 6). Note that profiles from 2 to 5 denote from inner bank to center of the river course.

Table 6: Dune height observed at the BOM area for each profile and survey period showing larger values for outer profiles

		Time-period							
H [m]		1	2	3	4	5	6	7	8
Profiles	2	0,78	0,37	0,66	0,59	0,52	0,47	0,42	0,28
	3	1,02	0,50	0,66	0,63	0,59	0,50	0,43	0,35
	4	0,71	0,47	0,72	0,69	0,60	0,52	0,42	0,35
	5	0,84	0,76	0,73	0,68	0,62	0,54	0,44	0,40

The water level in both areas fluctuates between 4 to 7m, depending on the upstream discharges. Consequently, the obtained data responds according to the similar water depth conditions field studies of Holmes & Garcia (2008) in the Missouri river and Toniolo (2013) for the Tanana river. Both studies, with water depths ranges within 4.84-6.46m and 5.14-5.90m, measured dune heights between 0.32–1.25m and 0.60–1.20m and dune lengths moving from 5.70–140.00m or 41.30–66.70m, respectively.

When comparing dune height and length for each of the selected dunes, the general trend for both study areas shows that on average the higher the dune, the longer. Furthermore, analyzing the dune steepness values in the field it is possible to obtain additional geometrical information. The results presented in BEM oscillate between 0.0019 and 0.0256 and in BOM from 0.003 to 0.021. A generic calculation considering BEM and BOM conditions show values of transport stage within a range from 50 to 120. The obtained values fit in the hyperbolic behavior of dune steepness with transport stage (τ_*/τ_{*c}) observed in the work of Yalin and collaborators (Yalin 1972; Yalin and Karahm 1979) and Allen (1982). Figure 21 displays the compilation of data of Bradley (2017) and the area in which the observed data cloud of BEM and BOM is found.

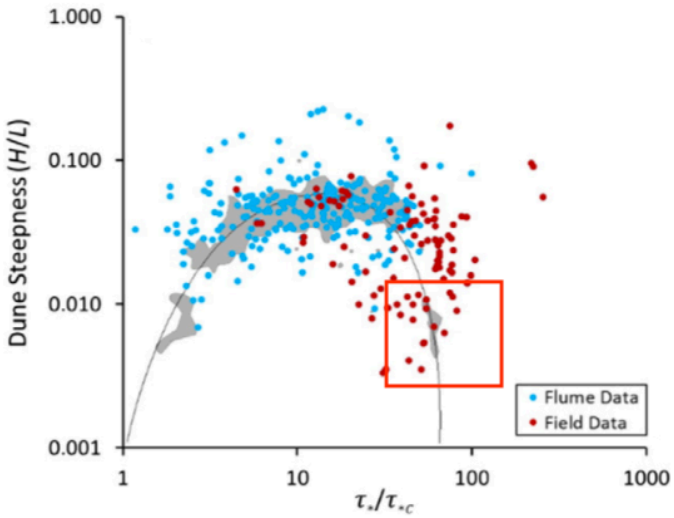

Figure 21: Aspect ratio (H/L) of dunes plotted as a function of transport stage (τ_*/τ_{*c}). The shaded area represents the data cloud from Yalin (1972). 254 points from flume experiments and 99 from field observations were added by Bradley (2017). An approximate location of the cloud data of BEM and BOM is pointed out by the red box. Source: Bradley (2017)

3.3. Dune migration rate

Migration rates go from close to zero values up to a maximum of 154 cm/day or 88 cm/day for the BEM and BOM areas, respectively, with a vast majority group oscillating within a range between 0 and 50 or 0 and 20 cm/day.

Migration rates are shown to scale weakly with dune height for the BEM area, agreeing with the results obtained by David Gaeuman (2007). On the other hand, results in the BOM area display on average a more constant migration behavior for all dune heights. Nevertheless, despite the observed migration rate and dune height trend, and besides certain data points, sand dunes are shown to migrate more or less equally in all the profiles' domain, preserving a migration rate range basically related to the discharges at each time period, regardless of the dune height.

An analysis between migration rate and discharges at Tiel during the corresponding period illustrates a tendency between both parameters (Figure 22). The migration rate is shown to be larger to higher discharges, suggesting that it responds not in a linear way but exponentially to the discharge. Hence, low discharge values generate low or practically null migration rates, while high discharge values are associated with greater migration rates. The daily averaged discharges extend from 928m^3/s to 2.729m^3/s in the BEM area and from 921m^3/s to 1.935m^3/s in the BOM area.

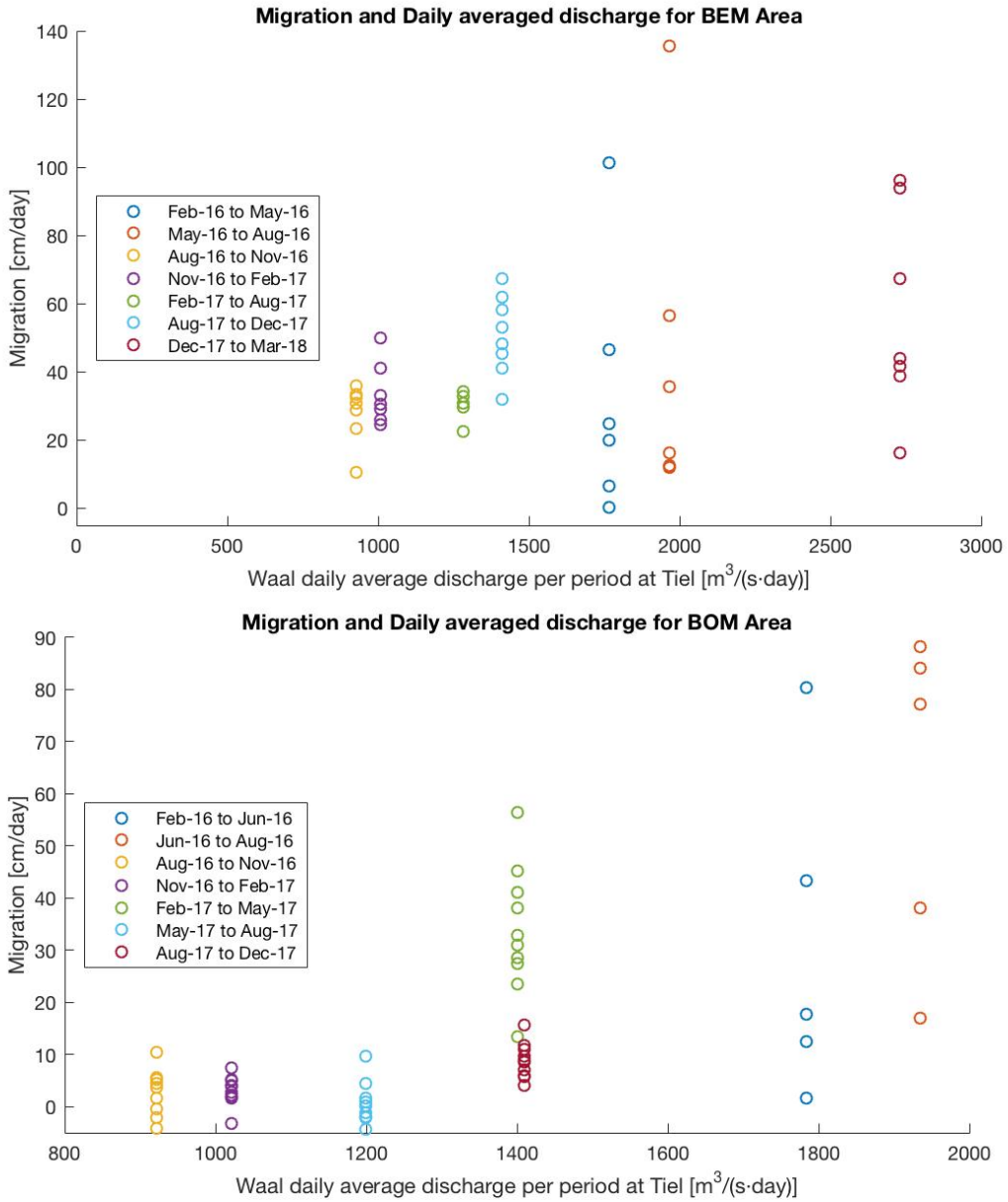

Figure 22: Daily-averaged upstream discharges per period related to the migration rate of dunes per period. BEM area (top) and BOM area (bottom)

To avoid undesired clusters of those dunes that are being tracked in all profiles respect to dunes that might not have been followed throughout all the profiles and time-periods, the considered data in Figure 22 is the all-profiles-averaged data for each dune. The higher migration rate values for BEM than for BOM while considering the same average discharge periods, are justified taking into account the different characteristics of each area. The analysis at the BOM area focus on the inner part of the curve where the flow is mainly displaced towards the outer bank. Consequently, lower velocities, lower water depths and thus lower bed shear stresses than the width-averaged are found in BOM. This particularity of the area is resumed in the necessity of higher upstream discharges to obtain the same transport regime as in the centered-width located BEM area.

3.4. Dune growth or decay rate

Growth rates fluctuate from 0.81 cm/day to -0.86 cm/day and from 0.788 to -0.47 cm/day for the BEM and BOM areas, respectively. Positive values represent a growth in dune height while negative characterize a decay in height dimensions during the considered period. At the BEM area, 47 dunes could be followed obtaining 26 growing and 21 decaying dunes. Specifically, for the BOM area there is a preponderance of decaying rates among the totality of the time periods. Out of the 60 followed dunes, 52 decayed while only 8 grew, 5 of them corresponding to the same period (Jun-16 to Aug-16) with only growing development.

For both areas there is a unique and clear trend. The higher the dune, the lower its growth (or the higher its decay). The analysis presents expected results, since the higher the dune, the closer to the new equilibrium state for a same increment in discharge, resulting in lower growth rates. Whereas, still considering high dune heights, the further it is found to a new equilibrium state for a decrease in discharge, producing a steep decay in dune height.

The analysis is extended focusing on the relation between growth rate and the average upstream discharge at Tiel per period (Figure 23). The considered data is the all-profiles-averaged data for each dune.

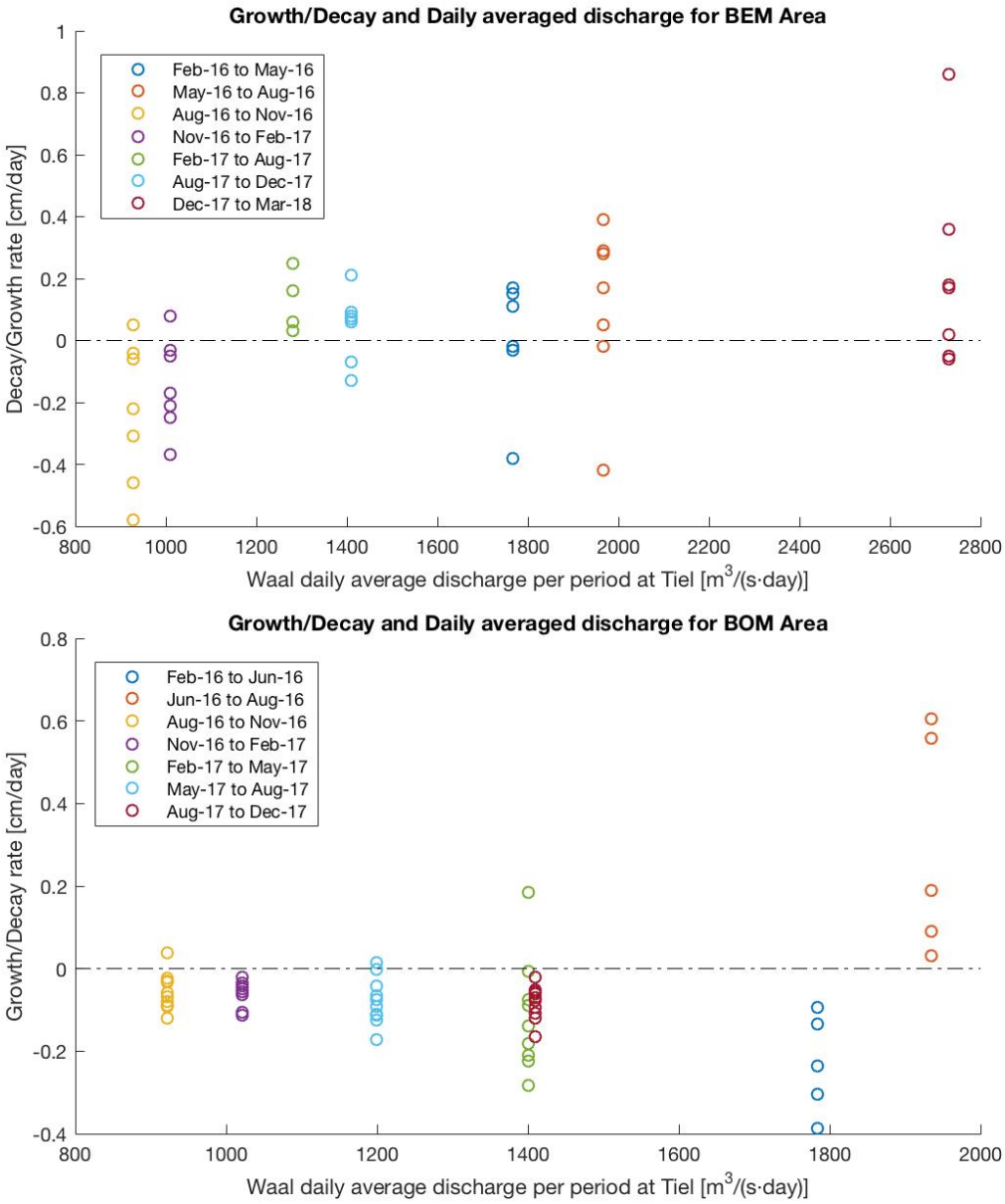

Figure 23: Daily-averaged upstream discharges per period related to the growth or decay rate of dunes per period. BEM area (top) and BOM area (bottom)

Results in the BEM area show growing development for daily-averaged discharge periods above 1250m^3/s, with a significant increase in growth rate as the mean discharge is increased. Contrarily, decaying behavior is observed for discharges below 1000m^3/s and increased decay rates for lower discharge values. In section 2.1 (Areas selection), using the Shields formulations and the approximate characteristics of the area it is discussed that a discharge of 400m^3/s results as an estimated threshold for the sediment motion at BEM. Furthermore, Figure 23 (top) suggests that the suspended load transport regime or bed load transport regime threshold is located between 1000 and 1200m^3/s, as predominant bed load transport is shown to lead to an increase in dune height while an increase in suspended load transport results in a decrease of the dune height (Naqshband et al. 2014).

The same principle can be used to explain the results at the BOM area, but due to the particular characteristics of the area the transport regime threshold is displaced to higher discharge values, between 1800 and 1900m^3/s. For lower upstream discharge periods, the motion limit is surely surpassed at the considered inner bank, as there is dune height decay, but the predominant transport regime is suspended load transport. As the discharge increases, so does the sediment transport in form of suspended load, and higher decay ratios are observed. Further increasing discharges overcome the threshold of the transport regime and as the bed load transport becomes predominant the dunes grow.

Aware of the flow recirculation in river curves, the dune behavior for the BOM area was intended to be analyzed depending on their location upstream or downstream of the profile, meaning right before or after the curve, or else conditioned on their location in the inner or outer profile. Nevertheless, the data did not show any effect trends on growth or migration.

4. Model

Modelling river dune behavior requires the inclusion of several phenomena. Dune evolution is dependent on the interaction of flow and sediment transport, both bed load and suspension transport. Several numerical and experimental studies illustrate the importance of the predominant sediment transport in the dune's behavior. Hence, an increase in bed load transport is shown to lead to an increase in dune height while an increase in suspended load transport will result in a decrease of the dune height (Smith & McLean, 1977; Fredsøe, 1981; Kostaschuk & Best, 2005, Naqshband et al., 2014). Furthermore, bed load transport is often assumed to contribute to the migration of dunes (e.g., Jerolmack and Mohrig, 2005; Kostaschuk et al., 2009). Recirculating eddies can develop at steep lee sides of dunes, resulting in a flow separation zone where flow rotation and reverse circulation can be found (Paarlberg, 2009; Warmink, 2014). Alongside, the understanding of dune amalgamation, superposition and splitting is crucial for dune comportment mechanisms (Gabel, 1993; Martin & Jerolmack, 2013). The presence of superimposed small river dunes on larger dunes, which migrate at higher velocities than the host dunes, are responsible for trough filling and merging of dunes, as well as dune splitting due to the flow separation zone.

Several process-based morphodynamic bed evolution models had been developed in the past, focusing on different scales, dimensional approaches or considering the occurrence of diverse phenomena (e.g. Nabi et al., 2013). The consideration of more physical processes has a direct implication on the accuracy of the model, but have as a consequence a considerable increase on the computational time. Therefore, given the purposes of this project and the necessity of a tool to support the large scale company model within a low computational time, the dune evolution model of Van Duin (2017) was chosen as the most suitable, which is based on the Paarlberg et al (2009) model. Van Duin (2017) model was selected, and not earlier versions of the dune model, as it introduced two different sediment transport formulas accounting for both bed load sediment transport and suspended sediment transport. Nevertheless, the model was used to simulate up to upper-stage plane bed regime, so a parameter calibration to only dune regime conditions is needed.

4.1. Model description

The basis of the Van Duin (2017) model is the dune evolution model developed by Paarlberg et al. (2009). Paarlberg et al. (2007) improved the morphodynamic sand wave model of Nemeth et al. (2006), based on the numerical model of Hulscher (1996). The model is a 2DV (two-dimensional, horizontally integrated) approach of a unique sand dune with unidirectional flow and considers shallow water equations. It uses an eddy viscosity turbulence closure in combination with partial slip boundary conditions, determined from flume experiments (Paarlberg et al., 2005). The model enables the consideration of a parameterization of the flow separation zone (Paarlberg et al., 2007), as well as 3 different transport equation formulas: a) the Meyer-Peter and Müller (1948) bed load formulation, b) the Nakagawa & Tsujimoto (1980) pick-up and deposition model and c) the Meyer-Peter and Müller (1948) formulation with a spatial lag via a relaxation equation.

The model consists of three decoupled modules: the flow module, the sediment transport module and the bed evolution module (see schematization in Figure 24). The hydrodynamic model predicts flows and water levels over the model domain, based on the bed levels at the start of each calculation step. This information is then used to determine the sediment transport regime, derived from the bed shear stress along the domain. Finally, the transport gradient, accretion or erosion estimates, is used to update the bed levels for the next calculation step through the Exner-equation. The governing equations for each of the models can be found outlined in the work of Van Duin et al. (2017).

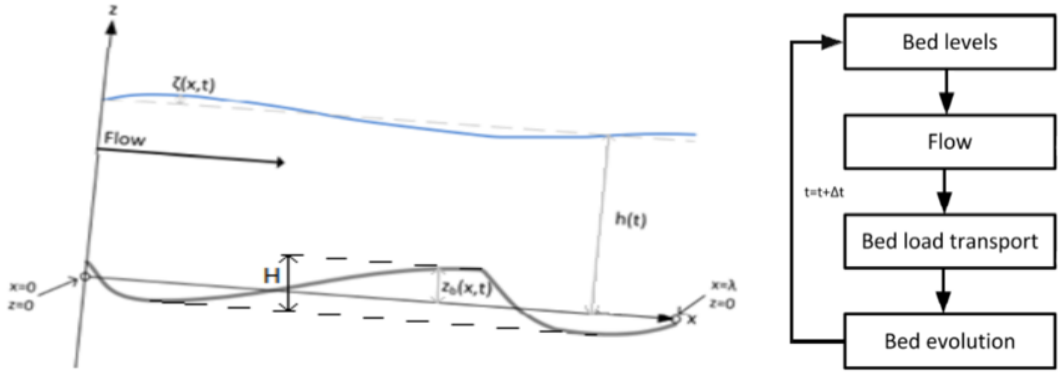

Figure 24: Schematized model (Van Duin, 2017)

Morphological models must deal with a high degree of uncertainty regarding the processes which occur and the manner in which the system reacts to them as morphology is at the end of a chain of the following inter-related processes (STOWA-RIZA, 1999).

Boundary conditions

The boundary conditions are defined at the water surface ($z = h+\zeta$), not allowing flow or shear stress on the surface (equations 1 and 2) and a kinematic condition at the boundary bed ($z = z_b$), yielding that there is no flow through it (equation 3).

$$u\frac{\partial \zeta}{\partial x}\Big|_{z=h+\zeta} = w \tag{1}$$

$$\frac{\partial u}{\partial z}\Big|_{z=h+\zeta} = 0 \tag{2}$$

$$u\frac{\partial z_b}{\partial x}\Big|_{z=z_b} = w \tag{3}$$

where u and w are the velocities in the x and z directions, respectively, and ζ is the water surface elevation, defined as the deviation from the average water depth, h.

A time- and depth-independent eddy viscosity is assumed, therefore, a partial slip condition at the bed (equation 4) is necessary to represent the bed shear stress correctly.

$$\tau_b = A_v \frac{\partial u}{\partial z}\Big| = S u_b \tag{4}$$

wherein, τ_b [m^2/s^2] represents the volumetric bed shear stress, u_b the flow velocity at the bed, A_v denotes the eddy viscosity, and the resistance parameter S [m/s] controls the resistance at the bed.

$$A_v = \frac{1}{6}\beta_1 \kappa u_* \tag{5}$$

$$S = \beta_2 u_* \tag{6}$$

where β_1 and β_2 are calibrating parameters, κ=0.407 the Von Kármán constant and u_*, the friction velocity.

Paarlberg et al. (2009) calibrated β_1 and β_2 to flume experiments setting their values to 0.5. Furthermore, Paarlberg & Schielen (2012) showed that both calibration coefficients needed to be reduced to 0.2 to get realistic river scale simulations. Hence, a reduction of the β-coefficients is expected in this project, which implicitly diminishes the value of A_v and S, reducing the bed shear stress, τ_b.

Finally, the model uses periodic upstream and downstream boundary conditions. These conditions involve that the flow at the downstream boundary of the model is used as an input at the upstream boundary. Therefore, the predicted dune can be depicted multiple times in order to present a multiple sand dunes field.

Pick-up and deposition model

The pick-up and deposition model of Nakagawa & Tsujimoto (1980) is chosen for the computation of the sediment transport. The model calculates the bed transport and the suspended load sediment transport by means of a pick-up and deposition model of a sediment particle. The sediment pick-up rate (probability of a particle being picked up in s^{-1}) is determined by:

$$p_s(x) = F_0 \sqrt{\frac{\Delta g}{D_{50}}} \theta(x) \left[1 - \frac{\theta_c}{\theta(x)}\right]^3 \tag{7}$$

where F_0 is a model parameter 0.03, Δ the specific gravity, θ is the Shields parameter, and θ_c is the bed slope corrected critical Shields parameter.

The deposition is calculated by equation 8:

$$p_d(x) = \int_0^\infty p_x(x-s)\, f_s(s)\, ds \tag{8}$$

where $f_s(s)$ determines the probability that picked-up sediment is deposited a distance s away from the pick-up point (x-s). This distribution function is defined by Nakagawa & Tsujimoto (1980) as follows:

$$f_s(x) = \frac{1}{\Lambda} e^{\left(-\frac{s}{\Lambda}\right)} \tag{9}$$

where Λ is the mean step length and s stands for the distance of sediment motion from the pick-up point. This step length is the only way in the model in which a form of suspended load transport is included. Particles with large values of step lengths can be seen as suspended sediment, as it is picked up, remains in suspension accordingly to Λ and finally settles down.

Shimizu et al. (2009) suggested a sediment particle step-length principle calculated as follows:

$$\Lambda = \frac{u_*}{w_s} e^{\left(-\alpha \frac{w_s}{u_*}\right)} \frac{C}{\sqrt{g}} h \tag{10}$$

where *C* is a constant parameter, *h* is the water depth, *g* the gravity, u_* is the friction velocity, w_s the particle settling velocity and α, the dimensionless step length.

The dimensionless step length α is delimited by θ', the dimensionless grain shear stress, and is defined by:

$$\alpha(\theta', h) = \begin{cases} \alpha_{min} \dfrac{h}{h_{ref}} \; for\; \theta' < \theta'_{min} \\ \left[\alpha_{min} + (\theta' - \theta'_{min}) \dfrac{\alpha_{max} - \alpha_{min}}{\theta'_{max} - \theta'_{min}}\right] \dfrac{h}{h_{ref}} \; for\; \theta'_{max} > \theta' > \theta'_{min} \\ \alpha_{max} \dfrac{h}{h_{ref}} \; for\; \theta' > \theta'_{max} \end{cases} \tag{11}$$

Applying the flume experiments calibrated formula on a river scale, the step-length will be increased with increasing water depths, therefore dividing the water depth by a reference depth, h_{ref}, allows to standardize the step-length to both flume and river scenarios.

4.2. Model sensitivity and setup

The model of Van Duin (2017) was run under 3 different transport equations and calibrated upon the flume experiments dataset of Venditti et al. (2005a, 2005b). Therefore, the model has not been calibrated to larger-scale observed river data. The transition from small-scale flume data to field magnitudes requires the modification of several parameters. The new values will be validated on the previously selected and analyzed dune data (see chapter 3.1).

4.2.1. Model setup and inputs

A first interpretation of the 3 possible transport equations from Van Duin (2017) showed that the Nakagawa & Tsujimoto (1980) model with the Shimizu et al. (2009) is able to represent proper dune height hysteresis effects respect to a passing floodwave, as observed by Martin & Jerolmack (2013). Inversely, the Meyer-Peter and Müller (1948) bed load formulation and its extension with a linear relaxation equation (MPM and MPM+LRE), showed larger adaptation times during the rising limb of the floodwave than during the falling stage.

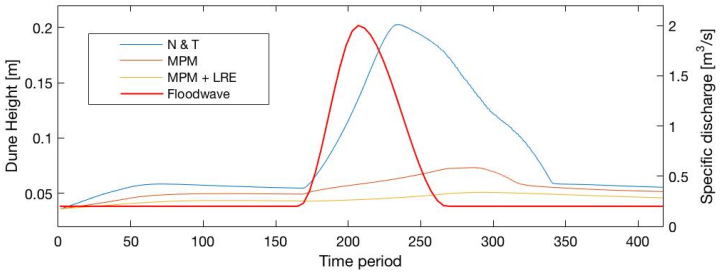

Figure 25: Dune height hysteresis for different transport equations

Therefore, the considered version of the model uses the Nakagawa & Tsujimoto (1980) stochastic sediment-transport approach with a pick-up and deposition model. The suspended transport is contemplated with the Shimizu et al. (2009) sediment particle step-length principle. The selected sediment transport formulation (N&T), inhibits the contemplation of the parameterized flow separation line of Paarlberg et al. (2007). Although the model includes a numerical stability analysis for the dune length at each time-step, dune length is assumed directly related to the water depth with a factor of 7, to reduce the computational time. Avalanching is enbled in the model.

The model workspace grid is defined to be 120 longitudinal points in the x-direction, each point referring to a meter, and 25 points in the vertical z-direction. The end time of simulation is set to 10000 seconds, with calculation time steps of 240 seconds, meaning that the complete simulation period takes 417 time steps. Regarding the company methodology and thus a future use of the model, the model will be executed for periods of 6 months (182 days). Therefore, each time-step of 240 simulated seconds will correspond to 10.37 hours (Morphological factor of 155).

4.2.1.1. Area dependent input parameters

Each area to be modelled has its own morphological conditions that can be considered to be constant in time. Therefore, the BOM area presents on average a finer grain size than the BEM area. Tthe former is located in the downstream area of the Boven Merwede while the later belongs to the upstream Beneden Merwede where lower discharges are expected, due to the bifurcation of the Boven Merwede not far upstream. On the other hand, river bed slope is also different in both areas. Nevertheless, these two parameters are not even constant through the extension of the selected profiles, which can contribute to the instability of the model. Physically speaking, a succession of coarse and fine pathways or differences in the bed slope can lead to an unreal increase or decrease of the transport capacity. After all, in reality there will be much more gradual transitions, for that after analysing all the possible existing values, a final bandwidth of values per each parameter and area were selected.

D_{50} interval

The D_{50} values were extracted from the work of Mol (2003), who by analysing large-scale soil samples conducted by Fugro (2002) determined all sorts of grain sizes for the entire Nordelijk Deltabekken. The raw data often showed abrupt fluctuations per place. As both areas cover an area of approximately two lineal kilometers, the following values are considered to be the upper and lower bound of possible median grain sizes and the selected mean to work with:

Table 7: Range of possible grain size, D_{50}, for each area

D_{50} [mm]	Min	Average	Max
BEM	0.7	**0.83**	0.9
BOM	0.5	**0.63**	0.75

Bed Slope interval

Due to the lack of precise river bed slope data for the area and the varying conditions in space, the bed slope values were obtained from the different profiles (3 profiles per 8 different time-periods in the BEM area and 5 profiles x 9 time-periods in the BOM area). Hence, the different values were calculated as the mean height difference of the first and last 50 profile points (out of 2450 points for BEM and 1850 calculation points for BOM), and their relative distance difference.

Table 8 presents the maximum, mean and minimum obtained values in m/m, as well as the first, second and third quartiles. For the BOM area, values are also shown without the consideration of the 9th time-period and the 1st profile, for the same reasons as they were omitted during the dunes selection (see chapter 2.2):

Table 8: Range of possible bed slope, i, for each area

	BOM			***BEM***
Bed Slope Values [m/m]	**All time-periods and profiles data**	**Without 9th time-period**	**Without 9th time-period and 1st profile**	**All time-periods and profiles data**
Max	3,49E-04	3,49E-04	3,49E-04	2,23E-04
75%	2,00E-04	2,06E-04	2,06E-04	1,56E-04
Average	**1,62E-04**	**1,65E-04**	**1,72E-04**	**1,25E-04**
25%	1,06E-04	1,06E-04	1,09E-04	8,51E-05
Min	4,26E-05	4,26E-05	4,26E-05	1,75E-05

Therefore, for the BEM area on average the bed slope will be considered **1.25E-04 m/m**, with a possible range of values between 1.1E-04 m/m – 1.5E-04 m/m. As for the BOM area, the average bed slope value resembles to **1.65E-04 m/m**, within a bandwidth between 1.4E-04 m/m – 1.9E-04 m/m.

4.2.1.2. Simulation dependent input parameters

Initial Dune profile

Each simulation starts with its own initial dune dimensions. Out of all the selected dunes data, the average slope values for the stoss and lee side were calculated, obtaining a value of 1.29% for the stoss side and -3.22% for the lee side. Hence, a generic dune profile is created responding to these slope values, having dimensions of 65 metres long and 0.8 metres height (Figure 26), according to the average values of Feb-16 at the BOM area. From this standard profile all the other input profiles are obtained by modifying each point respectively to the new maximum dune height. The initial dune length is not modified from the generic 65 meters long, which lay within the observed lengths of each survey period. Nonetheless, the model is expected to correct the dune length to the water depth conditions at the early time steps.

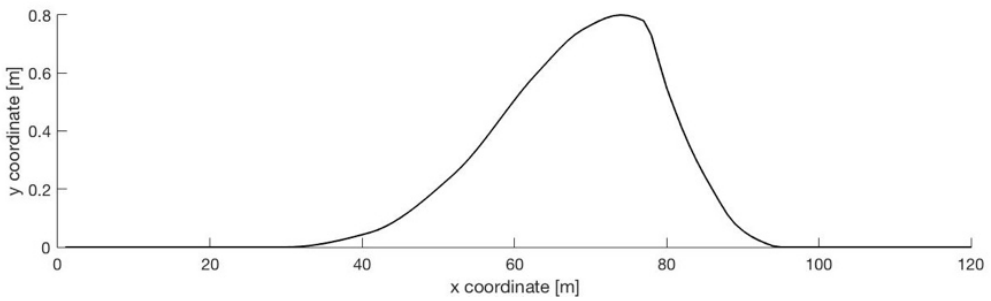

Figure 26: Initial dune profile shape, flow is expected from left to right

Floodwave

Along with De Vries & Van de Wiel's practice of forecasting the morphodynamics for the following 6 months, the model runs will be executed for the same period of time, which is then divided in 417 time steps. Thus, for each simulation, its corresponding width-averaged specific discharge [m^2/s] is obtained as the velocity [m/s] times water depth [m] for the particular area, these two as outcomes of the Delft3D model. To obtain the last two parameters, the extensive upstream discharge measured data at the river Waal (Tiel) and river Maas (Megen) are reduced and interpolated to 417 equally spaced time points of 10.37 hours. Therefore, for each pair of boundary discharges, the water depth and velocity values at each precise area are obtained out of the results of 37 Delft3D model runs, each concerning different upstream discharge conditions.

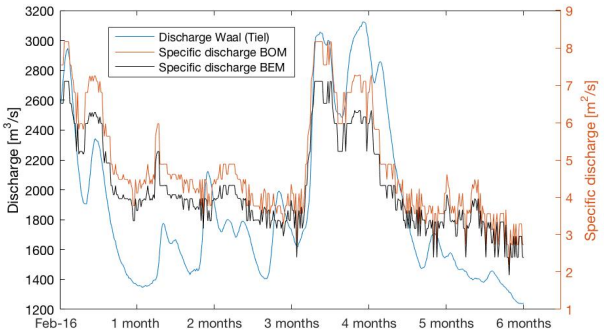

Figure 27: Superposition of BEM and BOM simulated specific discharge values and upstream discharge at Tiel

4.2.2. Sensitivity Analysis

To get an insight on the model's performance and be able to understand the effects of the different model inputs and parameters, a simple sensitivity analysis is done on dune height. The analysis will lead to the decision of which model parameters to change for the calibration and in what amount.

The parameters that are proportionally increased and decreased to see their implication on the model results are: the bed slope, the sediment grain size, d_{50}, the β_1 and β_2 values and the step-length module parameters (h_{ref}, the F_0-constant, the dimensionless step length α and the dimensionless grain shear stress θ').

The different runs are done on a real scenario (*Default Scenario*) from February 2016 to December 2017 at the BOM area, according to the corresponding specific discharges. No extension of the analysis will be done for the BEM area, as the sensitivity effects of each parameter that is intended to be examined is equally observed in both areas. The initial considered dune height and dune length agrees with the mean values observed for February 2016. The default values of β_1, β_2 and step-length model parameters correspond to the calibrated parameters of Daggenvoorde (2016). The rest of the considered values, listed in Table 9, correspond to the mean values found at the BOM area.

Table 9: Default Scenario input parameters for the sensitivity analysis

Input	Magnitude
β-values [-]	0.235
Bed slope i [m/m]	1.65*10^-4
D_{50} [mm]	0.63
h ref [m]	0.1166
α_{max} [-]	400
α_{min} [-]	50
θ'_{max} [-]	0.85
θ'_{min} [-]	1.30
F_0 [-]	0.025
Transport equation	Nakagawa & Tsujimoto (1980)
Step-Length model	Shimizu et al. (2009)

*Bed Slope, i [Default $\pm$ 0.2*10^{-4}]*

The effects of modifying the bed slope are basically seen during high discharge periods or increasing discharges (increasing phase of the floodwave). High bed slopes imply higher maximum dunes height during floodwaves, while low bed slopes have the opposite effect with slightly less perceptual infliction (Figure 28).

D_{50} [0.5 - 0.8mm]

The grain size influences equally every time-period dune height. Higher D_{50} generate lower dunes and lower D_{50} higher dunes (Figure 28).

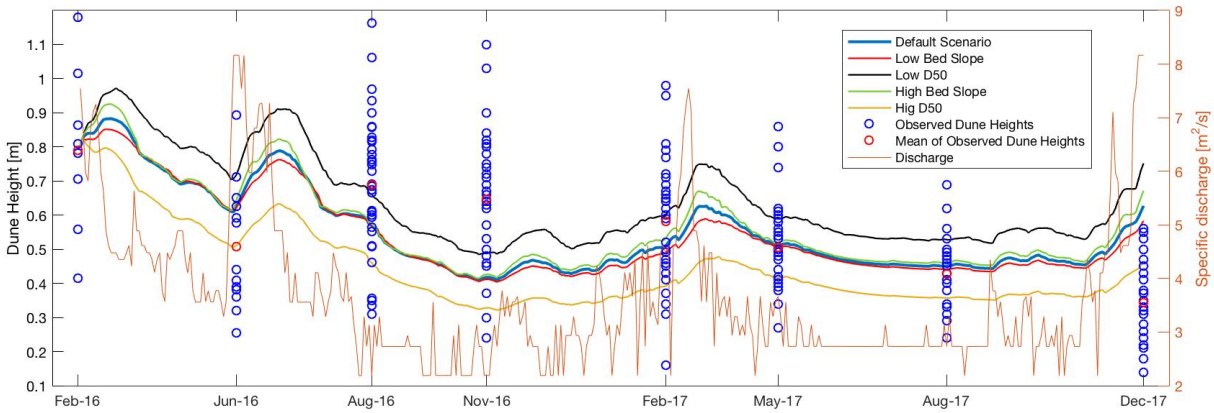

Figure 28: Dune height evolution for different bed slope, i, and grain size, D50

β-values [0.215 – 0.255]

As shown in Figure 29, lowering β_2 implies a general reduction of all the dune heights throughout the simulation period. Lowering β_1 by an equal amount shows the same consequences as the decrease of bed slope, with practically equal outcomes as the Default Scenario during the falling limb of the peak discharge and obtaining lower dune heights and lower maximum heights at the rising phase of the peak discharge. Analogously, increasing the β-values results in the opposite effects.

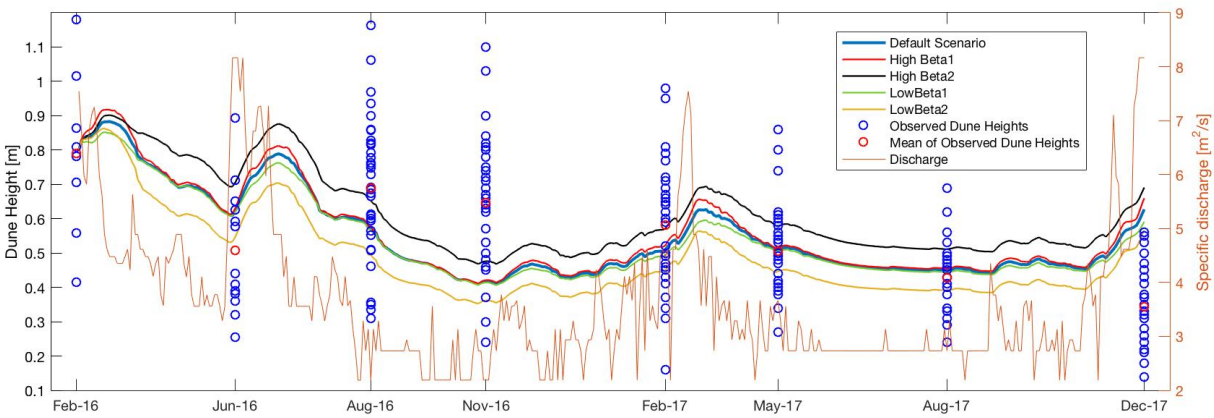

Figure 29: Dune height evolution for different β-values

Step-Length model

In the study, Van Duin (2017) shows that the resulting dune morphology (dune height, length and general shape) significantly depends on the bed load transport formulation used. Within the N&T transport equation, the model enables three different considerations to calculate the step-length, as being constant, or following the Shimizu et al. (2009) or the Sekine & Kikkawa (1992) model. After applying the three formulations to the conditions on the area (Figure 30), the Shimizu et al. (2009)

was chosen as the most feasible one as it best fits the morphological development shown by the surveyed data.

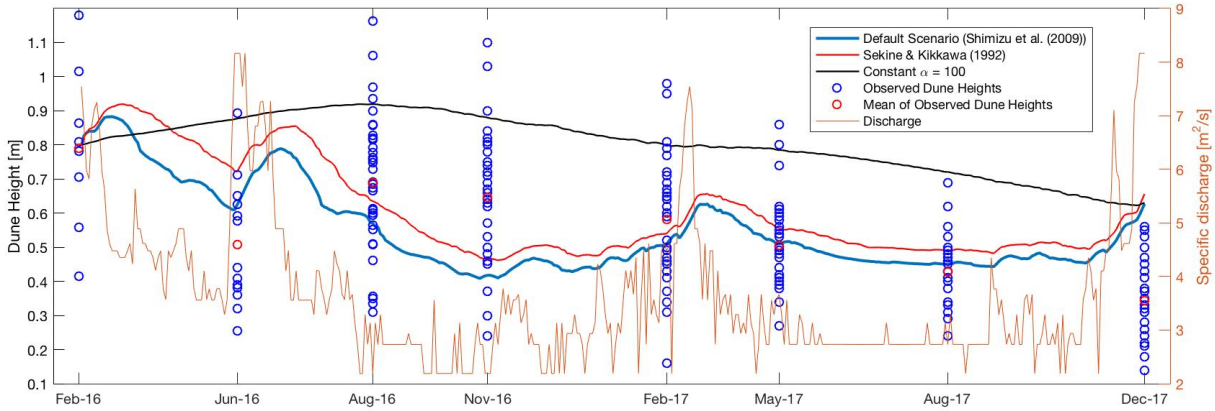

Figure 30: Dune height development for different Step-length-model principles

Shimizu et al. (2009) step-length model is determined by the reference height h_{ref}, the F_0-constant, the dimensionless step length α and the dimensionless grain shear stress θ'. Reducing the reference height implies a reduction in dune height, as the step-length is increased which simulates more load suspended transport. On the other hand, increasing its value generates overall higher dunes (Figure 31). An increase in F_0 directly derives in an increase in p_s (see equation 7), more bed load transport and therefore higher dunes (Figure 31). By reducing it the opposite result is obtained.

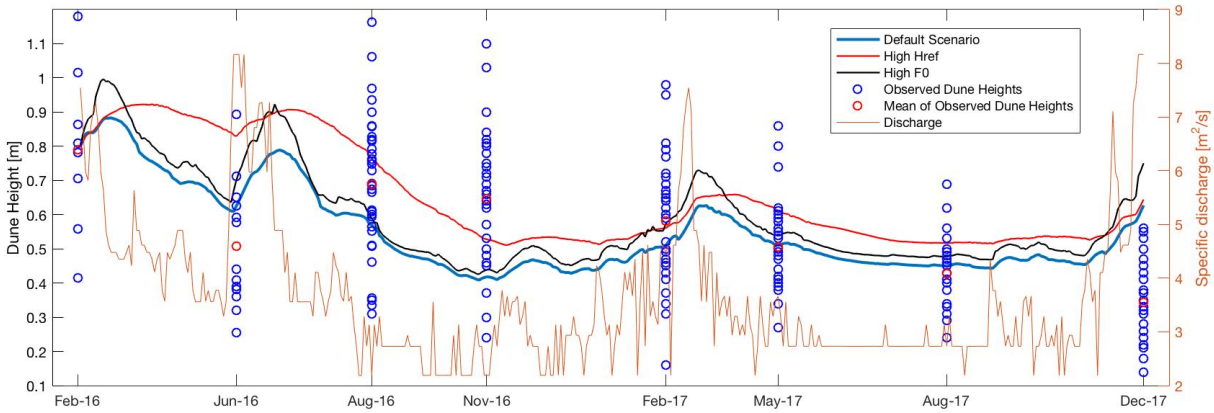

Figure 31: Dune height evolution increasing the F_0-parameter to 0.03 and increasing the h_{ref} to 0.3166

The Shimizu et al. (2009) step-length model principle suggests that the step length is constant in the dune regime, increases linearly with the dimensionless grain shear stress in the transitional regime, and is again constant at higher values in the upper-stage plane bed regime, Figure 32. The three regimes are delimited by the θ'_{min} and θ'_{max} values, which are dependent on the flow and sediment characteristics. The constant step-length values for dune regime and upper-stage plane bed regime are defined by the α_{min} and α_{max}, respectively.

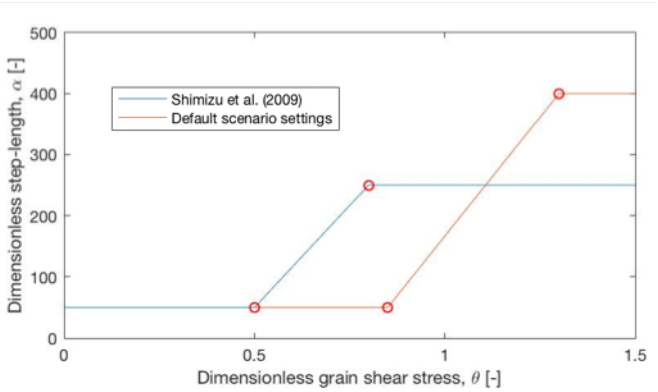

Figure 32: Step-length-model principle

If α-values are increased or θ'-values decreased, the model is shifted up and the overall step

length increases, which results in more suspended transport. Hence, maximum dune heights are smaller. The default scenario never presents θ' values higher than 0.7, therefore, the simulation lays in the dune regime for all the time-steps. Figure 33 (red line) shows the results of a new simulated scenario with a lowered θ'_{min} and θ'_{max}, reduced to 0.45 and 0.9, respectively. The effects of these changes are clearly seen during the peak discharge after Jun-16, after Feb-17 and before Dec-17, when the new transitional regime is reached, resulting in lower dune heights. Changing these values vice versa results in a reduction of the step-length and more bed load transport will be considered, the transport mode responsible for the development of higher dunes.

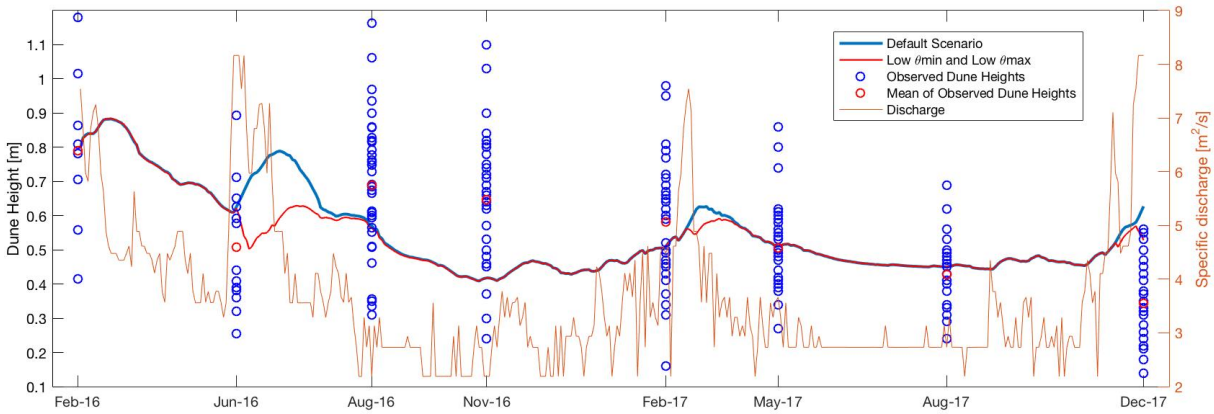

Figure 33: Dune height evolution varying the transitional regime bound (θ'_{min} = 0.45) and upper-stage plane bed regime bound (θ'_{max} = 0.9)

4.3. Calibration and validation

The insights of the sensitivity analysis have been used to understand how the model would behave to any parameter change in the process of calibrating the model. The flow module highly underestimates the outcoming water depths. Nevertheless, the model presents a good morphodynamic behavior. Therefore, since the dune length is calculated as a simple factor of 7 respect to the water depths, being likewise underestimated, the calibration will be done upon dune height. The model results will be compared and validated to the previously analyzed surveyed data.

The target of the calibration is set by the Nash-Sutcliffe-Efficiency (*NSE*, see equation 12). *NSE*-values will be computed by comparing (1) the average input conditions (initial dune height, bed slope, *i*, and grain size, d_{50}) model results at each period to the mean of the observed dune heights and (2) the most extreme conditions model results to the standard deviation bounds (Nash & Sutcliffe, 1970).

$$NSE = 1 - \frac{\sum_i (f_i - y_i)^2}{\sum_i (y_i - \bar{y})^2} \qquad (12)$$

where *i* is the survey period, y_i is the average observed dune heights at the i^{th} period, f_i the simulated value at the i^{th} period, and $\bar{y}$ the average value of all the observations y_i. An efficiency of 1 (*NSE* = 1) represents a perfect simulation, while 0 or negative values mean that a better prediction could be given by using the mean of the observed values. Therefore, the aim of the calibration is to achieve *NSE*-values as high as possible. Negative but close to 0 values will be accepted taking in mind the large observation heights range and the ambiguity of the chosen calibration values.

Validation on mean observation heights and average input conditions model results

Figure 34 shows the calibrated BEM and BOM dune height development prediction plots, respectively. The calibration was carried out adapting the sediment transport parameters and the β-values. The final model step-length parameters slightly differ depending on the simulated area. Due to the particular conditions at the BOM area, where only the most shallow inner part of the curve was considered and due to considering the input discharge as the width-averaged discharge, the model miscalculated values for the water depth are closer to the observed ones, which implies a necessary reduction in the h_{ref} value to better fit the surveyed dune heights progress. Moreover, the step-length model limits θ_{min} and θ_{max}, had to be adjusted to each area, Table 10.

For the modelled period, the dimensionless bed shear stress, θ', at the BOM area does not reach values higher than the lower limit, for which step-length in the area is considered constant throughout the entire period (dune regime). In the BEM area values higher than 0.35 are just obtained in particular points with increasing high discharges. Therefore, in the BEM area, the step-length is generally supposed constant but linearly dependent on the θ' in several limited transition regime periods. No upper-stage plane bed was observed in the surveys, consequently the maximum θ'_{max} limits are never exceeded.

Table 10: Calibrated model parameters

Parameter	BEM	BOM
h_{ref}	0.4166	0.2166
$\alpha_{min} - \alpha_{max}$	50 – 400	50 – 400
$\theta'_{min} - \theta'_{max}$	0.35 – 1.10	0.85 – 1.35
F_0	0.03	0.03
$\beta_{1,2}$	0.245	0.245

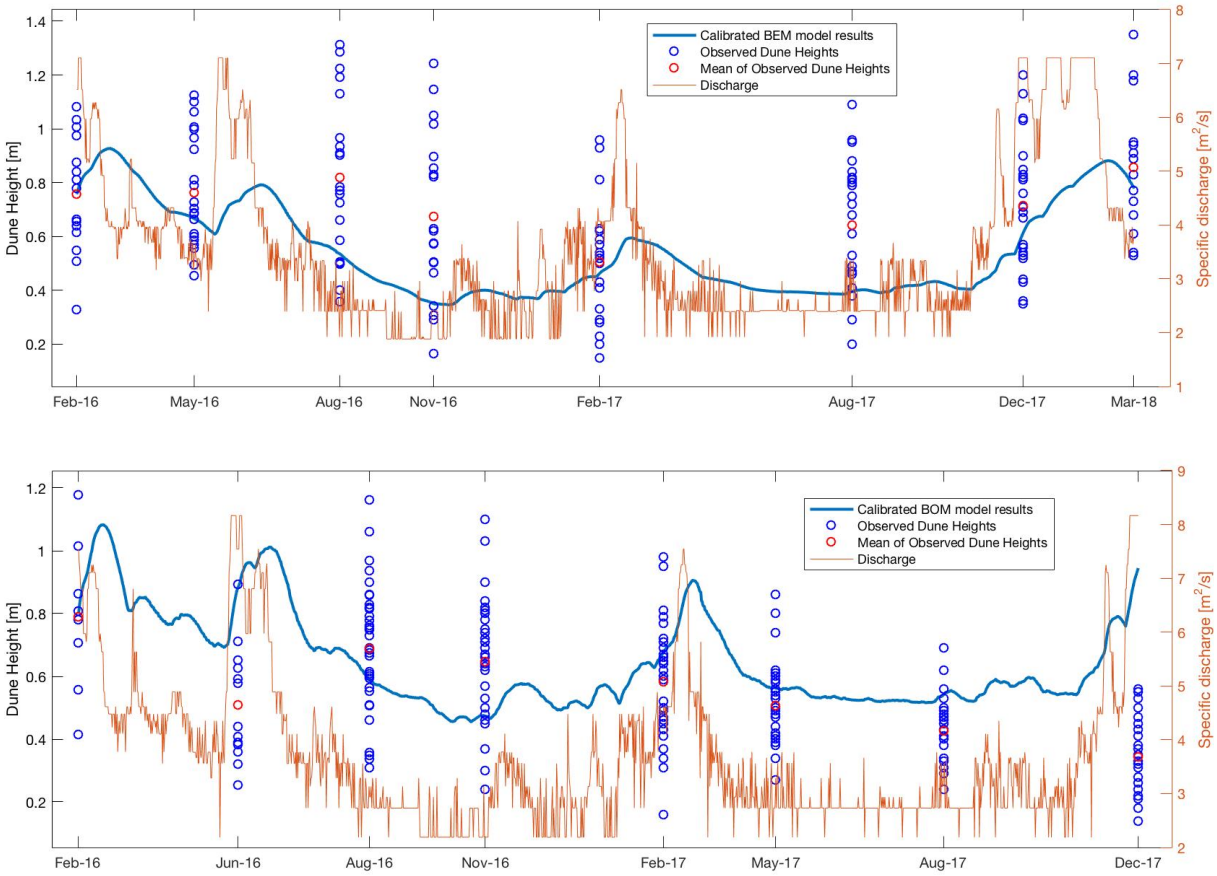

Figure 34: Average input conditions model results and observed dune heights. BEM Area (top) and BOM Area (bottom)

The validation of the model simulated to the mean observed dune heights at the BEM area gave an *NSE*-value of -2.3. The *NSE*-value at the BOM area resulted in -5.13. Negative values mean that the model does not reproduce the averaged dune heights in a sufficient manner. Nevertheless, the dune

evolution is well simulated and all the solution points lay within the range of observed values (except for the last survey period at BOM, Dec-17).

Figure 35 shows a scatter plot for each area of the validation results, where mostly all simulated points are shown to lay within or close to a 30% deviation of the desired observed values. At the BEM area, all the simulated values are found under the y=x line, which shows an underestimation of the average dune heights. At the BOM area the predictions lay at both sides of the line but results in Jun-16 and Dec-17 are clearly overestimated, coinciding with two periods with high discharges at the rising limb of a floodwave.

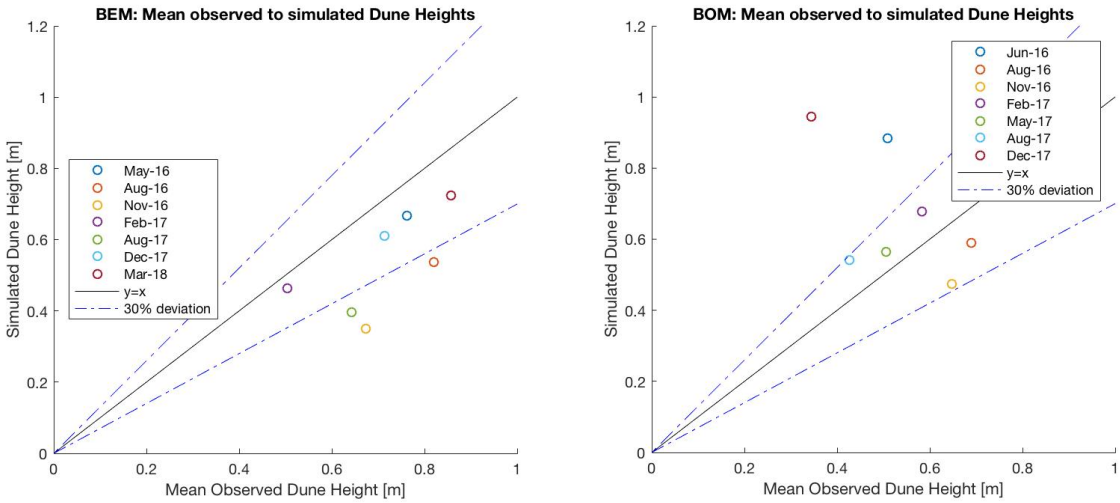

Figure 35: Validation results of the average input conditions calibrated models to the mean observed dune heights

Validation on standard deviation range of surveyed heights and extreme input conditions model results

As each dune cannot be modelled individually and the surveyed dune heights present a range of observed values, the models are also run for the two most extreme scenarios for each survey-period. By doing so, the resulting dune heights for each scenario define an interval of possible solution values (Figure 36). That means an upper bound considering the highest dune height for that survey point, the highest bed slope value for the area and the lowest grain size, d_{50}, following the intervals defined in section 4.2.1.1. The lower bound is computed vice versa, with the lowest values of dune height and bed slope and the highest of grain size.

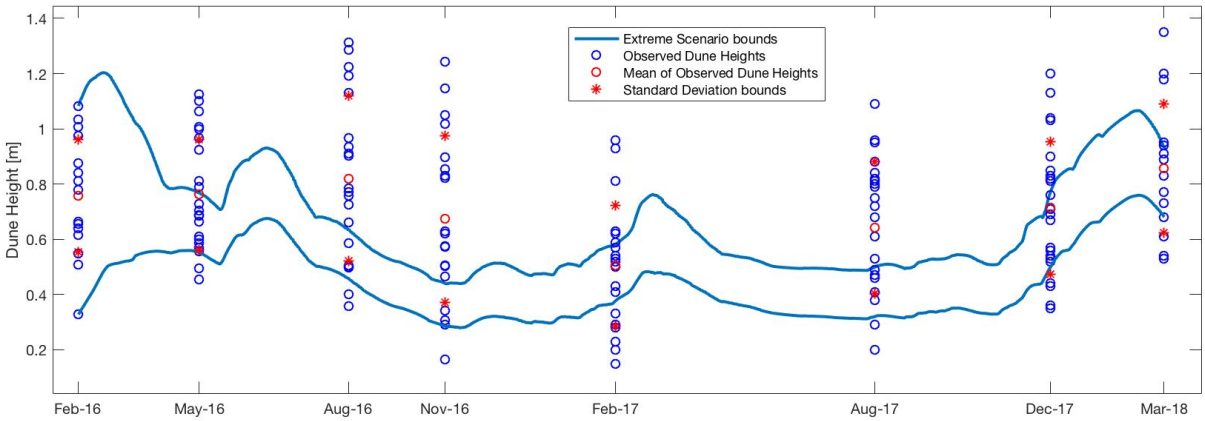

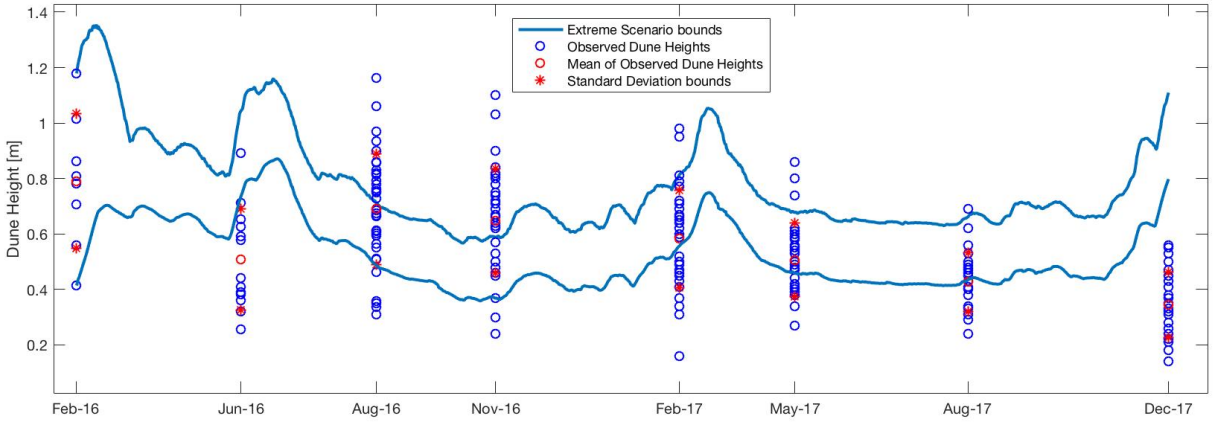

Figure 36: Extreme conditions model results and observed dune heights. BEM Area (top) and BOM Area (bottom)

This new approach defines an upper and lower bound of possible values, covering up a wider range of solutions. This interval can be compared to the upper and lower bounds that are defined by the standard deviation to the mean dune height of each time period. As previously, the new solution boundaries are plotted against the mean of the observed values (Figure 37) displaying the bandwidth of model dune height solutions. The upper and lower standard deviation values to each period average dune height are shown in red, to show the range in which the 68.2% of the measured data lays in and to be able to see the coverage of the model extreme conditions outcomes.

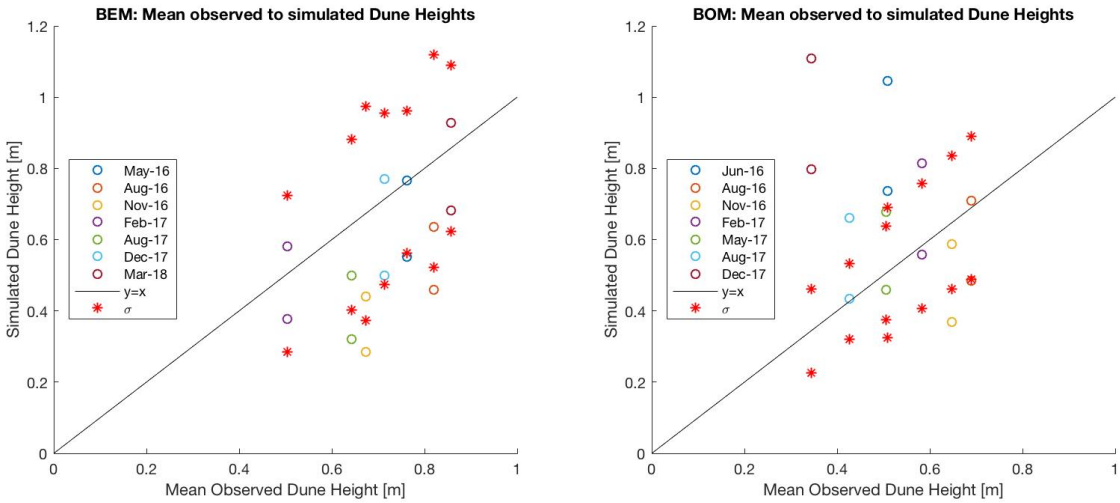

Figure 37: Upper and bottom boundary results of the calibrated models for the most extreme scenarios. The red scattered points define the 68.2% (standard deviation) range of the observed values

The BEM model presents accurate results for the lower limit, obtaining more than satisfactory *NSE*-values when comparing the lower simulated bound to the lower standard deviation at each surveyed period, 0.62. The BOM model presents a worse agreement with the lower bound, resulting in an *NSE*-value of -6.55. The first and the last survey periods (Jun-16 and Dec-17) exhibit lower dune heights than the expected dune height development for the upstream discharge situation. This is due to the specific flow conditions at the inner curve area where secondary flows appear and the main flow shifts to the outer river bank, leading to lower discharges within the studied perimeter and lower bed load transport. Consequently, the model results are completely overestimated. Excluding these periods, the *NSE*-value increases up to -0.87 (Table 11).

On the other hand, the BEM model simulates the upper limit in a more imprecise way, whereas the BOM model in a more precise way, obtaining values of -5.76 for BEM and -1.98, or -0.21 without considering the 1st and 8th observation points, for BOM. In the BEM area, the model generally underestimates the maximum values. In the BOM area the model mostly forecasts a better approach

to the upper limit, except for survey periods at the increasing phase of the floodwave where the simulated values exceed the maximum desired observation heights (Jun-16 and Dec-17).

Table 11: Nash-Sutcliffe-Efficiency values for the calibrated model results ((1) average and (2-3) extreme scenarios) to the (1) observed mean dune heights and (2-3) to the standard deviation (upper and lower) bounds. For BOM, results without considering Jun-16 and Dec-17 are also shown

***NSE* (simulated to observed)**	**BEM**	**BOM**
Mean dune height	-2.3	-5.13 (or -0.24)
Upper limit	-5.76	-1.98 (or -0.21)
Lower limit	0.62	-6.55 (or -0.87)

4.4. Model considerations and results

The model was set up to simulate periods of 6 months with a calculation time-step every 12 hours, following De Vries & Van de Wiel's needs. Therefore, the model considerations and results shown in this section are achieved modelling 7 different runs of 6 months from each of the surveyed points, except for the last time-period (Mar-18 for BEM and Dec-17 for BOM) in which no further data to compare the results is available.

4.4.1. Model considerations of use

When comparing the model results assessing extreme conditions and average input conditions, it can be observed that after a month of simulation for BEM, and two months for BOM, the extreme bounds are equidistant to the average conditions results (Figure 38).

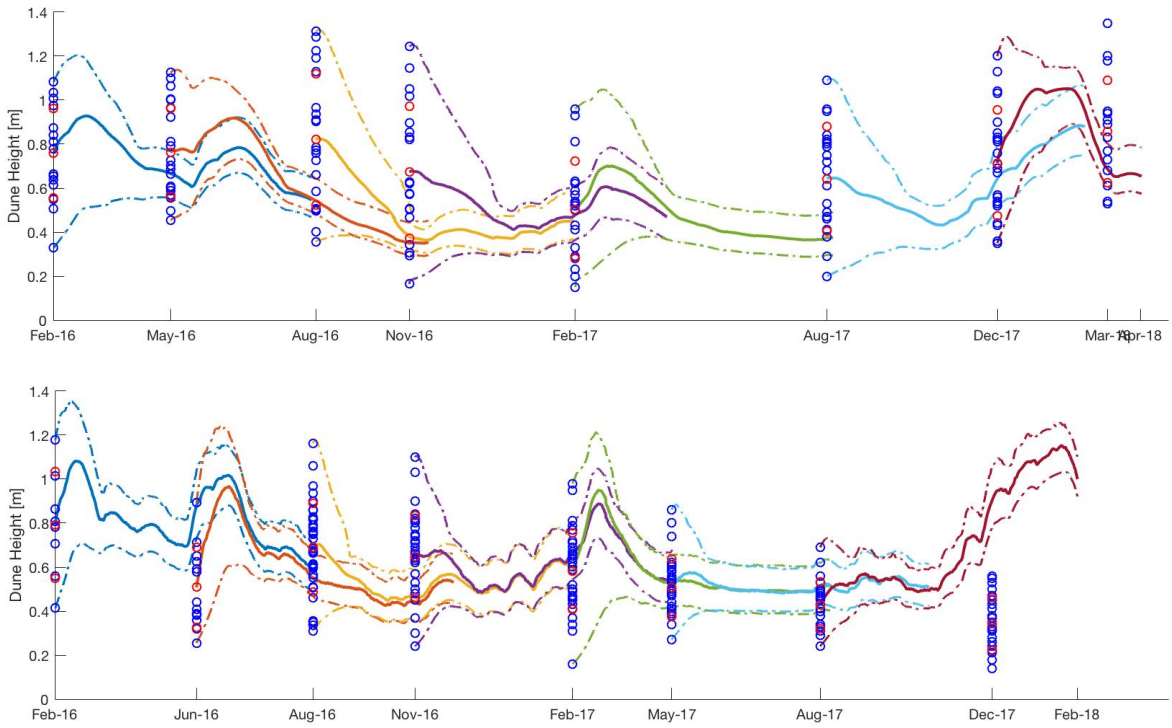

Figure 38: Dune evolution results for the most extreme conditions (dotted lines) and averaged conditions. BEM Area (top) and BOM Area (bottom). Blue dots represent each measured dune. Red dots refer to the mean and standard deviation values

Plots in Figure 39 display the height difference between the average input values results and the most extreme scenario upper and lower bounds (black and red lines, respectively). The outcomes show that when the extreme-scenario-model stabilizes, the BEM average-model results are on average 0.094m and 0.12m apart from the lower and upper bounds, respectively, and the BOM results

0.10m and 0.12m apart.

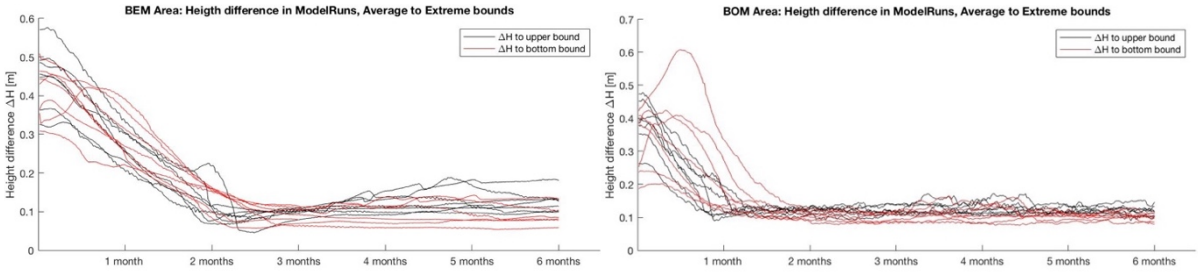

Figure 39: Difference in height from average conditions results to the upper and lower extreme bounds

Therefore, this analysis leads to the suggestion of using the model with the average input values and adding an additional limit to the model predicted results, *H,* of 0.12m to define the upper bound and subtracting 0.10m to define the lower bound (Table 12). This way the most extreme situation will be simulated, embracing a wider range of the observed dune height values in the surveys.

Additionally, during the calibration of the model, the BEM area showed a general underestimation of the upper boundary to the desired standard deviation range bound (*NSE* = -5,76). Hence, if the upper limit results are shifted up equally 0.32m, a best coverage of the observed dune heights is obtained, reaching a maximum *NSE*-value of -0.195 (Table 12). No additional upper limits are needed for the BOM area as the model already showed a better approach to the desired values. Despite the lower limit being generally overestimated for the BOM model no extension is proposed, since significant high dunes are the main concern for this project, ensuring in that way a safety factor for the lower predicted values.

Table 12: Definition of the simulated dune height [m] bounds, being H the resulting average-conditions model dune height

Range limits	**Lower limit**	**Upper limit**
BEM	*H* – 0.1m	*H* + 0.12m + 0.32m
BOM	*H* – 0.1m	*H* + 0.12m

4.4.2. Model performance

Further to the definition of the consideration of use and additional bandwidths, the model is meant to be used to predict future scenarios for which the discharges are unknown. The expected discharge values (stochastic forcing) are uncertain and may differ from the real ones, resulting in different model outputs. Therefore, a performance analysis is made for the current studied period, considering different quality sets of discharges with more or less accuracy, to determine their influence on the model results. First, three scenarios are run using different block-periods averaged discharges of the real measured data at Tiel and Megen. Consecutively, and to make it more realistic to a forecasting approach where the unavailability of exact discharges is a drawback, two more scenarios are regarded following statistical discharges at the same measuring stations from 1989 to 2014 for Tiel and 1996 to 2016 for Megen.

Exact measured data at Tiel and Megen:
- Daily-averaged discharges (Default scenario)
- 10 day blocks-averaged discharges
- Monthly-averaged discharges

Statistical discharges:
- Most frequent averaged discharge per month (Median discharge value of each month)
- Corrected most frequent discharge to real measurements

The histograms of all the long-term timeseries monthly-averaged discharges show a positive skewed, right-tailed distribution of occurrence (Figure 40, see APPENDIX C for the rest of the plots for each month). The spreading of possible discharges on average goes up to 3 to 4 times the most occurrence values. Therefore, it exemplifies the potential margin of error to underrate the real discharges in a particular month with wetter or dryer periods than the most occurrence conditions. For that, a last case scenario is modelled with a gentle correction of the considered most occurrence values respect to measured data

Criteria for the correction

- Corrected only those periods (months) with an estimation (median value) 30% higher or lower than the measured monthly-averaged discharge at the river Waal
- Months presenting lower but close to 30% deviations for the Waal and an estimated value at the river Maas highly deviated respect to the measured averaged discharge (more than 100%), are also corrected
- The correction is carried out up to a 15% deviation of the observed values

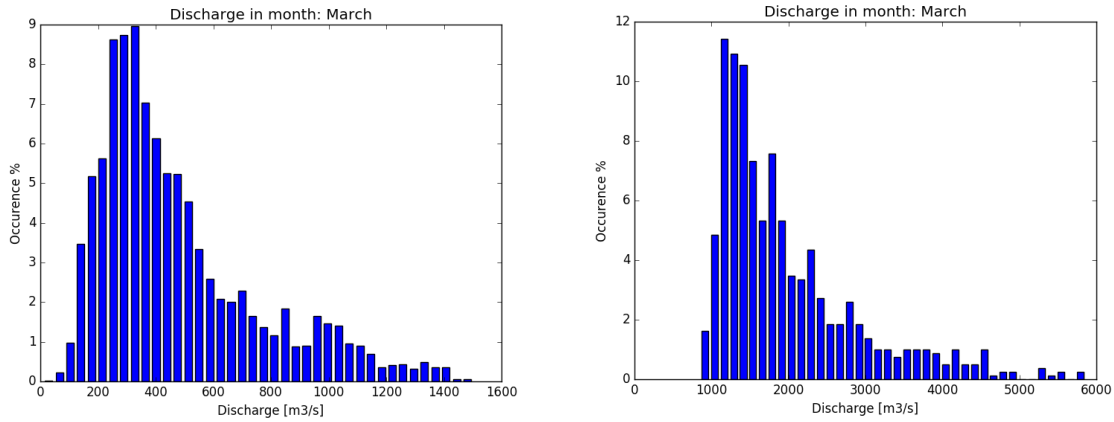

Figure 40: Monthly averaged histogram of the time series discharges for March. Megen (left plot) and Tiel (right plot)

The analysis of the performance has been done by computing (1) the percentage of observed data points included within the outcoming bound limits, (2) the covered percentage of the observed data range (maximum and minimum) and (3) the covered percentage of the range defined by the standard deviation to the mean observed values. In general, the different considered scenarios with measured data present similar results. Reducing the quality of the floodwave data, thus increasing the averaged block-periods, has low effects on the considered time-periods outcomes which are slightly being modified but still providing a reasonable and acceptable range of values. The lowest accuracy dune height predicted values are obtained with the poorest quality scenario, hence, considering the most imprecise discharges by simply assuming the discharge with more occurrence per month.

Performance results

The dune height evolution for all the considered scenarios is shown in Figure 41 for BEM and Figure 42 for BOM (All scenario-plots individually can be seen in APPENDIX C). A reduction in the discharge data quality by supposing larger averaged periods or more generalized monthly discharges results in a lower cover percentage of the observed dune heights standard deviation range, see Table 13. The ($\sigma_{min}/\sigma_{max}$) coverage values oscillate from 79.85% to 86.18% for the BEM area and from 36.58% to 41.33% for the BOM area, or 41.98% to 57.86% without considering the two failed to simulate Jun-16 and Dec-17 periods. Eventually, for the BOM area the best accuracy outcomes are found with the monthly-average scenario.

The ideal situation would be to cover 100% of the defined interval. Nevertheless, taking into account that the solution for the BEM area is given in a range of 0.52 meters and that on average the interval defined by the standard deviation is 0.495, it implies that covering 100% of all observation

points is not a feasible solution. Therefore, the obtained results, which show values greater than 80%, are more than acceptable. Likewise, but with lower accuracy results, the BOM model defines a range of 0.22m of possible dune heights while on average the observed data shows a distance of 0.315m between upper and lower standard deviation bounds. The simulated results for the area achieve a coverage width higher than 50% without considering the first and last periods, except for the most frequent discharges scenario. Hence, aware of the model hinders to properly predict the dune height hysteresis and the ambiguity of the last surveyed period data, the performance results are also acceptable.

Table 13: Dune height performance results. Additionally, for BOM the results without Jun-16 and Dec-17 are also shown

Dune Height	***Discharge Scenario***	***BEM***	***BOM***	
n points	Daily Averaged (Default Scenario)	67,22%	32,85%	44,45%
	10 Days-averaged	65,62%	33,03%	44,70%
	Monthly-averaged	63,04%	32,42%	43,85%
	Most frequent	61,71%	29,76%	33,97%
	Corrected Most Frequent	64,19%	31,93%	41,63%
Min/Max	Daily Averaged (Default Scenario)	63,39%	26,01%	32,88%
	10 Days-averaged	63,39%	23,75%	32,88%
	Monthly-averaged	63,39%	25,97%	32,88%
	Most frequent	59,98%	28,41%	32,88%
	Corrected Most Frequent	62,40%	27,82%	32,88%
$\sigma_{min}/\sigma_{max}$	Daily Averaged (Default Scenario)	86,18%	39,40%	55,15%
	10 Days-averaged	82,13%	36,58%	51,21%
	Monthly-averaged	80,56%	41,33%	57,86%
	Most frequent	79,85%	34,90%	41,98%
	Corrected Most Frequent	83,51%	40,26%	56,36%

The analysis is also supported by the percentage of number of points laying within the resulting bandwidth and by the coverage of all the surveyed data values. The later exhibits equal values for the real discharge measurements scenarios for BEM, meaning that the predicted interval fits in the observed data range between maximum and minim for all the periods. Statistical discharge scenarios instead, present gently smaller values as both underestimate the lower bound in Aug-16 and likewise 4 overestimates Feb-17, as that wet period was dryer than the most frequent expected winter. For BOM, all scenarios cover upper and lower bounds inside the minimum and maximum observed values for all periods but, as stated previously, they are all unsuccessful to predict Jun-16 and Feb-18.

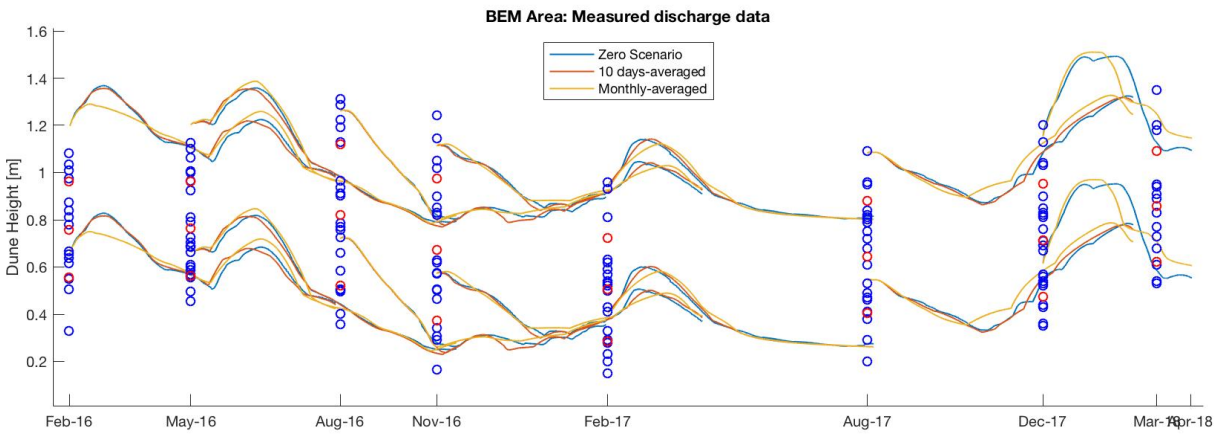

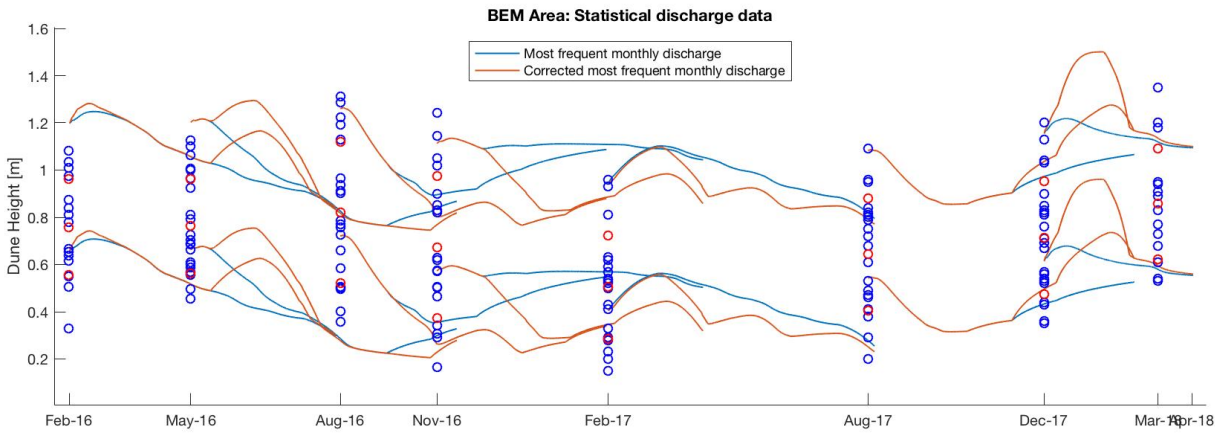

Figure 41: Dune height evolution for all the considered performance scenarios for the BEM area

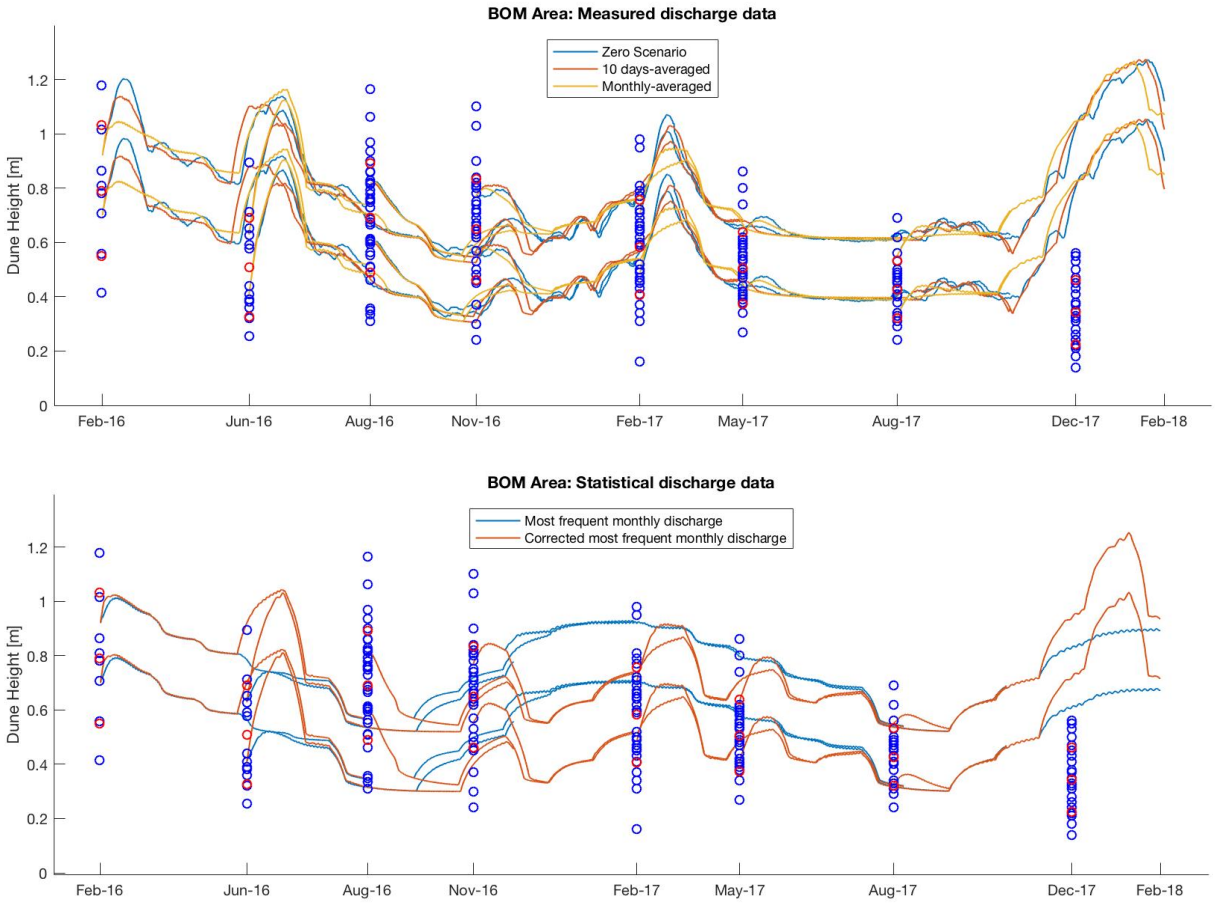

Figure 42: Dune height evolution for all the considered performance scenarios for the BOM area

5. Discussion

Throughout the elaboration of the present project, different steps were exposed to assumptions and criteria which involve a limitation and an uncertainty on the data, resulting on a hindrance on the accuracy of the final obtained results. Therefore, several remarks on the methodology and further developments or applications are necessary to be discussed.

In the absence of an accurate tool to collect the dunes data, as a result of the noisy profile bathymetry signals, criteria were used to manually select the dunes according to De Vries & Van de Wiel purposes. The outcoming range of dune characteristics is limited to the manual dune detection and data compilation procedure, disregarding much of the data from the profiles and generating a subjective uncertainty. The provided outputs are ambiguous, therefore, they should be supported by more data or a more encompassing selective methodology.

For a further study and to be able to overcome this issue, an open source MATLAB software is proposed (Bedforms-ATM). The Bedforms Analysis Toolkit for Multiscale Modelling is a wavelet-based toolkit to analyze the hierarchies and dimensionality of bed forms. The software provides a wavelength spectrum of bedform fields, Figure 43 left, and is able to discriminate bedform fields into three scale-based hierarchies for ripples, dunes and bars (Jerolmack et al. 2005), resulting on a less noisy and averaged-height centered profiles for sand dunes (without small scale ripples and large-scale bars), $h_{2,3}$ in Figure 43 right. The new profiles can be better analyzed with a zero-crossing tool to determine dune troughs and crest and extract every dune characteristic (e.g. Van der Mark & Blom, 2007).

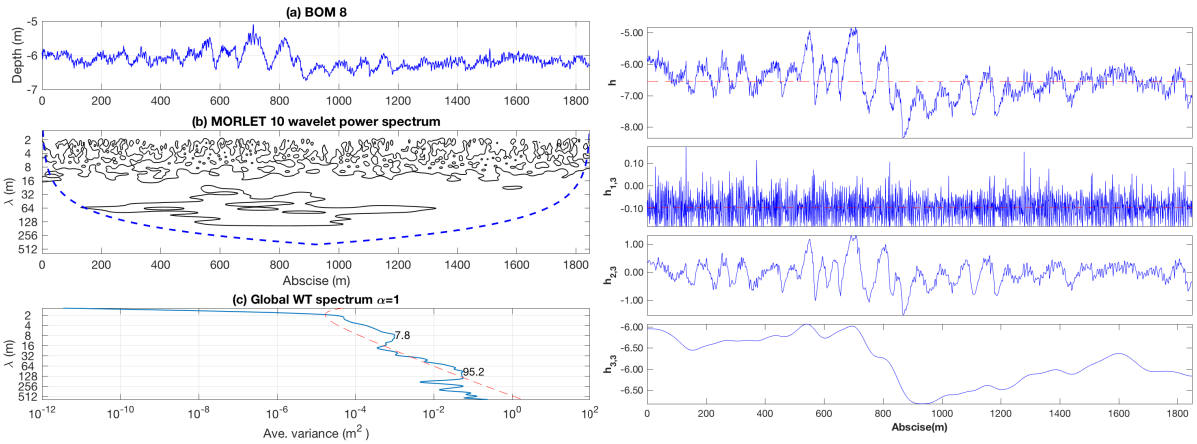

Figure 43: Results for the Wavelet Analysis (left) and bedform scale-based discrimination (right). Example for the BOM area

During the final days of the present project, the proposed methodology (tool) was implemented to support and validate the manually selected and collected data. The average results show a good agreement for the dune heights calculated in both areas (Figure 44). In the BEM area, the tool average results present slightly higher dunes whereas in the BOM area they present slightly lower dunes. Yet, the dune development is similarly displayed for the two areas.

Neither of the two procedures is totally reliable, as the manually dune selection is limited by the subjective criteria but the more encompassing tool methodology still detects some small bed fluctuations as dunes and splits longer dunes in two. However, the obtained results are closely similar for both areas, which validates the initial manually selected data.

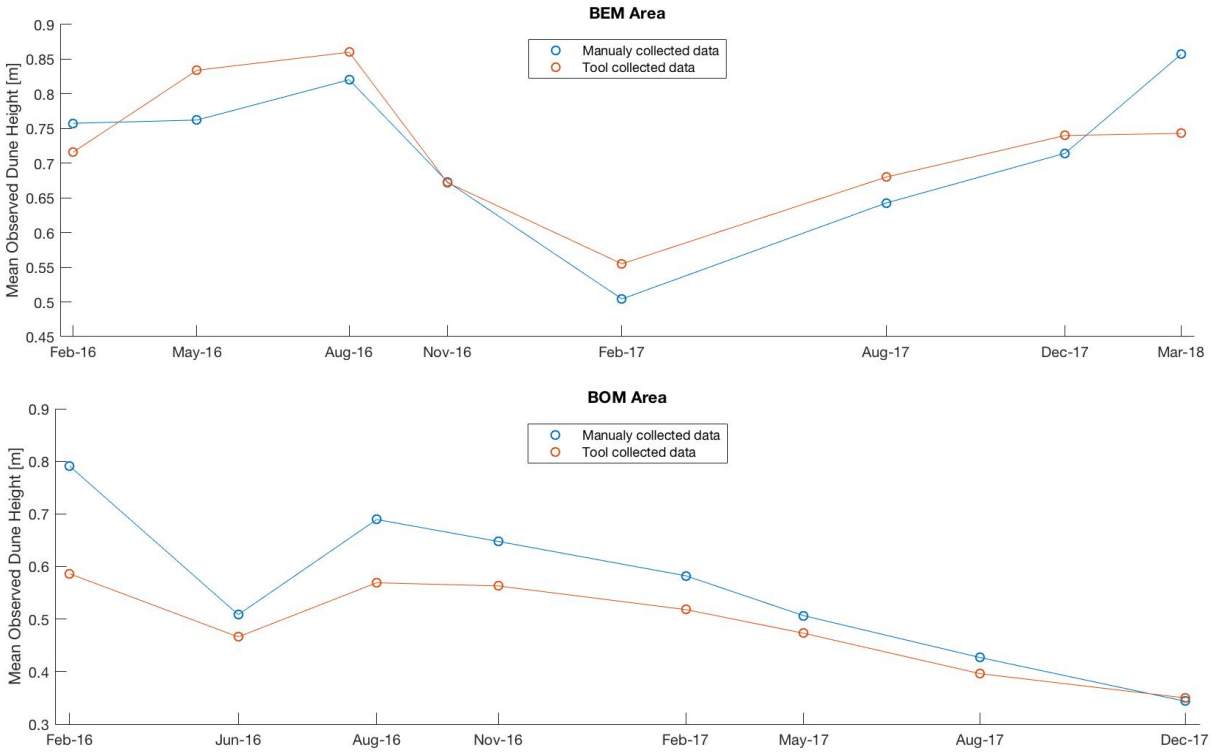

Figure 44: Mean dune heights at each survey period for the manual and tool (Bedforms-ATM + Van der Mark & Blom, 2007) selection of dunes and tool methodology. BEM area (top) and BOM area (bottom)

To propagate the upstream measured discharges at Tiel and Megen and get the specific hydrological data for each location, e.g. discharge, water depth, water level and flow velocities, 37 Delft3D model runs with pairs of varying upstream discharge conditions were used. The assumed data per each location is the average-width model simulated value, which results in a limitation for the simulation of locations with particular flow characteristics. Moreover, the morphological conditions are spatially dependent and exact data for each area is often a constraint, resulting in an interval of possible values. The simulated model outputs are noticeably dependent on the discharges Q (or specific discharge q [m^2/s]), bed slope, i, and grain size, d_{50}, and thus their limitation and ambiguity is a hindrance for the model accuracy.

The calibration of the model to the surveyed data of each area results in two different models with slightly different parameters. This contrast is linked to the difference in the hydraulic processes at each area. The BOM area was chosen for its particular characteristics, dealing with secondary flows effects and water surface tilting developing at the river bend. Therefore, the shallow, considered inner bank area presents lower discharges than the assumed river width-averaged values, forcing the reduction of the h_{ref} factor, stated as an important parameter for the scaling of the model to a river scale.

In addition to the dune height predictions of the model, the model is not able to give proper dune migration rates according to the observed ones. Nevertheless, the analysis on the migration and river discharges at Tiel in section 3.3 allowed to define a simple approach to determine an expected range of migration rates for a specific period of time. The relations between average daily discharge and migration rate per each area are presented in APPENDIX D. Furthermore, the tool performance for every considered scenario in section 4.4.2, is also shown.

The most extreme scenarios model predictions (considering the highest bed slope & the lowest grain size in the area, and the lowest bed slope & the highest grain size) define a range of possible dune heights within the range of the surveyed data. These limits are satisfactory for the BOM area. However, the BEM model showed to underestimate the predicted upper bound, for which an extension of 0.32m was proposed in order to embrace higher surveyed dunes.

The BOM model showed to simulate higher dunes and higher water depths for those few periods at the raising stage of the flood wave, suggesting that it fails to predict proper dune height and water depth hysteresis in the specific inner bend zone. The BEM model seems to predict a good hysteresis approach for the available survey data. However, further observation periods and its analysis are needed to understand the dune height hysteresis at the field during the rising and the falling limbs of a floodwave, in order to improve the model accuracy. The dune height hysteresis could be enlarged by assuming larger step-lengths, hence, by considering more suspended load transport at the increasing discharge stage which would reduce the dune height development and maximum value.

The models are meant to be used to forecast future scenarios. However, as no expected discharge data for the upcoming months was available, no future dune development scenarios were able to be presented. Nonetheless, a final model performance analysis was held considering lower quality discharge situations and supposing the most frequent discharges per month in the past. In that way, the worst real situations were simulated, in which almost no data for the computation of the expected discharge values per month is accessible. Results showed the possibility of considering large monthly blocs of averaged discharges, but suggest to at least correct the estimated values to an upstream analysis and evaluation of the rainfall and hydrological conditions in the catchment area, obtaining more accurate predictions to a possible wetter or dryer period.

Following the necessity of more data during specific hydrological events, which could lead to a proper model calibration by reducing the *NSE*-values, the analysis should be extended to other areas to determine the possibility to use one of the two different parameter models as a globally generalized model for all the areas. The particular hydrodynamics and characteristics of BOM suggest that its final calibrated model is very specific to the area, limiting its use to other non-equal locations, whereas the more common and englobing characteristics of the BEM area, straight river course within a groyne field, make its supposition and incorporation into the rest of the project area more feasible.

To run the model and extend its application to other areas, 4 main inputs are needed: (1) an initial dune profile, (2) an interval of grain size values, d_{50}, found in the area, (3) an interval of bed slope values, i, of the area and (4) the specific discharge, q, for the modelled period.

The whole project area is shown to be highly dominated by the ebb and flood tidal influences. Therefore, many downstream areas showed overturning flows, which mostly involves in the reversing of the dunes according to the predominant flow direction (visible in the Dordtsche Kil and downstream areas of the river Lek). Very likely, the application of the developed tool for the simulation and prediction of sand dunes behavior will result inaccurate in these areas. Therefore, a further study should consider an extension of the actual model or a different model to cover bi-directional flows.

6. Conclusions and Recommendations

6.1. Conclusions

The main purpose of this thesis was to develop a tool for the prediction of the river sand dune dynamic behavior using the Van Duin (2017) dune evolution model. Forecasting solutions are presented for dune height development, as well as for migration rates. Three research questions helped to follow the necessary steps to achieve the final results.

1. *Which are the most important areas for the development of sand dunes?*

Not all river branches are susceptible to develop sand dunes. Both morphological and hydrological conditions are spatially-dependent through the project extension. The hydrological conditions present also a variation in time which is governed by the upstream river discharges (at the river Waal, river Maas and river Lek) and the sea-boundary tidal influences. Therefore, sand dunes where found on the totality or parts of the following river branches: (1) Boven Merwede, (2) Beneden Merwede, (3) Nieuwe Merwede, (4) Amer, (5) Dordtsche Kil, (6) Lek and (7) Oude Maas.

The more downstream a river area is located, that is the closer to the sea-boundary, the higher are the effects of the ebb and flood currents due to the tides. If the upstream river discharge conditions are low and the tidal effects are considerably large, the area presents reverse flows for which dune shape and development is altered. The Dordtsche Kil, the river Lek and the Oude Maas show upstream or downstream pointing sand dunes, depending on the time-period analyzed.

According to the De Vries & Van de Wiel's interests on significant sand dunes that may require dredging and fitting in the dune evolution model limitations to simulate reverse flows, two areas were thoroughly studied. The first area, located at the Beneden Merwede (BEM), comprises a practically straight river segment delimited both sides within a groyne field. The groyne field ensures a concentration of the flow in the center part of the river course and provides more general, straightforward conditions. Small negative discharges are observed during a short stage for each tidal period, but the effects of it are negligible and predominant uni-directional flow can be considered. The second area lays at the inner bank of a river curve at the Boven Merwede (BOM). The area presents only downstream flow but complex hydrodynamics which endow interest to the dune analysis and further application of the model. Velocities in the considered area are lower, which derive to larger sediment deposition rates and lower water depths.

2. *What are the most important processes involved in dune characteristics and behavior?*

The analysis of the dunes data stated that the higher the dunes, the higher the length and the lower the growth ratio during the following period. Dune migration rates barely present a trend respect to the height and length values, suggesting that their rates respond only to the discharges. Dunes in the BEM area present higher values for dune height, length and migration than in the BOM area due to their difference in (1) specific discharges, (2) flow velocities, (3) water levels, (4) bed slope and (5) grain size. The data responds according to the most commonly used scaling relations which link dune dimensions to flow depth in rivers, e.g. Yalin (1964). The BEM area presents practically constant conditions across the river width. The BOM area deals with secondary flows effects and water surface tilting which develop at the river bend. Therefore, the shallow, considered inner bank area presents lower discharges and lower water depths. Moreover, dunes' data in the different parallel profiles prove that higher dunes are found the more to the center of the flow they are located, where discharges and bed elevations are higher.

The growth or decay rates and the daily averaged discharge per period allowed to vaguely determine the threshold between bed load and suspended or load sediment transport regimes. Predominant suspended transport is shown to influence on the decaying behavior of the dune height while the bed load transport in the growing development. At BEM, the sediment transport regime threshold is found at upstream discharges at Tiel between 1000 and 1200m^3/s, and the motion threshold at discharges around 400m^3/s. At BOM, due to the particular characteristics of the area, the

transport regime threshold is displaced to higher discharge values, between 1800 and 1900m^3/s.

At the BOM area, no data relations are found to the 3 dredging campaigns taking place in the nearby Ankervak location.

The occurrence of merging and splitting suggests that merging occurs during peak discharges, either at the increasing phase or the decreasing stage of the floodwave, not enough data to specify. Dune splitting seems to take place mainly during steady low discharges.

3. Can a dune evolution model simulate the observed dunes behavior?

The dune evolution model of Van Duin (2017) is capable of reproducing the morphodynamics, sediment transport gradients and dune height development during dune regime and transition regime, in a suitable order of magnitude. Hence, only few parameters had to be adapted to calibrate the results to the previously collected data.

Two different models with slightly different parameters were calibrated per each area. The shallow inner bank area defining BOM, presents lower discharges, q [m^2/s], and water depths, h [m], than the river width-averaged values that are being considered as inputs. Therefore, the h_{ref} factor which is responsible for the scaling of the model's sediment transport to a river scale, had to be decreased for the area from 0.4166m to 0.2166m to better fit the surveyed dune heights progression. Moreover, the step-length model limits, θ_{min} and θ_{max}, were adjusted to each area. The calibration could still be improved by better defining the step-length model parameter, to which more survey and reliable data would be needed.

The model resulting dune heights are shown to be sensible to the considered bed slope and grain size, which slightly vary within the area. Therefore, the interval of possible values for both input parameters define an upper and lower boundary of the model simulated dune heights. The resulting upper bounds for the BEM area underestimate the higher surveyed dune heights for which an additional upper limit extension of 0.32m is proposed to better cover the observed heights range.

A performance analysis varying the input discharge data quality proved that running the models with a monthly averaged discharge still predicts the dune development properly, in addition to reducing the computational time. These results evidence the ease of applying the model on a future scenario where the unknown discharges induce to work with generic estimated and inaccurate values. On a general basis, the best performance results, computed as the observed σ-range coverage for the simulated dune heights, dune lengths and migration rates, are found for the real daily-averaged measured data. The worst performance is shown for the broadest poor-quality scenario, which considers the most frequent monthly-averaged discharges on a 25 year timeseries statistical analysis. A last scenario correcting those months with a 30% or higher deviation to the most frequent discharges, presents closer results to the exact measured data scenarios, suggesting the need to correlate the input discharges for a future situation based on an evaluation and estimation of the upstream hydrological conditions and expected rainfall events in the river Rijn and river Maas catchment area.

The model predictions underestimate the water depths. The dune length is calculated as a simple factor of 7 times the water depths in the model, being likewise underestimated. However, dunes in the surveys are shown to oscillate on average between 80m and 90m long for the BEM area and 65m to 75m long for the BOM area. Therefore, its exact behavior prediction results irrelevant for the De Vries & Van de Wiel's dredging optimization.

Moreover, the model also fails to give proper dune migration magnitudes. The predicted migration rates are 3 to 4 times higher in the BEM area and 1 order of magnitude higher for the BOM area, from the surveyed 10ths of cm/day to the predicted 1.5-2.5 m/day values. Nevertheless, after the relation analysis on the migration rates and the daily average discharges at the river Waal (Tiel), two boundary limit functions defining a range of possible values for BEM and BOM were suggested.

6.2. Recommendations

The following recommendations are proposed to further studies or additional model applications:

Improvement of the models

The model results show accordance to the survey points data. Nevertheless, no survey periods lay during the expected maximum dune heights after a peak discharge. Therefore, in order to improve the model and in order to better predict the maximum dune heights and hysteresis during a floodwave, more survey points are needed. A special emphasis should be made on data recording the dune evolution during the pass of a floodwave.

Recommendations of use (for BEM and BOM models)

The models can be used to speculate the growth or decay of the range of dune heights present in the BEM area and BOM area over 6 months in advance. These results can be coupled to the new bathymetries predicted by the Delft3D model, in which the initial sand dunes re-appear, to determine their new characteristics and the maximum bed elevation. Therefore, it is possible to verify the predicted river depths to the minimal contractual depths, to which, if surpassed, the volume to be dredged can be approximated. For more information on the downstream movement of these bed patterns, the range of probable dune migration rates can be predicted by the approach given in APPENDIX D.

The steps to apply the model and obtain the results are the following:

- From previous survey (initial time-step, t_0) extract dune height and length and create input bedform profile with the averaged dune characteristics.
- Create floodwave input with the expected discharges for the considered period. Divide the discharges in steps of 12 hours (which are equivalent to steps of 240 seconds in the simulation). Discharges can be monthly averaged, although the shorter the averaged period the better.
- Simulate runs and apply the proposed upper and bottom extended limits (in section 4.4.1).
- From the model results extract the dune height range at the desired period of simulation.
    - Additionally, extract the range of expected migration rates.
- From the outcoming ranges and knowing the initial range of dune heights, the expected dune growth or decay can be computed.
- Apply the expected growth or decay range to the sand dunes on the Delft3D predicted bathymetry.

Recommendations to extend the model to other areas

The BEM model can be extended to practically every other river segment as long as the area does not present considerable reverse flow. Nevertheless, an analysis on the model results to past surveyed data should be done to validate it and suggest the new solution range limit extensions for the area.

Four main inputs are needed: (1) an initial dune profile, (2) an interval of grain size values, d50, found in the area, (3) an interval of bed slope values, i, of the area and (4) the specific discharge, q, for the modelled area and period. For specific hydrodynamic areas (river bends, confluences, bifurcations and other), working with general width-averaged discharges should be avoided and it is recommended to use the closest specific discharge characteristics for the considered perimeter.

Furthermore, a quick analysis simulating the most extreme scenarios at the considered area (highest bed slope and lowest grain size & lowest bed slope and highest grain size), will reveal the need to apply an additional limit extension or not to the range covered by the results of the two modelruns.

7. References

Aberle, J., Coleman, S., & Nikora, V. (2012). Bed Load Transport by Bed Form Migration. *Acta Geophysica , 60* (6), 1720-1743.

Best, J. (2005). The fluid dynamics of river dunes: A review and some future research directions. *Journal of Geophysical Research , 110*.

Bradley, R., & Venditti, J. (2017). Reevaluating dune scaling relations. *Earth-Science Reviews , 165*, 356-376.

Coleman, S., Zhang, M., & Clunie, T. (2005). Sediment-Wave Development in Subcritical Water Flow. *Journal of Hydraulic Engineering ASCE*.

Dörrbecker, M. (n.d.). *Wikipedia*. Retrieved March 2018, from Partition of Rhine and Meuse water among the various branches of their delta: https://en.wikipedia.org/wiki/Rhine–Meuse–Scheldt_delta#/media/File:Map_of_the_annual_average_discharge_of_Rhine_and_Maas_2000-2011_(EN).png

Daggenvoorde, R. (2016). *Upper Stage Plane Bed in the Netherlands.* University of Twente, Water Engineering and Management (WEM).

De Vriend, H. (1981). *Steady flow in shallow channel bends.* Civil Engineering and Geosciences, TU Delft, Hydraulic Engineering.

Fredsøe, J. (1981). Unsteady flow in straight alluvial streams. Part 2. Transition from dunes to plane bed. *Journal of Fluid Mechanics , 102*, 431-453.

Gabel, S. (1993). Geometry and kinematics of dunes during steady and unsteady flows in the Calamus River, Nebraska, USA. *Sedimentology , 40* (2), 237-269.

Gaeuman, D., & Jacobson, R. (2007). Field Assessment of Alternative Bed-Load Transport Estimators. *Journal of Hydraulic Engineering* , 1319-1328.

Gutierrez, R. (2016, November 21). Bedforms-ATM. *https://sourceforge.net/projects/bedforms-atm/* . Peru.

Holmes, R., & Garcia, M. (2008). Flow over bedforms in a large sand-bed river: a field investigation. *Journal of Hydraulic Resources , 46* ((3)), 322-333.

Hulscher, S. (1996). Tidal-induced large-scale regular bedform patterns in a three-dimensional shallow water model. *Journal of Geophysical Research , 101*, 20,727-20,744.

Hulscher, S., & Dohmen-Janssen, C. (2005). Introduction to special section on Marine Sand Wave and River Dune Dynamics. *Journal of Geophysical Research , 110*.

Jerolmack, D., & Mohrig, D. (2005). A unified model for subaqueous bedform dynamics. *Water Resources Research , 41* (W12421).

Julien, P., ASCE, & Klassen, G. J. (1995). Sand-dune geometry of large rivers during floods. *Journal of hydraulic engineering* .

Julien, P., Klaassen, G., Ten Brinke, W., & Wilbers, A. (2002). Case Study: Bed resistance of Rhine River during 1998 flood. *Journal of Hydraulic Engineering , 128* (12), 1042-1050.

Kennedy, J., & Odgaard, A. (1991). *Informal Monograph on Riverine Sand Dunes.* University of California. U.S. Army Engineer Waterways Experiment Station.

Kostaschuk, R. (2002). A field study of turbulence and sediment dynamics over subaqueous dunes with flow separation. *Sedimentology , 47* (3), 519-531.

Kostaschuk, R., & Best, J. (2005). Response of sand dunes to variations in tidal flow: Fraser Estuary, Canada. *J. Geophys. Res. , 110*.

Kostaschuk, R., Shugar, D., Best, J., Parsons, D., Lane, S., Hardy, R., et al. (2009). Suspended sediment transport and deposition over a dune: Río Paraná, Argentina. *Eart Surface Processes and Landforms , 34* (12), 1605-1611.

Martin, R., & Jerolmack, D. (2013). Origin of Hysteresis in Bed Form Response to Unsteady Flows. *Water Resources Research , 49*.

Meyer-Peter, E., & Müller, R. (1948). Formulas for bed load transport. (pp. 39-64). Stockholm: Proceedings of the 2nd meeting of the Int. Assoc. for Hydroaul. Environ. Eng. and Res.

Mol, A. (2003). *Morfologische gevolgen van rivierverruimende maatregelen langs de Merweden.* Universiteit Twente, WEM.

Nabi, M., Vriend, H., Mosselman, E., Sloff, C., & Shimizu, Y. (2013). Detailed simulation of morphodynamics: 3. Ripples and dunes. *Water Resour. Res. , 49*.

Nakagawa, H., & Tsujimoto, T. (1980). Sand bed instability due to bed load motion. *Journal of the Hydraulics Division , 106* (12), 2029-2051.

Naqshband, S., Ribberink, J., Hurther, D., & Hulscher, S. (2014). Bed load and suspended load contributions to migrating sand dunes in equilibrium. *Journal of Geophysical Research: Earth Surface , 119*, 1043-1063.

Paarlberg, A., & Schielen, R. (2012). Integration of a dune roughness model with a large-scale flow model. In: Murillo. *Proc. of River Flow 2012,*, (pp. 155-161). Costa Rica.

Paarlberg, A., Dohmen-Janssen, C., Hulscher, S., & Termes, A. (2009). Modelling river dune evolution using a parameterization of flow separation. *Journal of Geophysical Research. Pt. F: Earth surface , 114* (F01014).

Paarlberg, A., Dohmen-Janssen, C., Hulscher, S., & Termes, P. (2007). A parameterization of flow separation over sub-aqueous dunes. *Water Resources Research , 43* (12), W12417-1-W12417-10.

Paarlberg, A., Dohmen-Janssen, C., Hulscher, S., Termes, P., & Schielen, R. (2010). Modelling the effect of time-dependent river dune evolution on bed roughness and stage. *Eart Surface Processes and Landforms , 35* (15), 1854-1866.

Paarlberg, A., Dohmen-Janssen, C., Hulscher, S., van den Berg, J., & Termes, A. (2006). Modelling morphodynamic evolution of river dunes. In R. Ferreira, E. Alves, J. Leal, & A. Cardoso (Ed.), *International Conference on Fluvial Hydraulics: River Flow.* Lisbon: Taylor & Francis Group.

Sekine, M., & Kikkawa, H. (1992). Mechanics of Saltating Grains II. *Journal of Hydraulic Engineering , 118* (4), 536-558.

Shimizu, Y., Giri, S., Yamaguchi, I., & Nelson, J. (2009). Numerical simulation of dune-flat bed transition and stage-discharge relationship with hysteresis effect. *Water Resources Research , 45* (W04429).

Smith, J., & McLeam, S. (1977). Spatially-averaged flow over a wavy surface. *Journal of Geophysical Research , 82*, 1735-1746.

STOWA-RIZA. (1999). *Good Modelling Practice Handbook.* Dutch Dept. of Public Works, Institute for Inland Water Management and Waste Water Treatment. report 99.036, 167pp.

Ten Brinke, W., Willbers, A., & Wesseling, C. (1999). Dune growth, decay and migration rates during a large-magnitude flood at a sand and mixed sand-gravel bed in the Dutch Rhine river system. *Fluvial Sedimentology VI , 28*, 15-32.

Tsujimoto, T., Mori, A., Okabe, T., & Ohmoto, T. (1990). Non-equilibrium sediment transport: a generalized model. *Journal of Hydroscience and Hydraulic Engineering , 7* (2), 1-25.

Van Den Berg, J., & Van Gelder, A. (1993). Prediction of suspended bed material transport in flows over slit and very fine sand. *Water Resources Research , 29*.

Van der Mark, C., & Blom, A. (2007). *A new and widely applicable tool for determining the geometric properties of bedforms.* University of Twente, Water Engineering & Management (WEM). Enschede: Marine and Fluvial Systems.

Van Duin, O., Hulscher, S., Ribberink, J., & Dohmen-Janssen, C. (2017). Modeling of Spatial Lag in Bed-Load Transport Processes and Its Effect on Dune Morphology. *Journal of Hydraulic Engineering , 143* (2), 04016084.

Van Duin, O., Ribberink, J., Dohmen-Janssen, C., & Hulscher, S. (2012). Particle step length variation along river dunes. In R. Muñoz (Ed.), *Proceedings of the International conference on fluvial hydraulics. 1*, pp. 493-497. San Jose, Costa Rica: London, UK: CRC Press Taylor & Francis Group.

Van Stokkom, H. T., Smits, A. J., & Leuven, R. S. (2005). *Flood Defense in The Netherlands: A New Era, a New Approach.* International Water Resources Association.

Venditti, J., Church, M., & Bennet, S. (2005a). Bedform initiation from a flat sand bed. *Journal of Geophysical Research , 110* (F01009).

Venditti, J., Church, M., & Bennett, S. (2005b). Morphodynamics of small-scale superimposed sand waves over migrating dune bed forms. *Water Resources Research. , 41* (W10423).

Vriend, D. (1981). *Steady flow in shallow channel bends.* Delft.

Warmink, J. (2014). Dune dynamics and roughness under gradually varying flood waves, comparing flume and field observations. *Advances in Geosciences , 39*, 115-121.

Warmink, J., Dohmen-Janssen, C., Lansink, J., Naqshband, S., Van Duin, O., Paarlberg, A., et al. (2014). Understanding river dune splitting through flume experiments and analysis of a dune evolution model. *Earth Surface Processes and Landforms , 39*, 1208-1220.

Yalin, M. (1964). Geometrical properties of sand waves. *Journal of the Hydraulics Division , 90* ((5)), 105-119.

APPENDIX A: Dune Tracking

Figure 45: Detailed dune tracking lines for the BEM area

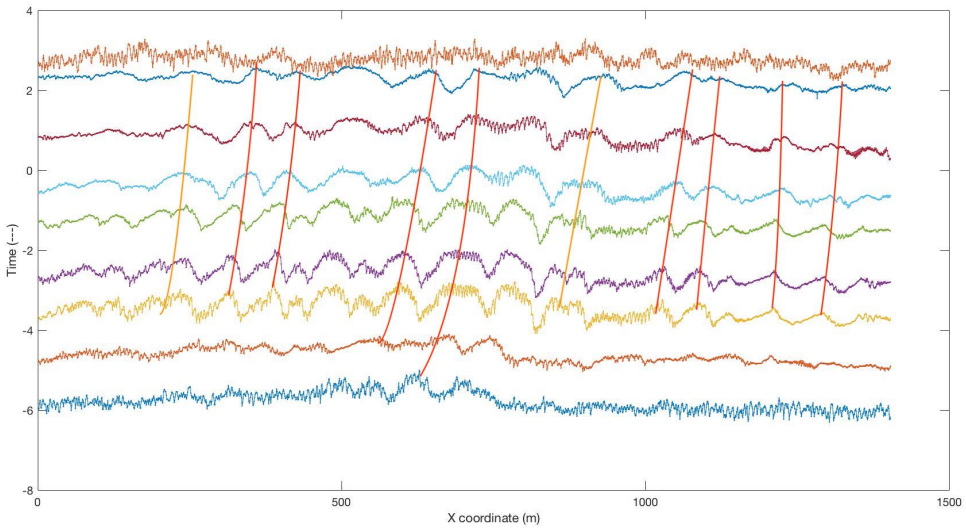

Figure 46: Cross section 2, and dune tracking lines (orange = not possible to track) for the BOM area

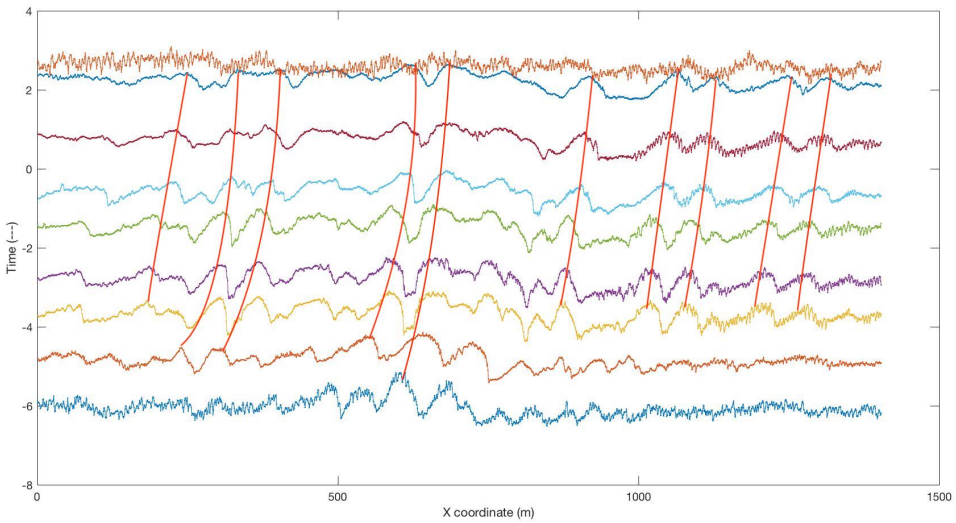

Figure 47: Cross section 3, and dune tracking lines for the BOM area

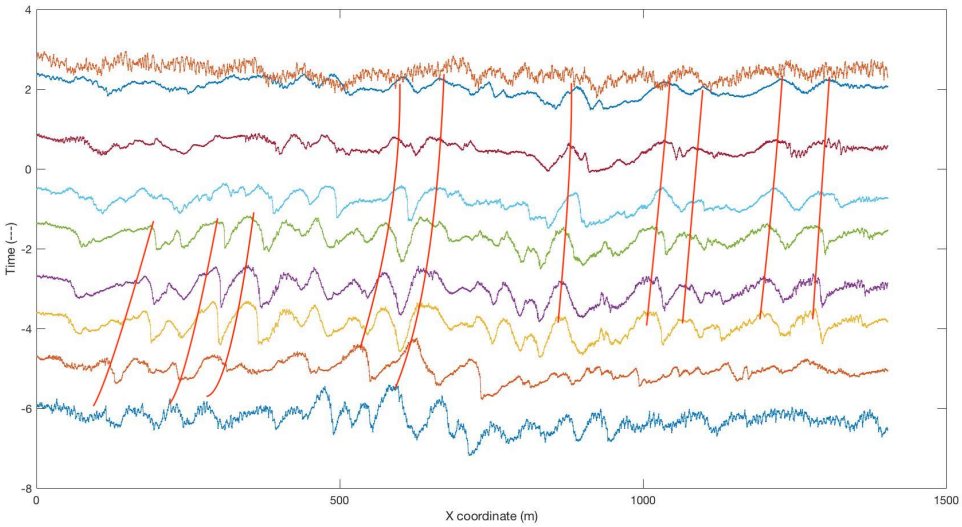

Figure 48: Cross section 4, and dune tracking lines for the BOM area

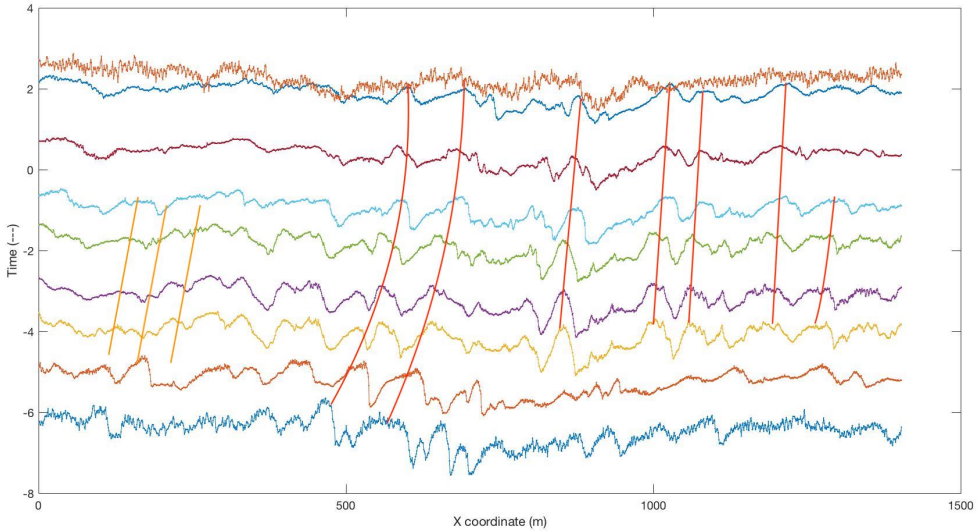

Figure 49: Cross section 5, and dune tracking lines (orange = not possible to track) for the BOM area

Table 14: Collected dune height data

Time-period	H MAX	H MEAN	H MIN	H Q1	H MEDIAN	H Q3
			BEM			
1	1,083	**0,758**	0,328	0,639	0,759	0,875
2	1,125	**0,762**	0,454	0,605	0,703	0,945
3	1,312	**0,820**	0,357	0,565	0,778	1,007
4	1,244	**0,673**	0,164	0,493	0,624	0,864
5	0,960	**0,504**	0,150	0,330	0,530	0,590
6	1,090	**0,643**	0,200	0,465	0,680	0,815
7	1,200	**0,714**	0,350	0,535	0,690	0,840
8	1,350	**0,857**	0,530	0,718	0,718	0,943
			BOM			
1	1,179	**0,791**	0,414	0,669	0,795	0,901
2	0,893	**0,508**	0,255	0,382	0,440	0,626
3	1,163	**0,689**	0,310	0,580	0,685	0,817
4	1,100	**0,648**	0,240	0,530	0,660	0,745
5	0,980	**0,582**	0,160	0,455	0,600	0,680
6	0,860	**0,506**	0,270	0,405	0,490	0,570
7	0,690	**0,427**	0,240	0,350	0,440	0,478
8	0,560	**0,344**	0,140	0,245	0,340	0,425

Table 15: Collected dune length data

Time-period	L MAX	L MEAN	L MIN	L Q1	L MEDIAN	L Q3
			BEM			
1	165,00	**83,28**	46,20	55,00	68,80	91,00
2	183,00	**87,81**	43,00	58,95	88,45	99,92
3	147,42	**80,14**	42,00	59,69	73,90	95,70
4	139,56	**86,88**	39,00	62,73	89,00	102,23
5	143,50	**85,58**	35,00	64,90	78,80	107,00

6	153,30	**73,57**	50,10	58,00	65,00	80,55
7	141,50	**88,29**	47,20	71,90	81,00	103,65
8	287,00	**137,64**	51,20	88,00	88,00	149,23
			BOM			
1	96,90	**64,68**	48,15	50,90	62,00	73,35
2	91,50	**67,44**	28,40	59,30	65,40	83,30
3	110,30	**70,73**	46,30	58,30	69,30	76,15
4	110,30	**72,26**	49,50	61,55	70,00	79,05
5	111,90	**71,25**	40,40	61,00	68,50	78,90
6	118,00	**75,30**	38,00	61,00	73,10	88,00
7	114,00	**78,37**	50,00	67,10	77,20	90,15
8	111,00	**77,81**	42,70	59,53	77,25	91,55

Table 16: Collected dune migration rate data

Time-period	***M MAX***	***M MEAN***	***M MIN***	***M Q1***	***M MEDIAN***	***M Q3***
			BEM			
1	107,23	**32,62**	-18,07	6,02	23,73	43,86
2	153,92	**41,52**	-4,82	13,43	24,22	54,49
3	43,94	**27,61**	4,55	22,39	28,48	33,83
4	54,70	**32,85**	2,48	26,82	34,44	38,39
5	64,97	**29,47**	6,10	22,87	29,38	32,74
6	75,33	**51,77**	25,83	45,00	50,75	61,67
7	125,64	**55,81**	7,69	21,79	47,95	94,26
			BOM			
1	62,53	**31,81**	1,72	10,18	32,63	51,77
2	80,84	**45,97**	0,84	32,53	37,11	74,58
3	20,97	**2,97**	-20,83	0,00	3,61	6,46
4	18,92	**2,84**	-12,16	0,81	3,60	6,22
5	56,86	**30,07**	7,14	20,43	29,43	38,00
6	16,19	**-0,14**	-12,38	-6,79	-0,05	4,17
7	17,36	**8,31**	-5,79	5,29	9,13	12,23

Table 17: Collected dune growth rate data

Time-period	***G MAX***	***G MEAN***	***G MIN***	***G Q1***	***G MEDIAN***	***G Q3***
			BEM			
1	0,810	**-0,007**	-0,458	-0,227	-0,064	0,175
2	0,597	**0,046**	-0,630	-0,163	0,053	0,216
3	0,156	**-0,223**	-0,861	-0,325	-0,187	-0,062
4	0,203	**-0,140**	-0,409	-0,262	-0,159	-0,027
5	0,311	**0,090**	-0,277	-0,028	0,138	0,189
6	0,492	**0,060**	-0,375	-0,088	0,058	0,217
7	1,179	**0,156**	-0,462	-0,147	0,192	0,401
			BOM			
1	0,030	**-0,270**	-0,472	-0,436	-0,294	-0,137
2	0,788	**0,278**	-0,055	0,018	0,182	0,565

3	0,063	**-0,058**	-0,235	-0,099	-0,062	0,008
4	0,045	**-0,059**	-0,216	-0,104	-0,045	-0,018
5	0,071	**-0,127**	-0,414	-0,193	-0,129	-0,043
6	0,067	**-0,080**	-0,267	-0,131	-0,062	-0,021
7	0,041	**-0,069**	-0,198	-0,114	-0,066	-0,027

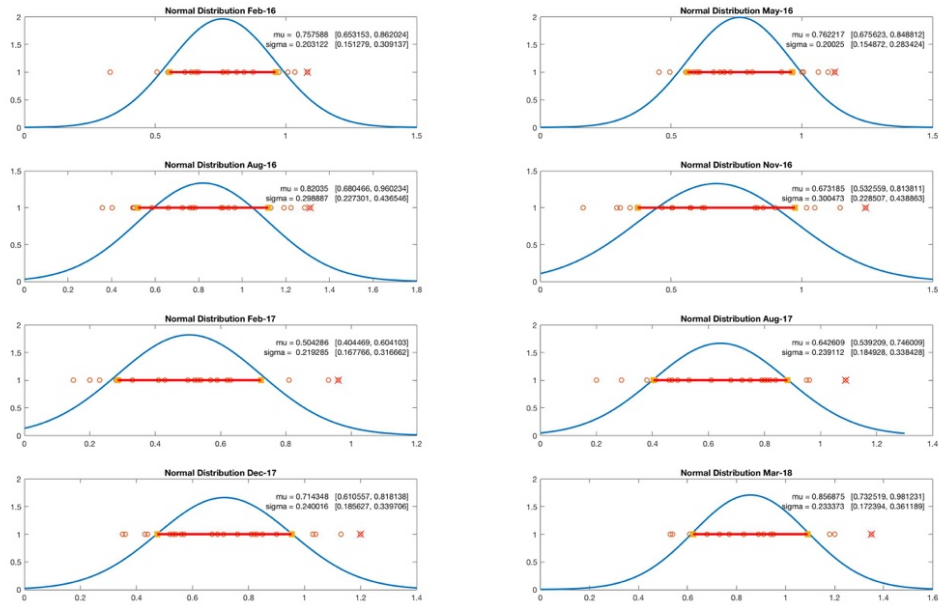

Figure 50: Dune height distribution for the BEM area

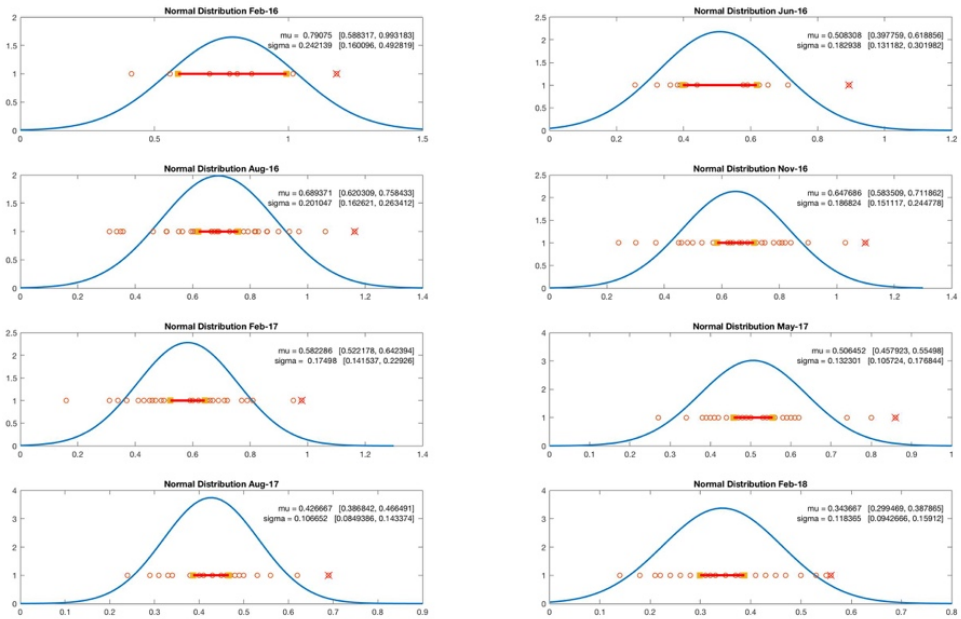

Figure 51: Dune height distribution for the BOM area

APPENDIX B: Data Analysis

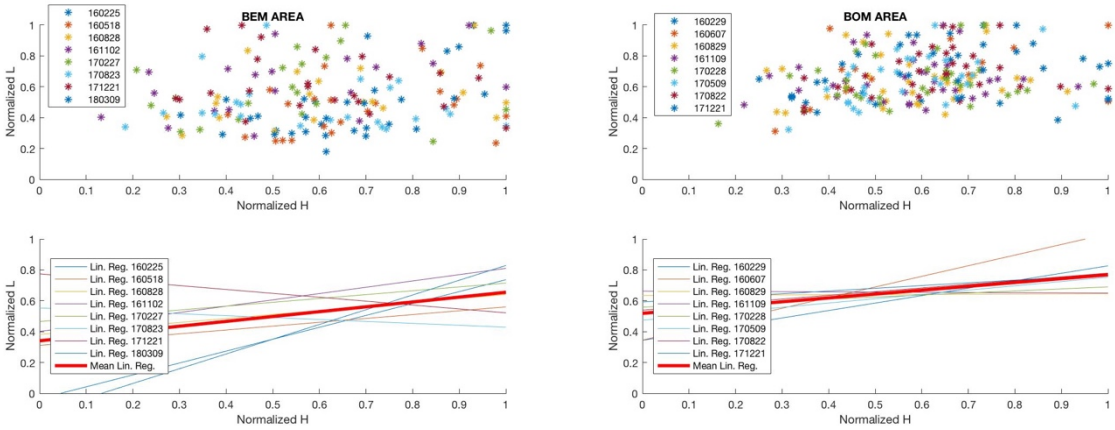

Figure 52: Normalized dune height (H) against normalized dune length (L)

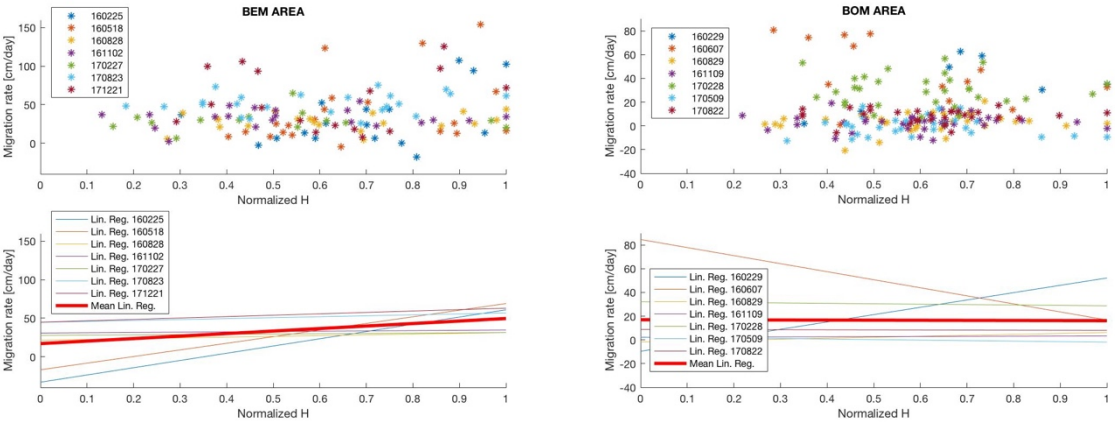

Figure 53: Normalized dune height (H) against migration rate (M)

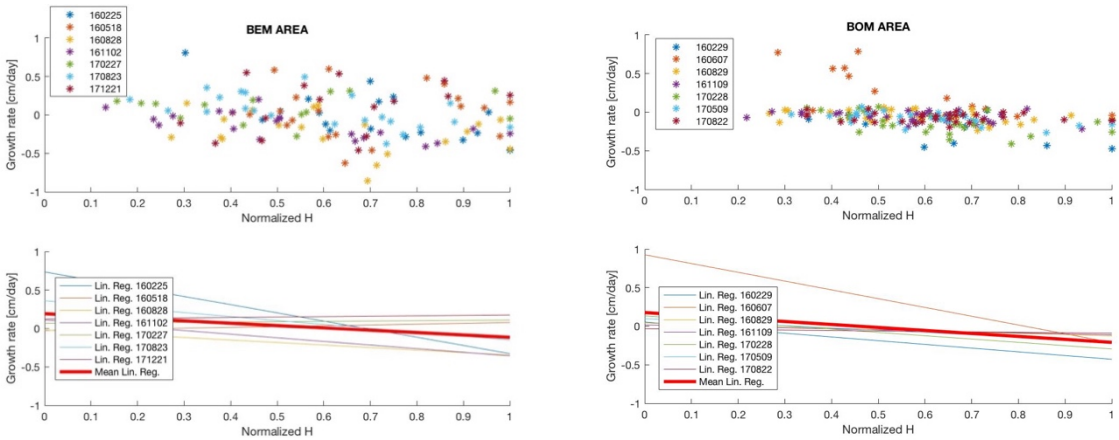

Figure 54: Normalized dune height (H) against growth/decay rate (G)

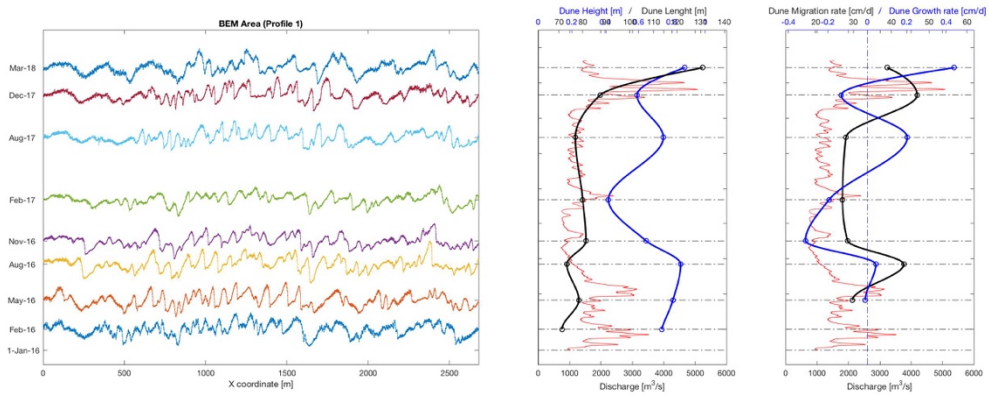
BEM Area (Profile 1)
Mar-18
Dec-17
Aug-17
Feb-17
Nov-16
Aug-16
May-16
Feb-16
1-Jan-16
X coordinate [m]
Dune Height [m] / Dune Lenght [m]
Discharge [m³/s]
Dune Migration rate [cm/d] / Dune Growth rate [cm/d]
Discharge [m³/s]

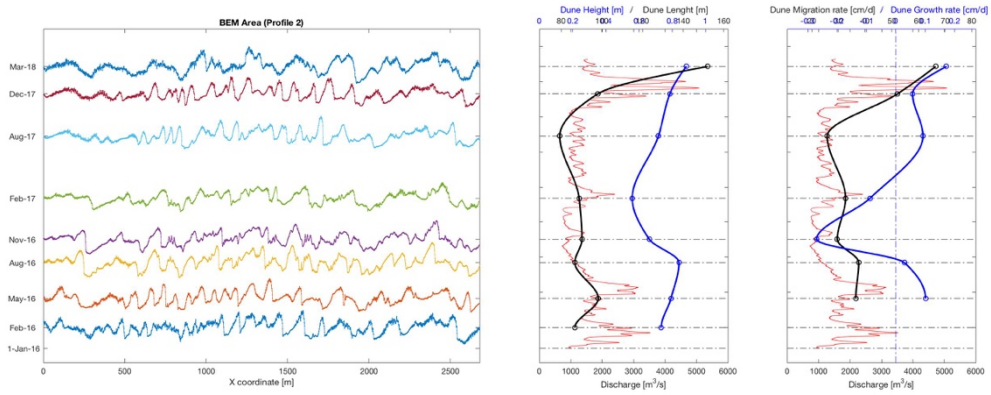
BEM Area (Profile 2)
Mar-18
Dec-17
Aug-17
Feb-17
Nov-16
Aug-16
May-16
Feb-16
1-Jan-16
X coordinate [m]
Dune Height [m] / Dune Lenght [m]
Discharge [m³/s]
Dune Migration rate [cm/d] / Dune Growth rate [cm/d]
Discharge [m³/s]

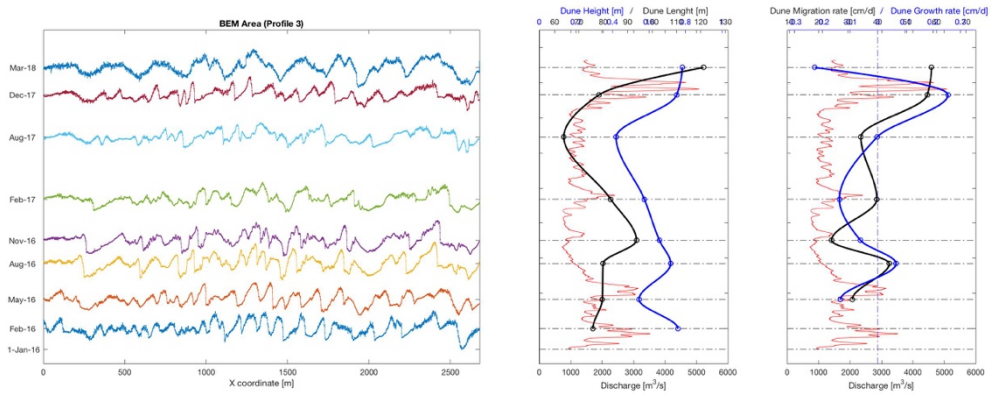
BEM Area (Profile 3)
Mar-18
Dec-17
Aug-17
Feb-17
Nov-16
Aug-16
May-16
Feb-16
1-Jan-16
X coordinate [m]
Dune Height [m] / Dune Lenght [m]
Discharge [m³/s]
Dune Migration rate [cm/d] / Dune Growth rate [cm/d]
Discharge [m³/s]

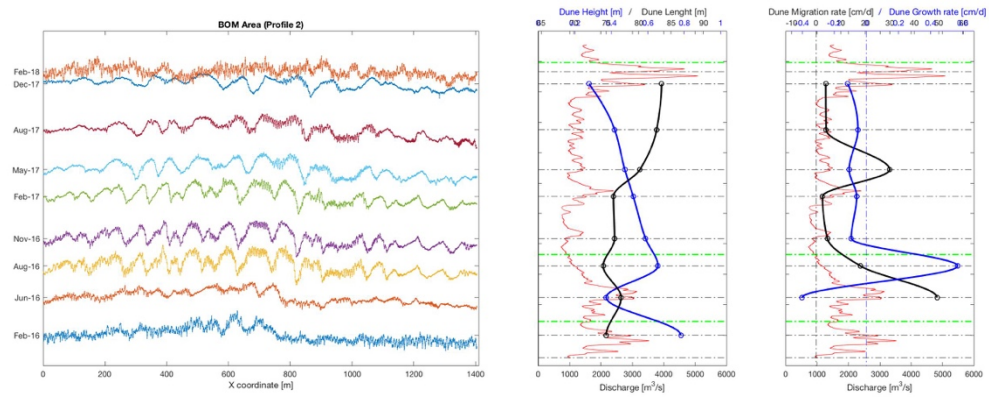
BOM Area (Profile 2)
Feb-18
Dec-17
Aug-17
May-17
Feb-17
Nov-16
Aug-16
Jun-16
Feb-16
X coordinate [m]
Dune Height [m] / Dune Lenght [m]
Discharge [m³/s]
Dune Migration rate [cm/d] / Dune Growth rate [cm/d]
Discharge [m³/s]

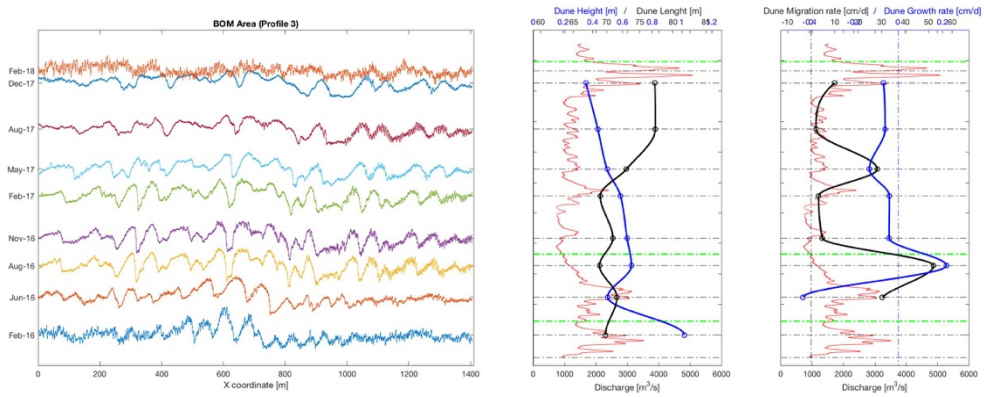
BOM Area (Profile 3)
Feb-18
Dec-17
Aug-17
May-17
Feb-17
Nov-16
Aug-16
Jun-16
Feb-16
X coordinate [m]
Dune Height [m] / Dune Lenght [m]
Discharge [m³/s]
Dune Migration rate [cm/d] / Dune Growth rate [cm/d]
Discharge [m³/s]

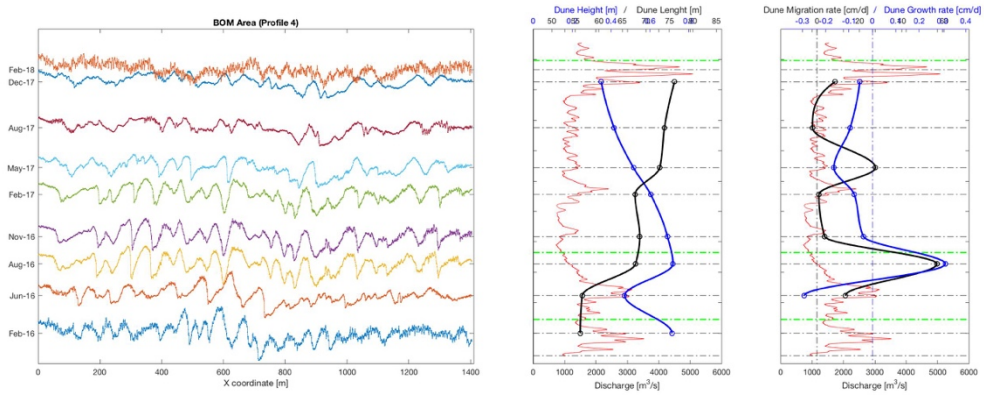
BOM Area (Profile 4)
Feb-18
Dec-17
Aug-17
May-17
Feb-17
Nov-16
Aug-16
Jun-16
Feb-16
X coordinate [m]
Dune Height [m] / Dune Lenght [m]
Discharge [m³/s]
Dune Migration rate [cm/d] / Dune Growth rate [cm/d]
Discharge [m³/s]

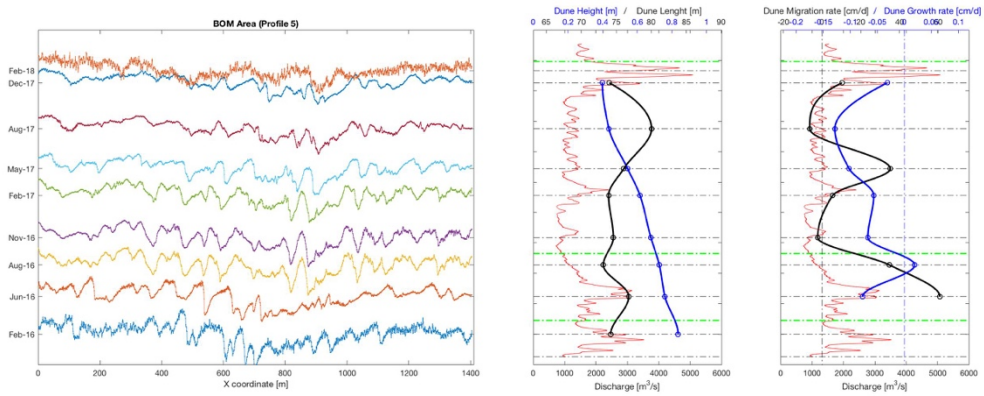
BOM Area (Profile 5)
Feb-18
Dec-17
Aug-17
May-17
Feb-17
Nov-16
Aug-16
Jun-16
Feb-16
X coordinate [m]
Dune Height [m] / Dune Lenght [m]
Discharge [m³/s]
Dune Migration rate [cm/d] / Dune Growth rate [cm/d]
Discharge [m³/s]

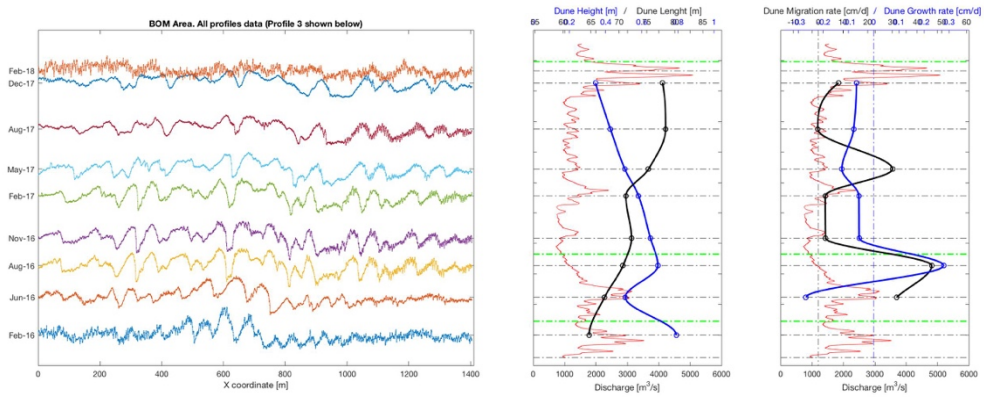
BOM Area. All profiles data (Profile 3 shown below)
Feb-18
Dec-17
Aug-17
May-17
Feb-17
Nov-16
Aug-16
Jun-16
Feb-16
X coordinate [m]
Dune Height [m] / Dune Lenght [m]
Discharge [m³/s]
Dune Migration rate [cm/d] / Dune Growth rate [cm/d]
Discharge [m³/s]

APPENDIX C: Model Results

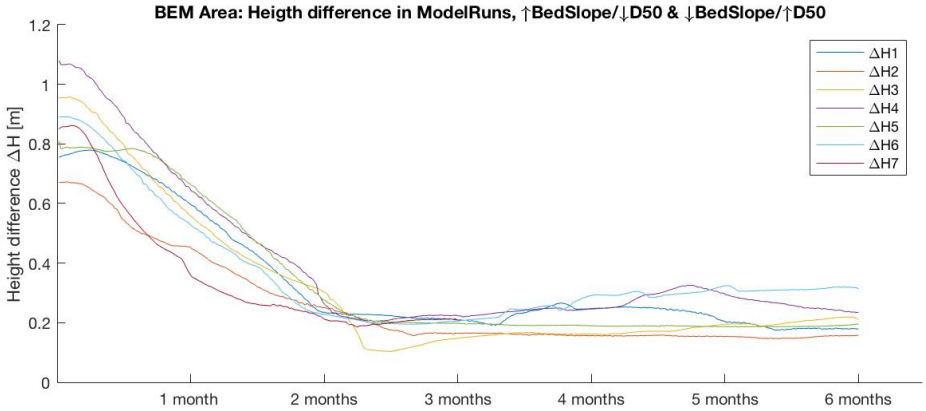

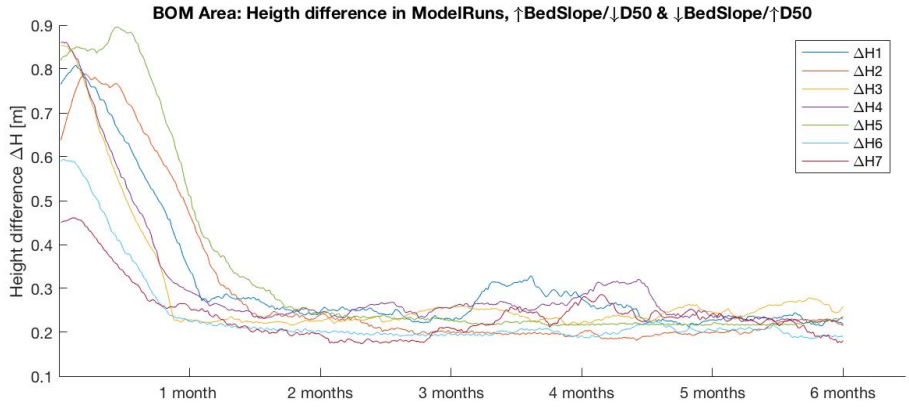

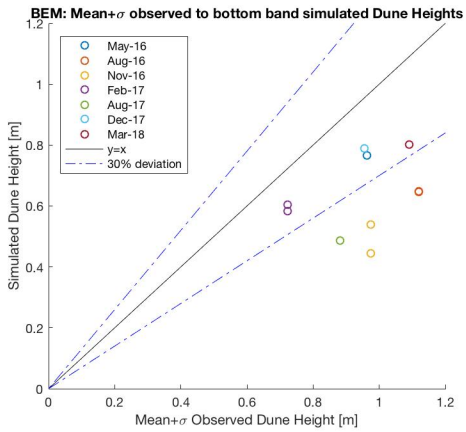

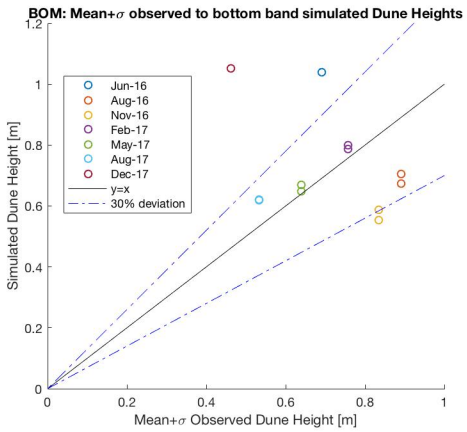

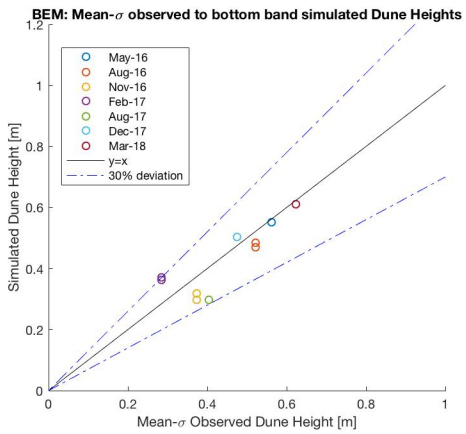

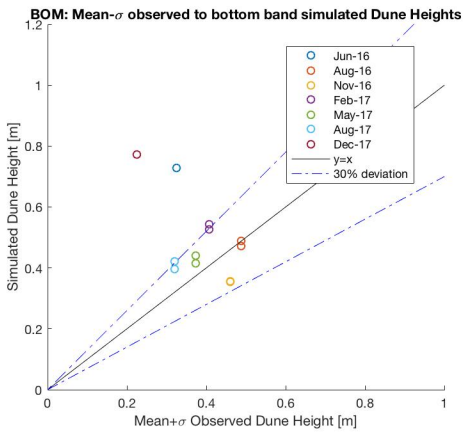

Performance analysis

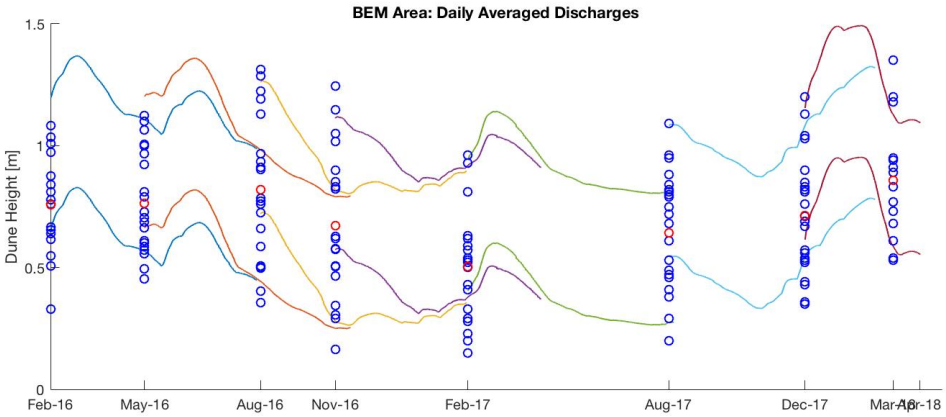

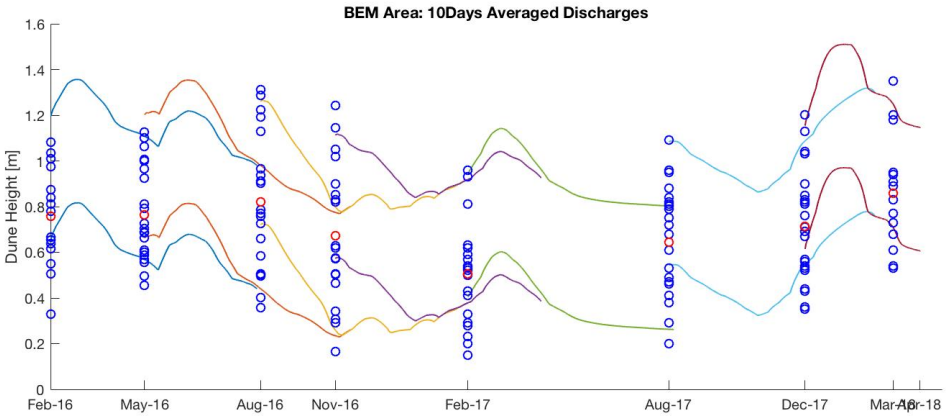

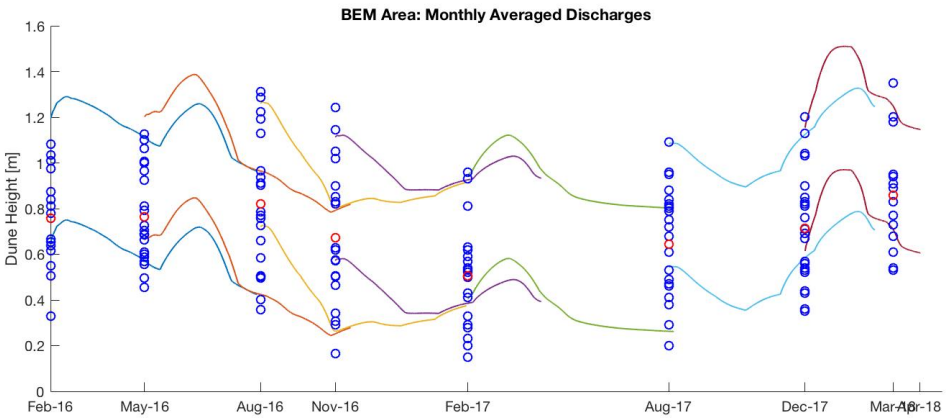

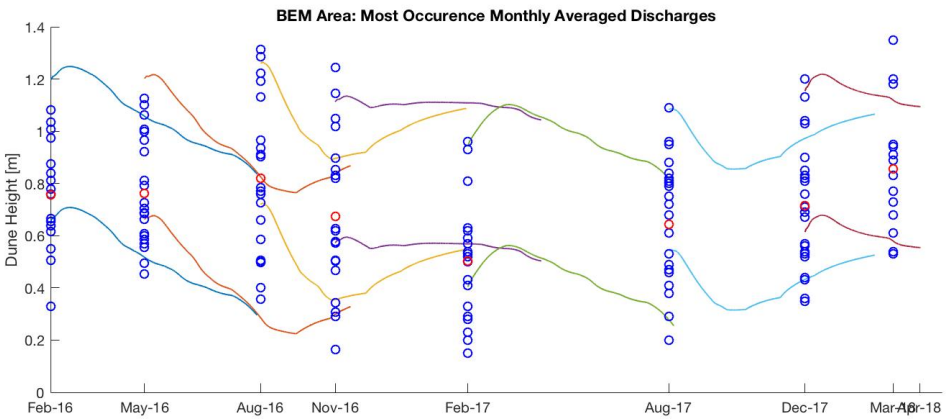

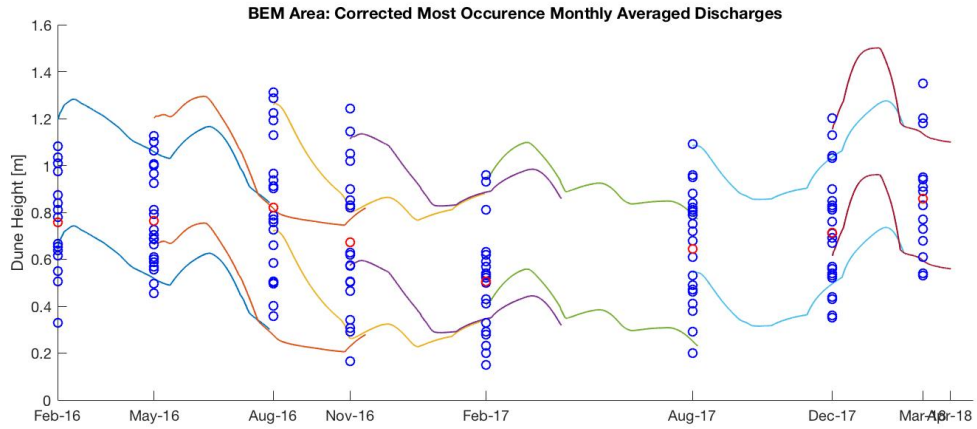
BEM Area: Corrected Most Occurence Monthly Averaged Discharges
Dune Height [m]
0
0.2
0.4
0.6
0.8
1
1.2
1.4
1.6
Feb-16
May-16
Aug-16
Nov-16
Feb-17
Aug-17
Dec-17
Mar-18
Apr-18

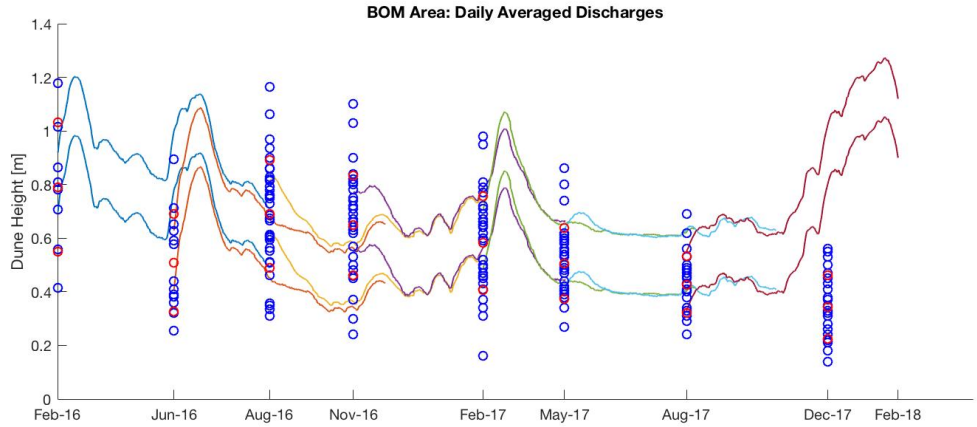
BOM Area: Daily Averaged Discharges
Dune Height [m]
0
0.2
0.4
0.6
0.8
1
1.2
1.4
Feb-16
Jun-16
Aug-16
Nov-16
Feb-17
May-17
Aug-17
Dec-17
Feb-18

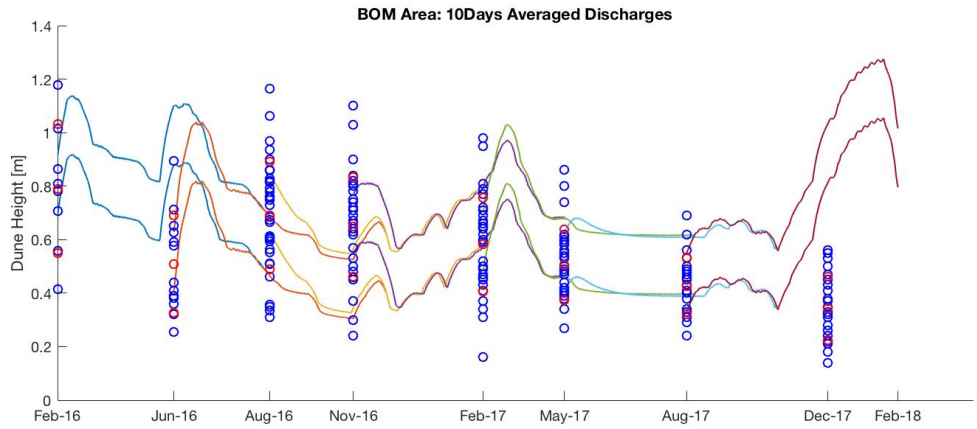
BOM Area: 10Days Averaged Discharges
Dune Height [m]
0
0.2
0.4
0.6
0.8
1
1.2
1.4
Feb-16
Jun-16
Aug-16
Nov-16
Feb-17
May-17
Aug-17
Dec-17
Feb-18

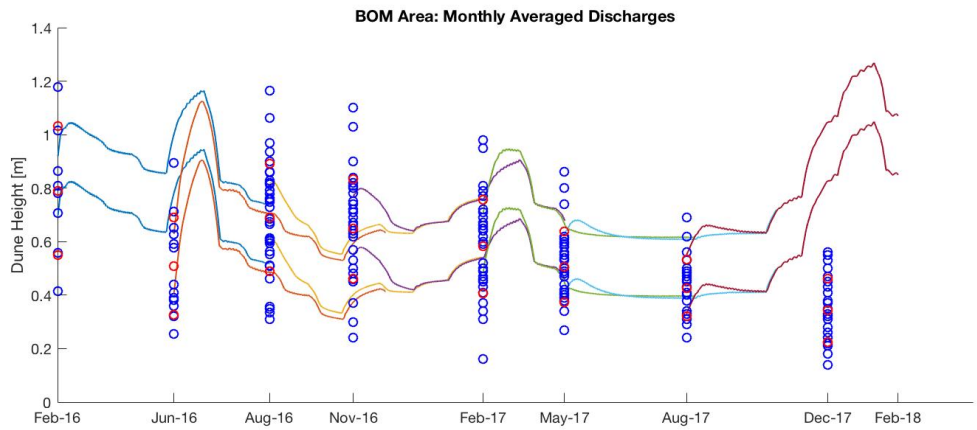
BOM Area: Monthly Averaged Discharges
Dune Height [m]
0
0.2
0.4
0.6
0.8
1
1.2
1.4
Feb-16
Jun-16
Aug-16
Nov-16
Feb-17
May-17
Aug-17
Dec-17
Feb-18

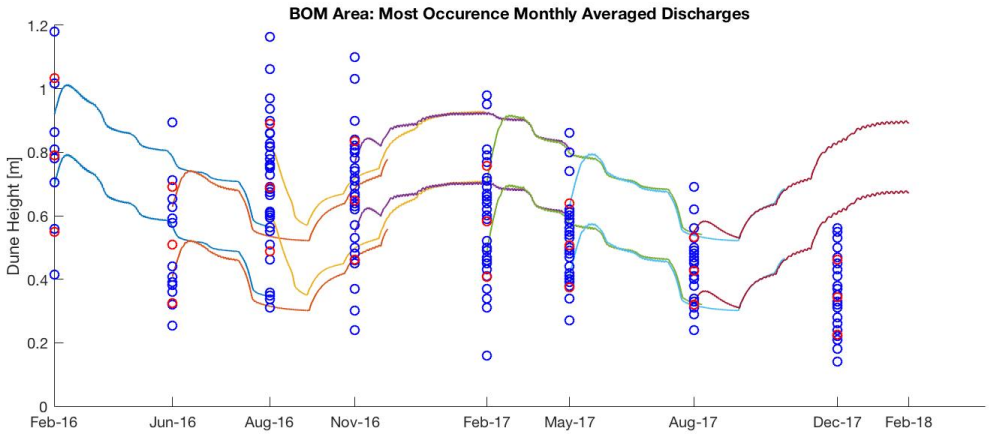

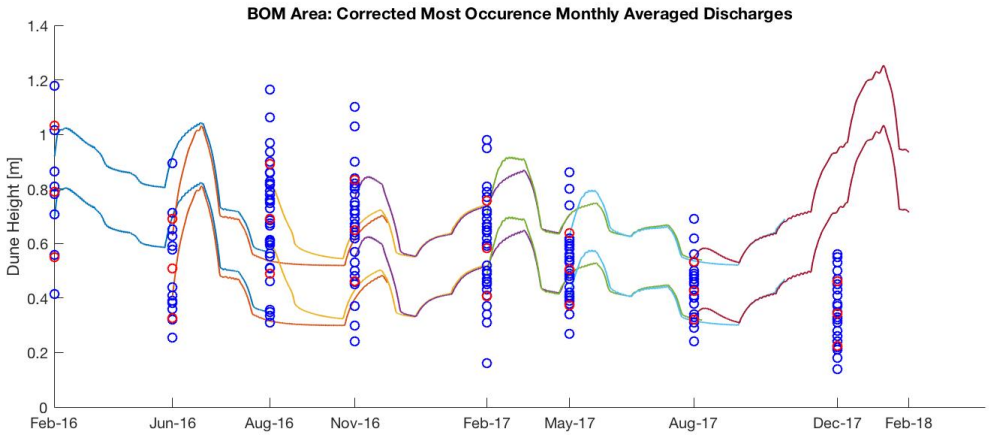

Model Performance	***Discharge Scenario***	***H BEM***	***H BOM***	
n points	Daily Averaged (Zero Scenario)	67,22%	32,85%	44,45%
	10 Days-averaged	65,62%	33,03%	44,70%
	Monthly-averaged	63,04%	32,42%	43,85%
	Most frequent	61,71%	29,76%	33,97%
	Corrected Most Frequent	64,19%	31,93%	41,63%
Min/Max	Daily Averaged (Zero Scenario)	63,39%	26,01%	32,88%
	10 Days-averaged	63,39%	23,75%	32,88%
	Monthly-averaged	63,39%	25,97%	32,88%
	Most frequent	59,98%	28,41%	32,88%
	Corrected Most Frequent	62,40%	27,82%	32,88%
$\sigma_{min}/\sigma_{max}$	Daily Averaged (Zero Scenario)	86,18%	39,40%	55,15%
	10 Days-averaged	82,13%	36,58%	51,21%
	Monthly-averaged	80,56%	41,33%	57,86%
	Most frequent	79,85%	34,90%	41,98%
	Corrected Most Frequent	83,51%	40,26%	56,36%

Statistical monthly discharges at river Maas (Megen) 1996-2016

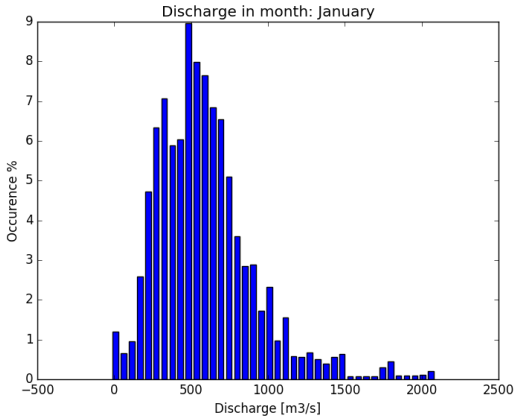

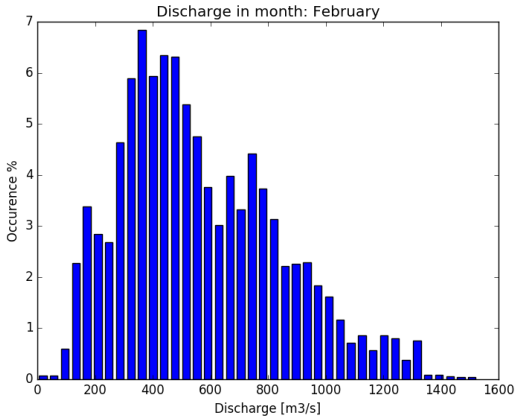

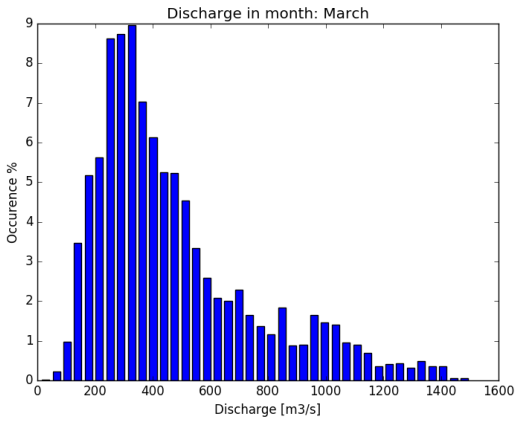

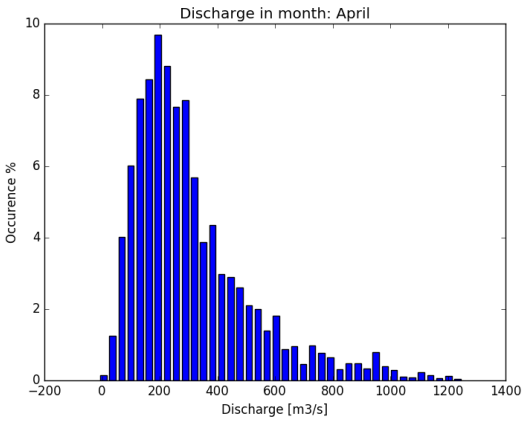

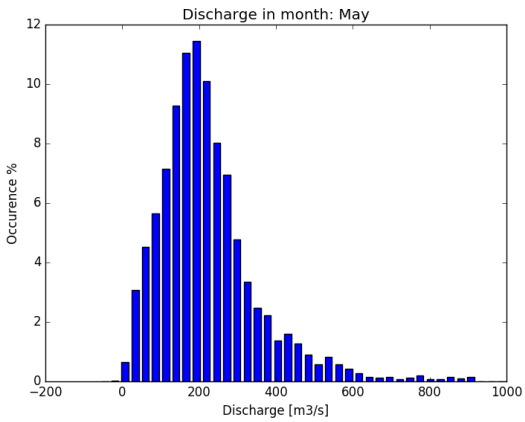

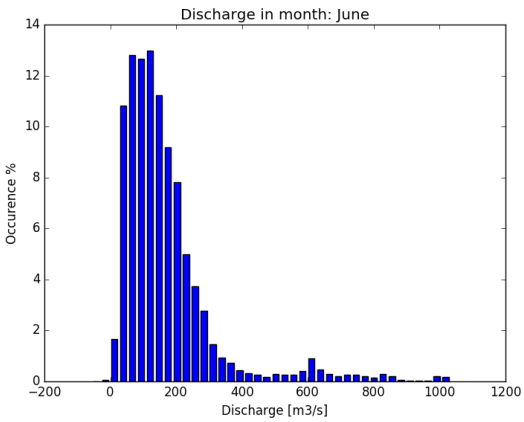

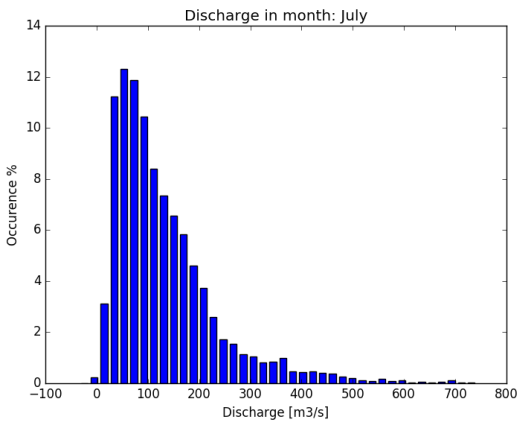

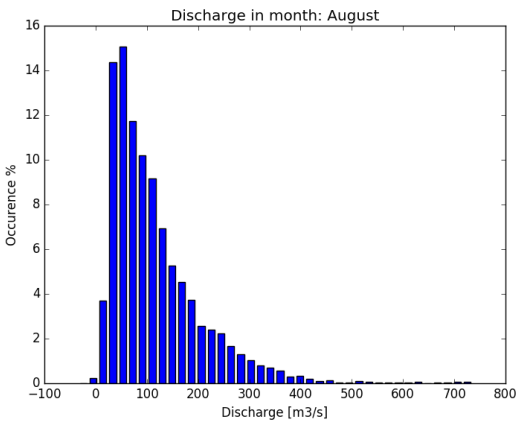

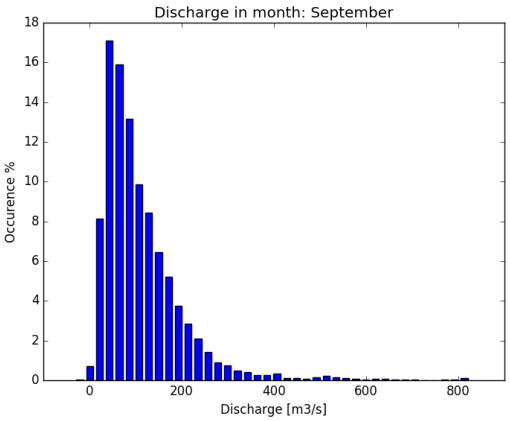
Discharge in month: September
Occurence %
Discharge [m3/s]

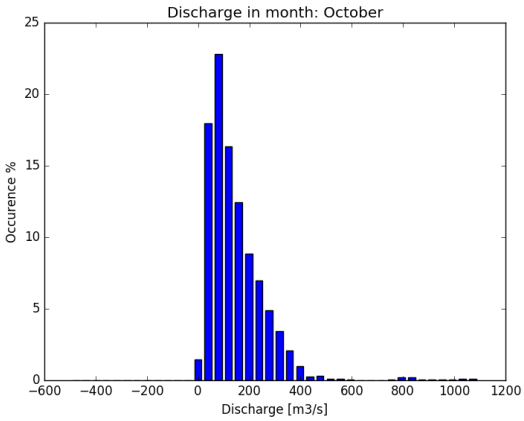
Discharge in month: October
Occurence %
Discharge [m3/s]

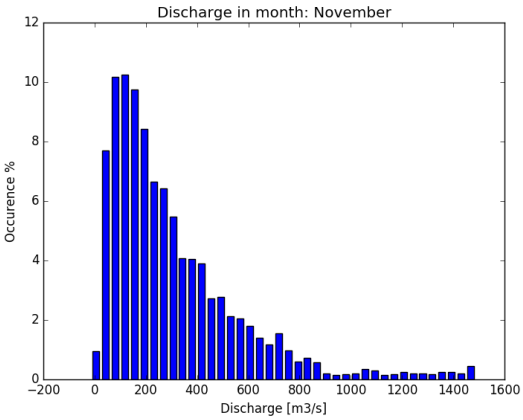
Discharge in month: November
Occurence %
Discharge [m3/s]

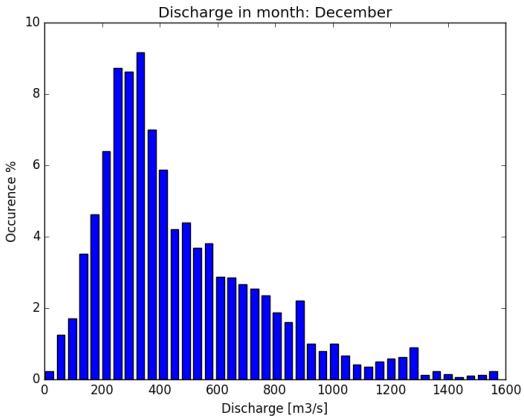
Discharge in month: December
Occurence %
Discharge [m3/s]

Statistical monthly discharges at river Waal (Tiel) 1989-2014

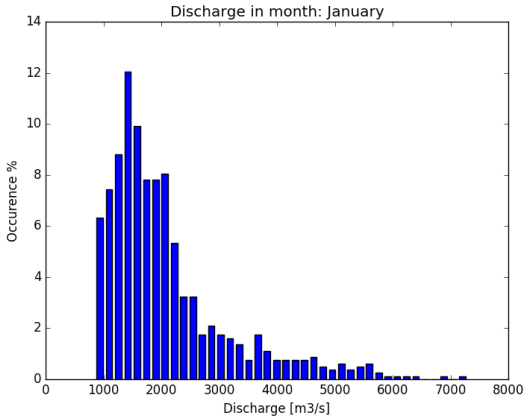

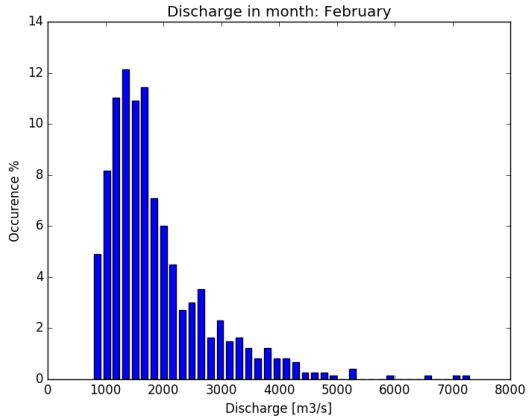

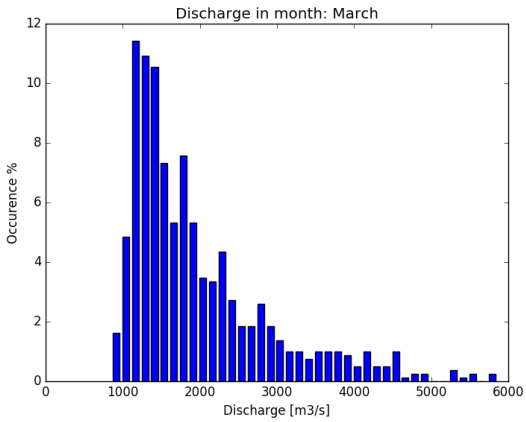

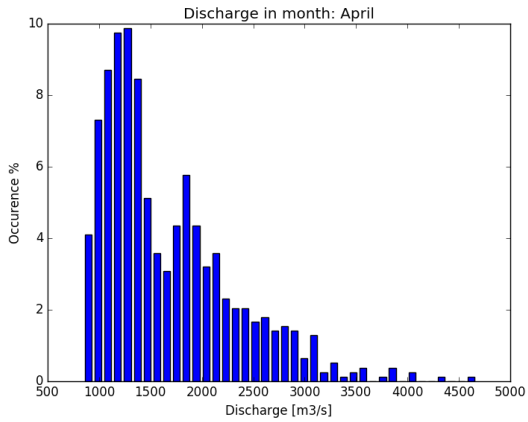

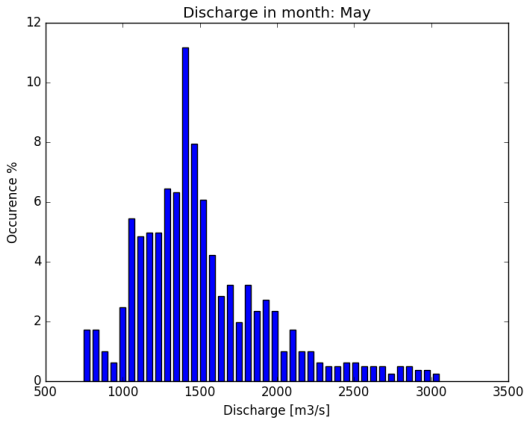

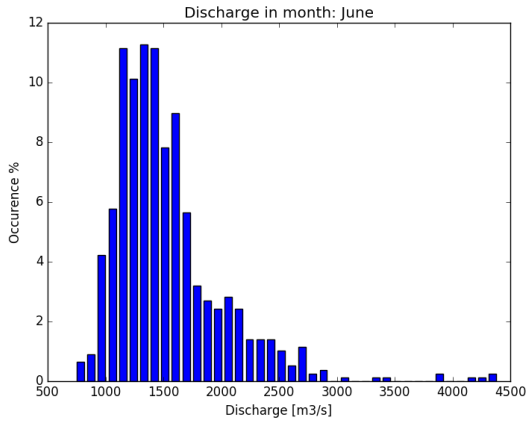

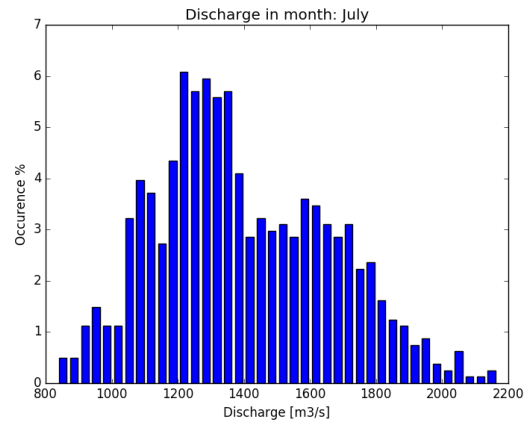

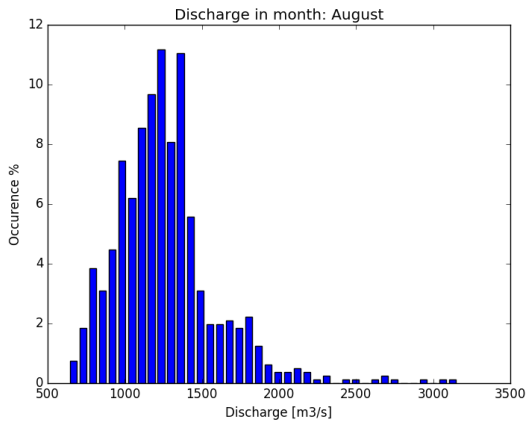

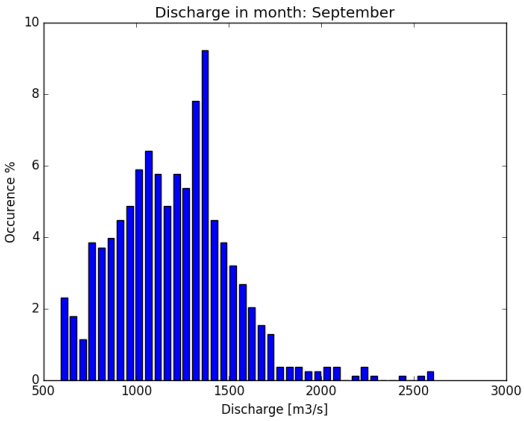
Discharge in month: September
Occurence %
Discharge [m3/s]

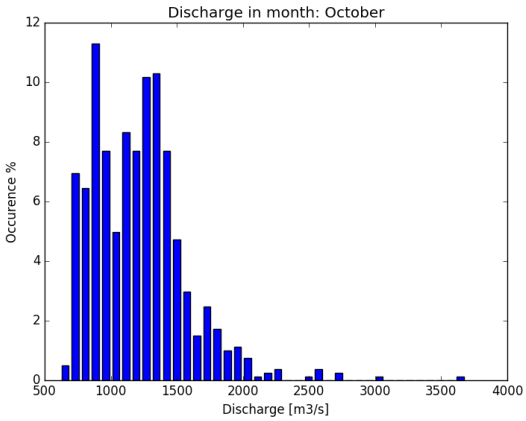
Discharge in month: October
Occurence %
Discharge [m3/s]

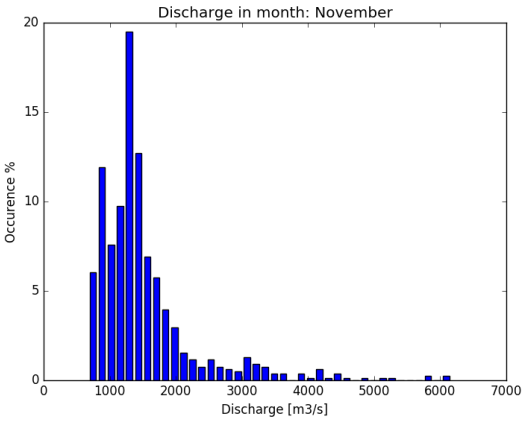
Discharge in month: November
Occurence %
Discharge [m3/s]

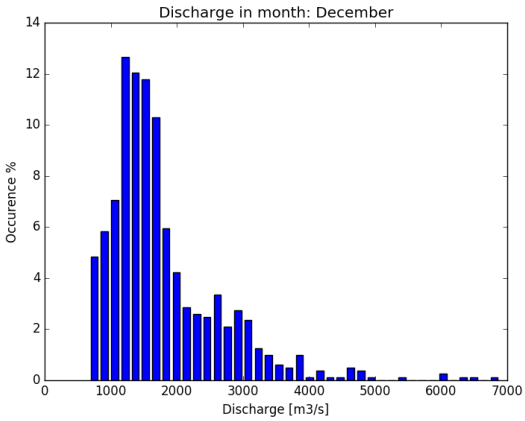
Discharge in month: December
Occurence %
Discharge [m3/s]

APPENDIX D: Dune migration rate estimation approach

The migration rate presents a clear exponential tendency to the average discharges at Tiel, where higher discharges lead to higher migration rates. Therefore, the following formulas are suggested to estimate the range of possible migration rates depending on the upstream discharge at Tiel, Table 18. Each boundary limit functions were found as a quadratic fit of the first quartile, *Q1* and third quartile, *Q3* of the surveyed values for each period.

Table 18: Definition of the simulated migration rates [cm/day] bounds, being Q the daily averaged discharge at Tiel [m^3/s]

Range limits	**Lower limit**	**Upper limit**
BEM	$3.3*10^{-6}*Q^2-0.00012*Q$	$-1.2*10^{-6}*Q^2+0.029*Q+3.5$
BOM	$1.5*10^{-5}*Q^2-0.011*Q-3$	$2.1*10^{-5}*Q^2-0.0042*Q$

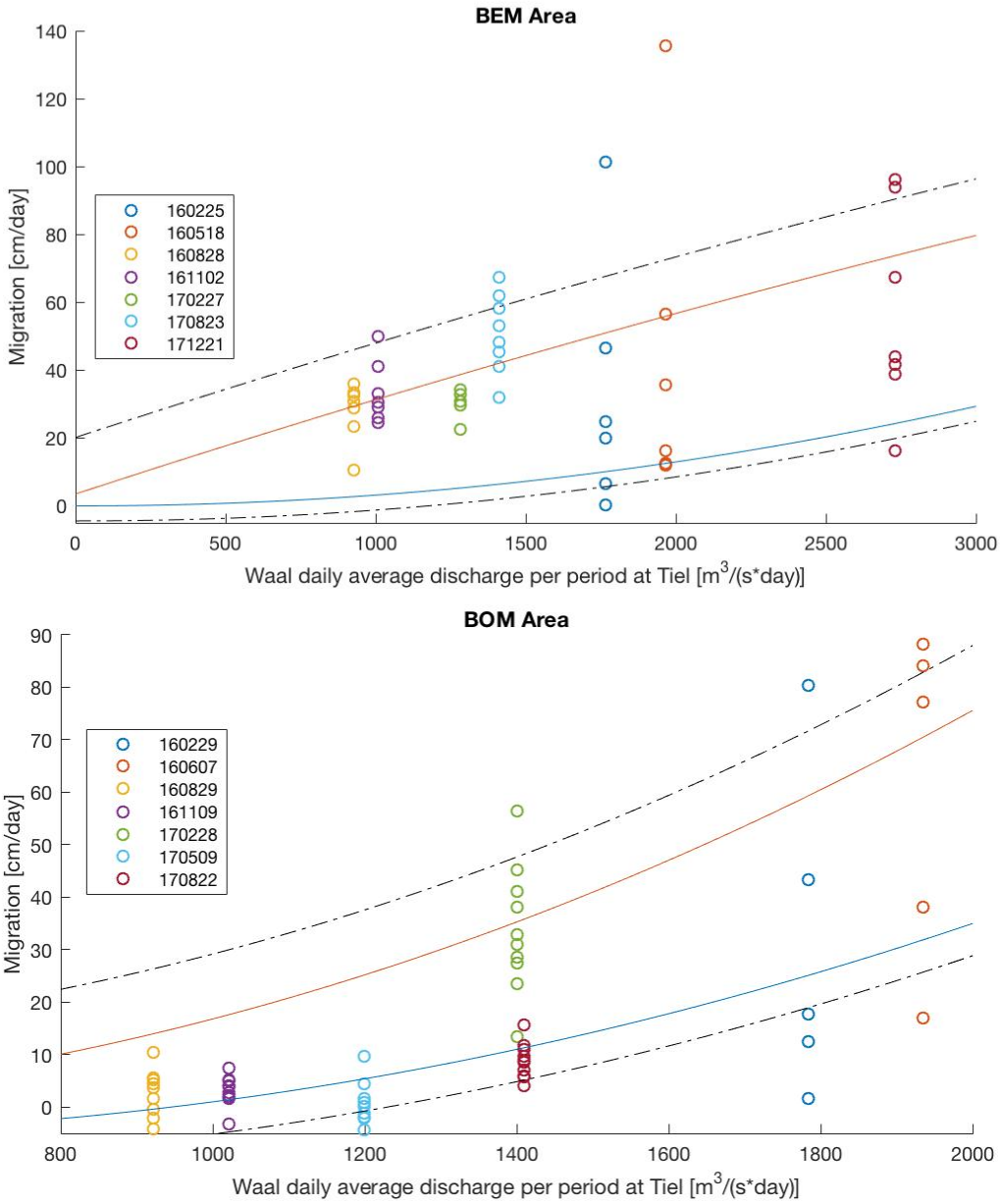

Figure 55: Visual representation of the function limits and extended bounds and the measured data

The basic fitting equations present residuals higher than 30cm/day for some of the data points, therefore, an extension of the boundary limits is proposed (dotted lines in Figure 55). The additional margins were calculated adding the average distance to the closest limit of those surveyed values that lay outside of the functions bandwidth, Table 19. The function boundaries encompass 52% of the observed migration values for the BEM area and 45% for the BOM. The suggested extensions of 16.67cm/day or 12.37cm/day for the upper limit and 4.41 or 6.15 for the lower limit, for BEM and BOM areas respectively, show more englobing results in which 80.85% and 76.67% of the points lay within the delimited area.

Table 19: Results of the defined bandwidth of possible dune migration rates, and the additional limits, to the surveyed data

	BEM			BOM		
	Excluded points within bandwidth (out of 47)	**% points included**	**Averaged distance to closest limit [cm/day]**	**Excluded points within bandwidth (out of 60)**	**% points included**	**Averaged distance to closest limit [cm/day]**
Functions bandwidth	23	52%	±14,0023	33	45%	±7,6591
To upper limit			16,6661			12,3715
To bottom limit			4,4124			6,1511
Functions bandwidth + additional limits	9	80,85%	±14,2957	14	76,67%	±4,9945
To upper limit			17,1119			6,0409
To bottom limit			4,4392			4,5759

Migration Rate Tool Performance

The migration rate approach is totally dependent on the averaged considered discharges at the river Waal. Therefore, it presents the following performance results for the different considered scenarios (notice that the averaged discharge is the same for the 3 exact measured discharge scenarios):

Table 20: Migration rate performance results. Values shown for function delimited area and the extended margins area

		BEM		BOM	
Migration Rate	***Discharge Scenario***	***Functions***	***Functions + Additional margin***	***Functions***	***Functions + Additional margin***
n points	Measured	47,30%	76,03%	50,47%	75,69%
	Most frequent	56,86%	77,10%	40,15%	70,52%
	Corrected Most Frequent	48,91%	77,99%	46,57%	76,40%
Min/Max	Measured	28,39%	69,64%	41,53%	68,02%
	Most frequent	30,68%	68,35%	42,08%	68,07%
	Corrected Most Frequent	26,51%	67,60%	43,42%	70,78%
$\sigma_{min}/\sigma_{max}$	Measured	52,62%	88,72%	54,28%	84,84%
	Most frequent	59,29%	80,40%	47,20%	72,63%
	Corrected Most Frequent	49,24%	85,03%	53,08%	80,58%

The general trend states that the maximum ($\sigma_{min}/\sigma_{max}$) coverage values are found for the real measured data scenario, followed closely by the corrected most frequent monthly-averaged discharges and finally the broadest poor-quality scenario. However, for the BEM area and considering the results given by the functions bounds, the most frequent scenario presents the best accuracy results. The draught conditions during Feb-17 and Aug-18 period are responsible for this change in trend. Discharge values are overestimated when considering the most frequent discharges per month, shifting to the right of the plot in Figure 55, resulting in higher migration rate bounds and an increase of the bandwidth region, which then covers 100% of the periods observed data.

The obtained accuracy results show simulated ranges covering around 50% of the standard deviation range of observed data, and higher than 80% considering the additional suggested margins. This transforms to around 30% for BEM and 40% for BOM cover results of the complete bandwidth of measured migration rates, or lower than 70% for both areas adding the extreme limits.

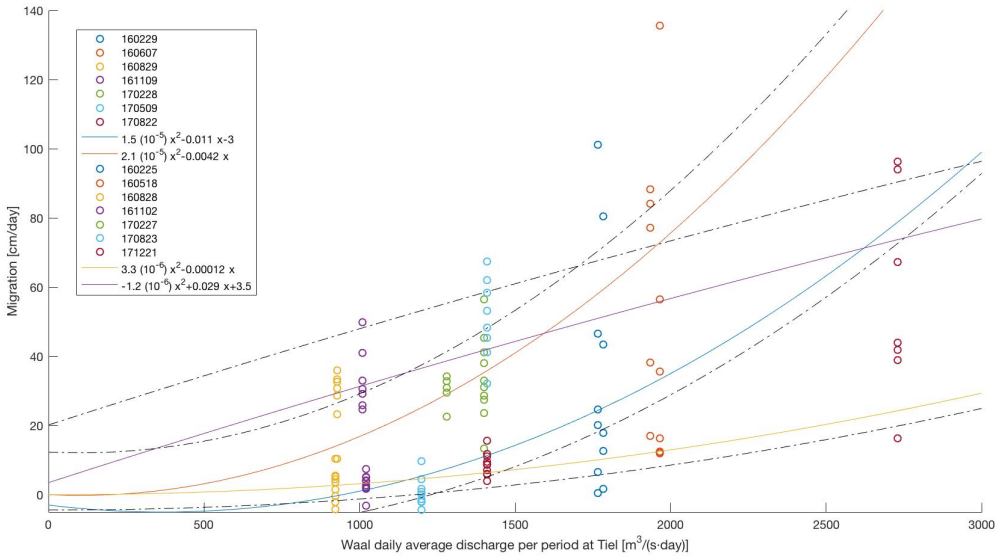

Figure 56: Superposition of BEM and BOM dune migration rate ranges